Novel neurotherapeutic strategies for alleviating chronic pain

Thesis submitted for the degree

of

Doctor of Philosophy

by

Mariia Belinskaia, MSc

Supervised by
Dr Gary W. Lawrence

Co-supervised by

Prof. J. Oliver Dolly

School of Biotechnology
Dublin City University
Ireland

May 2023

Declaration

I hereby certify that this material, which I now submit for assessment on the programme of study leading to the award of Doctor of Philosophy is entirely my own work, that I have exercised reasonable care to ensure that the work is original, and does not to the best of my knowledge breach any law of copyright, and has not been taken from the work of others save and to the extent that such work has been cited and acknowledged within the text of my work.

Name: Mariia Belinskaia Student ID No: 18212868

Signed: Date:

Acknowledments

I have a lot of people to thank for this thesis. Not least my supervisor Dr Gary Lawrence and Prof. J. Oliver Dolly for providing both practical and intellectual direction in this project. I can never repay their hard work, patience, and perseverance.

I am especially grateful too for all the efforts and kind words of encouragement from my colleagues at 'International Centre for Neurotherapeutics'; Dr Caren Antoniazzi, Dr Seshu Kumar Kaza, and Dr Tomas Zurawski. Their years of experience, practical help, advice, and critical feedback were invaluable. Special thanks to ICNT's most popular PA, Geraldine Jordan, for good jokes in dark times!

It was a pleasure to work with such great minds and I wish every success in career and in life to all the team. Without their help this thesis would not be possible.

To my family, mam and dad, Daria, and Marta, I don't know what I would have done without your endless kind words of support and encouragement. Your belief in me was unwavering.

To Brian, thank you for walking this winding road with me with all its peaks and potholes. I could not have asked for a better partner on this journey.

I would also like to thank all members of School of Biotechnology and Science Foundation Ireland for making this work possible through grant funding awarded to Prof. Oliver Dolly.

Publications

1) M. Belinskaia, T. Zurawski, S. K. Kaza, C. Antoniazzi, J. O. Dolly and G. W. Lawrence (2022). "NGF Enhances CGRP Release Evoked by Capsaicin from Rat Trigeminal Neurons: Differential Inhibition by SNAP-25-Cleaving Proteases." Int J Mol Sci 23(2), doi:10.3390/ijms23020892.

2) C. Antoniazzi, M. Belinskaia, T. Zurawski, S. K. Kaza, J. O. Dolly and G. W. Lawrence (2022). "Botulinum Neurotoxin Chimeras Suppress Stimulation by Capsaicin of Rat Trigeminal Sensory Neurons In Vivo and In Vitro." Toxins (Basel) 14(2), doi:10.3390/toxins14020116.

3) M. Belinskaia, J. Wang, S. K. Kaza, C. Antoniazzi, T. Zurawski, J. O. Dolly and G. W. Lawrence (2023). "Bipartite activation of sensory neurons by a TRPA1 agonist allyl isothiocyanate is reflected by complex Ca^{2+} influx and CGRP release patterns: enhancement by NGF and inhibition with VAMP and SNAP-25 cleaving botulinum neurotoxins. " Int J Mol Sci 24(2), doi:10.3390/ijms24021338.

Table of Contents

List of Figures

List of Tables

Abbreviations used

A.A., acetic acid

AbD, antibodies dilution buffer

AbW, antibodies wash buffer

AchE, acetylcholinesterase

AITC, allyl isothiocyanate

AP, alkaline phosphatase

ARA-C, cytosine arabinoside

AUC, area under the curve

BDNF, brain-derived neurotrophic factor

BCA, bicinchoninic acid

BK, bradykinin

BoNT, botulinum neurotoxin

BoNT/X, BoNT serotype where X can be A, B, C, D, E, F, or G

BOTOX®, botulinum toxin A-haemagglutinin complex

BSA, bovine serum albumin

$[Ca^{2+}]_i$, intracellular calcium concentration

CAP, capsaicin

[CAP], capsaicin concentration

CFA, complete Freund's adjuvant

CGRP, calcitonin gene-related peptide

Chimera /EA, chimeric toxin containing LC and translocation domains of BoNT/E and binding domain of BoNT/A

Chimera LC/E-BoNT/A, chimeric toxin containing LC of BoNT/E attached to full-length BoNT/A

CIP, congenital insensitivity to pain

CIPA, congenital insensitivity to pain with anhidrosis

CLR, calcitonin receptor-like receptor

CMF-HBSS, Ca^{2+} and Mg^{2+}- free Hanks' balanced salt solution

CNS, central nervous system

CPZ, capsazepine

DC, di-chain

DAG, diacylglycerol

DCU, Dublin city university

DIV, days *in vitro*

DMEM, Dulbecco's modified Eagle's medium

DMSO, dimethylsulfoxide

DPBS, Dulbecco’s phosphate-buffered saline

DRG, dorsal root ganglion

DRGNs, dorsal root ganglia neurons

EC_{50}, half-maximum effective concentration

EGTA, ethylene glycol-bis(β-aminoethyl ether)-N,N,N′,N′-tetraacetic acid

ELISA, enzyme-linked immunosorbent assay

ERK1/2, the extracellular signal-regulated kinase 1/2

FBS, foetal bovine serum

HBS, HEPES buffered saline

HBS-HK, 60 or 100 mM KCl modified HEPES buffered saline

HBS-LB, HEPES buffered saline with 10 µg/ml BSA

H_C, binding domain

HC, heavy chain

HEPES, 4-(2-hydroxyethyl)-1-piperazineethanesulfonic acid

$H_{N,}$ translocation domain

$(His)_6$, polyhistidine purification tag

HSAN, hereditary sensory and autonomic neuropathy

ICNT, International Centre for Neurotherapeutics

IgG, immunoglobulin G

IP3, inositol 3-phosphate

K^+, potassium ions

KO, knockout

LC, light chain

LDCVs, large dense-core vesicles

LDS, lithium dodecyl sulphate

Mab, monoclonal antibodies

MAPK, mitogen-activated protein kinase

MOPS, 3-(n-morpholino)propanesulfonic acid

Mr, relative mobility molecular mass

NF-200, neurofilament 200

NGF, nerve growth factor

NSAIDs, non-steroidal anti-inflammatory drugs

NSF, N-ethylmaleimide-sensitive factor

NT, neurotransmitter

P_2X_3, purinergic receptor 3

p75NR, p75 neurotrophin receptor

Pab, polyclonal antibodies

PI3K, phosphatidylinositol 3-phosphate kinase

PKC, protein kinase C

PLCγ, phospholipase C-gamma

PNS, peripheral nervous system

PVDF, polyvinylidene fluoride

RAMP1, receptor activity-modifying protein 1

SC, single-chain

SDS, sodium dodecyl sulphate

SDS-PAGE, sodium dodecyl sulphate-polyacrylamide gel electrophoresis

SNAP, soluble NSF attachment protein

SNAP-25, synaptosomal-associated protein with Mr=25 k

$SNAP\text{-}25_A$, truncated product of SNAP-25 cleavage by BoNT/A

$SNAP\text{-}25_E$, truncated product of SNAP-25 cleavage by BoNT/E

SNARE, SNAP receptor

SP, substance P

SSVs, small synaptic vesicles

SV2, synaptic vesicle protein 2

TBST, tris-buffered saline (TBS) supplemented with 0.1% (v/v) Tween-20

TFA, trifluoroacetic acid

TG, trigeminal ganglion

TGNs, trigeminal ganglia neurons

TNC, trigeminal nucleus caudalis

TNFα, tumour necrosis factor alpha

TrkX, tropomyosin receptor kinase sub-type where X can be A, B or C

TRPA1, transient receptor potential cation channel subfamily A member 1

TRPV1, transient receptor potential cation channel subfamily V member 1

VAMP, vesicle-associated membrane protein

VGCC, voltage-gated calcium channel

Abstract

Thesis title: Novel neurotherapeutic strategies for alleviating chronic pain

Author: Mariia Belinskaia

Calcitonin gene-related peptide (CGRP) in trigeminal ganglion neurons (TGNs) contributes to neurogenic inflammation and chronic migraine (CM). Trafficking of transient receptor potential (TRP) cation channels to plasmalemma has been implicated in TGN sensitisation by inflammatory agents, such as nerve growth factor (NGF), and could potentiate CGRP exocytosis. Its Ca^{2+}-dependent release from sensory fibres is mediated by synaptosomal-associated protein with Mr=25 k (SNAP-25), syntaxin-1, and vesicle-associated membrane protein isoforms 1/2/3 (VAMP1/2/3). Hence, moderation of CGRP release and TRP trafficking by botulinum neurotoxins (BoNTs) is a potential therapeutic strategy for CM.

Cultured TGNs from neonatal rats were exposed to activators of TRP subfamilies V1 and A1; capsaicin (CAP) and allyl isothiocyanate (AITC). This caused dose-dependent increases of intracellular Ca^{2+} $[Ca^{2+}]_i$, revealed by confocal fluorescence monitoring in Fluo-4 loaded cells, and CGRP secretion quantified by ELISA. However, AITC differed from CAP by inducing a complex bi-phasic response. BoNT type A (/A) cleaved SNAP-25 and reduced neuropeptide exocytosis evoked by low [CAP], but not high concentrations that elevated $[Ca^{2+}]_i$ more extensively. The toxin partially reduced CGRP release stimulated by AITC, but raising the concentration of this agonist failed to induce the high $[Ca^{2+}]_i$ necessary to fully overcome BoNT/A blockade. Chimeras created by gene recombination, BoNT/EA and LC/E-BoNT/A that both removed a larger fragment of SNAP-25 then /A, partially blocked CGRP secretion evoked by AITC, but extensively inhibited the release evoked by low and high [CAP]. VAMP1/2/3-cleaving BoNT/DA effectively blocked CGRP release evoked by all [CAP] and [AITC].

Herein, it was discovered that NGF provokes Ca^{2+}-dependent CGRP exocytosis that was susceptible to blockade by SNAP-25 and VAMP1/2/3 cleaving proteases. In addition, the neurotrophin enhanced CAP- and AITC-stimulated release, although this effect was more pronounced at low [agonist]. The NGF-induced enhancement of stimulated exocytosis did not require extracellular Ca^{2+}. BoNT/EA was a more effective inhibitor of NGF-enhanced CGRP secretion stimulated by high [CAP] than BoNT/A. On the other hand, all the BoNTs inhibited AITC-stimulated secretion enhanced by NGF to similar extents. BoNTs with distinct protease activities might expand their therapeutic utility for CM in addition to currently used BoNT/A.

1. General introduction

1.1 Regulated exocytosis is involved in the transmission of pain signals in peripheral and central nervous systems

Pain is an unpleasant sensation aimed to protect the organism from tissue damage. It is also essential in the healing process when the injured area is hyper-sensitised. In this case, innocuous stimuli are sensed as painful (a condition termed allodynia) and noxious triggers elicit more robust responses (hyperalgesia) compared to non-damaged tissues (Basbaum et al., 2009). Alterations in pain signalling can lead to persisting and debilitating pain even after the tissue damage has healed; this is termed chronic pain. In Europe, 20% of the adult population suffers from chronic pain (van Hecke et al., 2013), which poses a severe challenge to the European economy and healthcare system. In many cases, modern analgesics can provide only a short period of relief and are often ineffective. Moreover, they might produce severe side effects, and some are addictive. Considering these negative factors together, more effective, long-lasting, safe, and non-addictive anti-pain treatments are urgently needed.

1.1.1 Structure and function of the sensory nervous system

The sensation of pain is usually initiated within the peripheral nervous system (PNS) by a specialised high-threshold sensory neurons called nociceptors. These are pseudo-unipolar neurons, whose peripheral fibres, primarily non- or thinly myelinated C- and Aδ-fibres, innervate tissues and organs. Central projections of these sensory neurons form synapses with second-order neurons of the central nervous system (CNS). Cell bodies of nociceptors are clustered in ganglia: those that innervate most tissues of the body are in dorsal root ganglia (DRG), and those which innervate the head are in trigeminal ganglia (TG). Activation of nociceptors results in signal transmission from DRGs or TGs to second-order neurons in the dorsal horn or trigeminal nucleus caudalis (TNC), respectively. Then the signal is transmitted through ascending pathways to cortical structures via the thalamus, activating distinct areas depending on properties of the signal such as location and intensity of the stimulus or emotional aspects of pain (Fig. 1.1) (Basbaum et al., 2009). Feedback on the received signal is provided by descending pathways including structures such as the midline periaqueductal gray and the rostral ventral medulla (Heinricher et al., 2009).

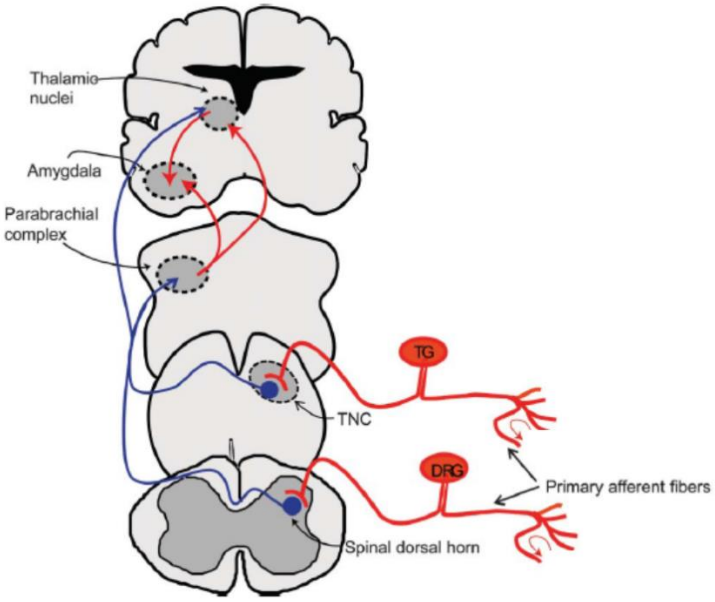

Figure 1.1 Illustration of the ascending pain pathway
Primary sensory neurons in DRGs and TGs detect noxious conditions at their peripheral fibres and transmit signals to second-order neurons in the spinal dorsal horn (from DRG neurons [DRGNs]) or in trigeminal nuclei caudalis (TNC, from TGNs) in brainstem. From there, CNS neurons pass signals providing information about the location and intensity of the signal to the thalamus and thence to the somatosensory cortex. Another subset of CNS neurons transmits information to the amygdala via the parabrachial nucleus, contributing to the emotional component of pain. The illustration is taken from (Iyengar et al., 2017).

1.1.2 Ca^{2+} regulated exocytosis participates in noxious signal transmission in the PNS and CNS

Nociceptors express on their surface receptors and channels responsible for detection of noxious heat, cold, chemical, or mechanical stimulation. Once these pain transducers are activated, they generate action potentials which are propagated along the nerve fibre by voltage-gated ion channels before the transmission of signals to second-order neurons by regulated Ca^{2+}-dependent exocytosis (Basbaum et al., 2009). Signals are passed between neurons and from neurons to non-neuronal cells by chemical messengers called neurotransmitters. These include different molecules like amino acids, such as glutamate, which is the most abundant neurotransmitter in the CNS, acetylcholine which transmits signals in the neuromuscular junction and many other locations, or neuropeptides like calcitonin gene-related peptide (CGRP) which is a potent vasodilator and one of the key components in neurogenic inflammation (Basbaum et al., 2009), (Iyengar et al., 2017).

For storage and release, neurotransmitters are packed into membrane delimited organelles called vesicles. Fast-acting neurotransmitters such as glutamate and

acetylcholine tend to be stored in small synaptic vesicles (SSVs) whereas neuropeptides are located in large dense-core vesicles (LDCVs); the terms used are derived from the appearance of the different vesicle types in electron micrographs. Another difference between SSVs and LDCVs lies in their location and trafficking cycle within the presynaptic terminals: swellings along or at the end of nerve fibres are where the chemical neurotransmitters get released (Martens and McMahon, 2008). SSVs are filled and stored in the cytoplasm at nerve terminals. Some of them are docked to the plasmalemma at specialised regions of the nerve terminal called active zones that oppose regions of the post-synaptic cell having elevated densities of neurotransmitter receptors. Once SSVs have released their contents, they undergo local refiling with neurotransmitters (Sudhof, 2014).

Neuropeptides are synthesised on ribosomes at the endoplasmic reticulum and processed through the Golgi. Peptide-containing vesicles are delivered by axonal transport to release sites, where LDCVs contents are secreted (Nicholls, 1994). By contrast to SSVs, LDCVs are not clustered in nerve terminals, although some of these vesicles release their content into the synaptic cleft. Instead, most frequently, LDCVs exocytosis is observed in non-synaptic sites and, in general, neuropeptides must diffuse over longer distances before interacting with their receptors in comparison to fast neurotransmitters acting at synaptic clefts. Moreover, neuropeptides tend to elicit longer-lasting changes and, hence, are often considered to be neuromodulators rather than neurotransmitters. After the release of LDCVs' contents, their membrane components are usually internalised and then undergo degradation rather than being re-utilised like SSVs (Nicholls, 1994).

1.1.3 Regulated exocytosis is mediated by a SNARE complex

A central role in regulated exocytosis is attributed to soluble N-ethylmaleimide-sensitive factor attachment protein receptors (SNAREs). These are proteins that include vesicle-associated membrane protein (VAMP, also known as synaptobrevin), which is present on SSVs and LDCVs (Fig. 1.2 B), two plasmalemma proteins called synaptosomal-associated protein with Mr=25 k (SNAP-25, Fig. 1.2 D) and syntaxin-1 (Fig. 1.2 C). Together, they form a highly stable 'SNARE complex', the defining feature being a parallel four-helix bundle formed by so-called SNARE motifs of VAMP, syntaxin-1, and two of them in SNAP-25 (Rizo and Rosenmund, 2008). Assembly of the

SNARE complex involves several other proteins associated with pre-fusion steps termed docking and priming. Other proteins, including N-ethylmaleimide-sensitive factor (NSF) and the soluble NSF attachment proteins (SNAPs) are implicated in the disassembly of the complex. Initially, in active zones, the SNARE complex is partially formed (vesicles are docked and primed) (Sudhof, 2014). After activation of voltage gated calcium channels (VGCCs) by an action potential, extracellular Ca^{2+} flows inwards down a steep concentration gradient into the cytoplasm where it binds to Ca^{2+} sensors-proteins named synaptotagmins. These are evolutionarily conserved proteins, present on all synaptic vesicles, that bind Ca^{2+} by their two C2-domains (C2A and C2B) (Sudhof, 2012) (Fig. 1.2 A). When the ions bind to synaptotagmin, it drives zipping of the SNARE complex, which brings vesicular and plasma membranes close to each other. The energy released during SNARE complex zipping is transduced through transmembrane domains of the complex members into lipid bilayers resulting in membrane destabilisation. It is proposed that sufficient energy results from completion of complex assembly to overcome the energy barrier to fusion, drive the merger of the vesicle and plasma membranes and initiate the formation and widening of a fusion pore through which vesicular contents escape to extracellular space [reviewed in (Chapman, 2002), (Martens and McMahon, 2008)].

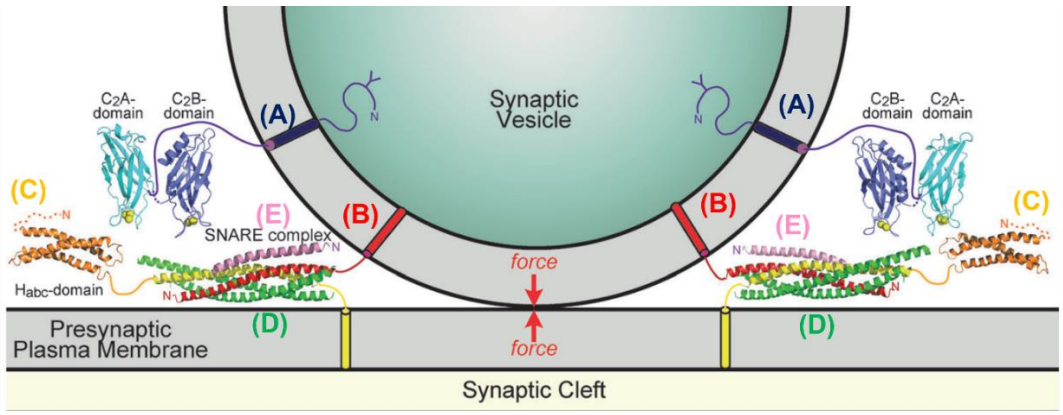

Figure 1.2 A schematic diagram of SNARE complex and synaptotagmin
Synaptotagmin (A) is present on the synaptic vesicle and binds Ca^{2+} (filled yellow circles) by its two domains: C2A (three Ca^{2+} ions) and C2B (two Ca^{2+} ions). This results in the zippering of a SNARE complex comprised of (B) VAMP; shown in red and (C) syntaxin-1; transmembrane anchor and SNARE domain shown in yellow and Habc domain in orange, plus (D) SNAP-25; in the presynaptic plasma membrane; green. A small cytoplasmic protein named (E) complexin, shown in pink, binds to the SNARE complex and plays both stimulatory and inhibitory roles to modulate vesicle fusion. Schematic modified from (Sudhof, 2014).

SNARE-dependent exocytosis plays a crucial role in pain signalling. It underpins chemical signal transmission from sensory neurons to CNS. Importantly, it is also involved in the release of pain-related mediators and translocation of pain-associated channels in peripheral fibres of nociceptors (see 1.1.4). Consequently, local modulation of exocytosis has considerable potential as a novel therapeutic approach for chronic pain.

1.1.4 SNARE-dependent exocytosis contributes to the trafficking of pain-related ion channels TRPV1 and TRPA1

As mentioned in 1.1.2 nociceptors express on their surface receptors to detect and transduce harmful stimuli. One of the most extensively studied are the transient receptor potential cation channel (TRP) subfamily V member 1 (TRPV1) and subfamily A member 1 (TRPA1). These TRPs are expressed primarily in peripheral peptidergic and non-peptidergic sensory neurons of TGs and DRGs and their essential role in nociception has been demonstrated by knockout (KO) from rodents (Caterina et al., 2000). Both channels are polymodal sensors that are activated by noxious temperature (>43 °C, TRPV1; <17 °C TRPA1) [reviewed in (Koivisto et al., 2022)], endogenous compounds and numerous chemicals. Activation of TRPV1 and TRPA1 leads to Na^+ and Ca^{2+} influx into neurons, triggering membrane depolarisation and leading to the release of neurotransmitters via a mechanism essentially the same as described above for synaptic neurotransmission.

TRP channels are composed of a homomeric tetramer of four subunits, a structural feature common to many types of cation channel. A single subunit of TRPV1 or TRPA1 consist of six transmembrane domains (S1-S6), a pore-forming linker between S5 and S6, and several cytosolic domains on N- and C-terminals (Fig. 1.3 A, B). The N-terminus of TRPV1 contains six ankyrin repeats that regulate the channel's function (Fig. 1.3 A). Additionally, there are two calmodulin (Cam/Ca^{2+}) binding regions located on the N- and C-terminus that regulate desensitisation of the channel. The C-terminus of TRPV1 contains a sequence known as the TRP box, which is highly conserved in other members of the TRP channels family. This region interacts with the pre-S1 and S5-S6 regions, thereby influencing the gating of the channel (Liao et al., 2013).

Ankyrin repeats domain of TRPA1 is more extensive than of TRPV1 and is located before cysteine and lysine residues, which are covalently modified by electrophiles, resulting in channel's activation (Fig. 1.3 B). The C-terminus of the channel contains calmodulin (Cam/Ca^{2+}) binding region, TRP-like region, which is a

topologically analogous to the TRP domain in TRPV1 and modulates the pore configuration. Another coiled-coil domain on C-terminal of TRPA1 mediates interactions between subunits in homotetramers (Paulsen et al., 2015).

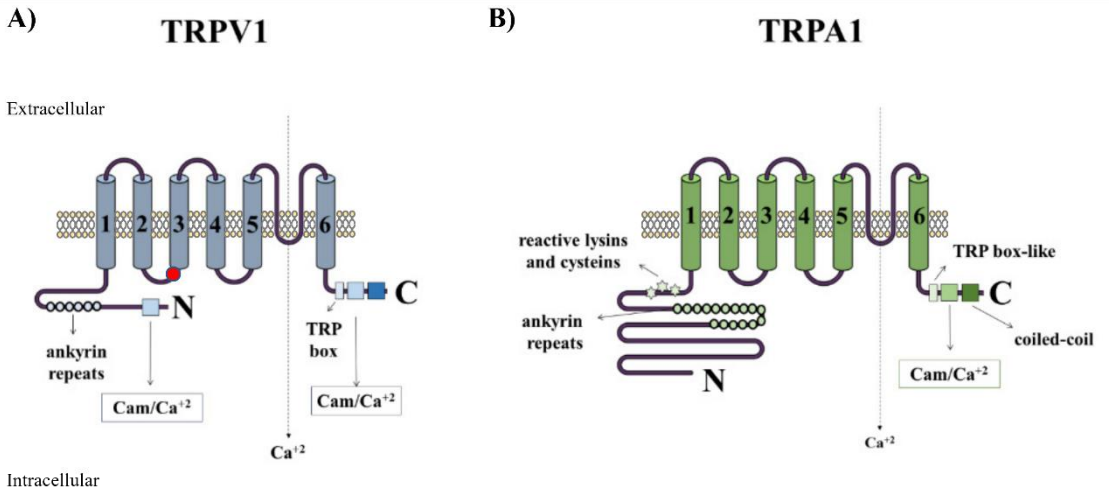

Figure 1.3 Graphical representation of TRPV1 and TRPA1 subunit structure
TRPV1 (A) and TRPA1 (B) are composed of six transmembrane domains (1-6). Transmembrane domains 5 and 6 form the central pore of the channels, with 1-4 arranged around them on the channel periphery. An extended linker between transmembrane coils 5 and 6 extends into the channel pore. (A) On N-terminus of TRPV1 are located ankyrin repeats and binding site for Ca^{2+} and Cam. The binding site for CAP is located on the linker between 2-3. On C-terminus are TRP box and binding site for Cam and Ca^{2+}. (B) N-terminus of TRPA1 has ankyrin repeats, reactive cysteines and lysins which are covalently modified by electrophilic agonists of the channels. C-terminus contains TRP box-like, binding site for Ca^{2+}. Illustration is modified from (Araujo et al., 2022).

Functional TRPV1 and TRPA1 channels can also assemble together in heterotetramers, which can modulate activity and sensitivity to various stimuli (Ferrandiz-Huertas et al., 2014).

TRP channels are synthesised on the endoplasmic reticulum and trafficked through the cisternae of the Golgi apparatus, where it undergoes posttranslational modifications, including glycosylation. In the trans-Golgi network, TRPs are sorted into transport vesicles, delivered to the plasmalemma (Fig. 1.4, left) and by constitutive exocytosis the channels are inserted into the cell membrane. This pathway maintains homeostasis of the channels and does not require elevation of intracellular Ca^{2+} to stimulate the fusion of the vesicles (Sudhof, 2014). Alternatively, TRPs can be sorted into secretory vesicles, which might also contain neuropeptides (CGRP), and they are delivered to the cell surface by regulated exocytosis (Ferrandiz-Huertas et al., 2014). In this case, the recruitment of TRPs to the cell surface in response to stimuli (i.e., regulated

exocytosis) involves Ca^{2+} influx into the cells. For example, activation of TRPV1 by capsaicin (CAP, V1 agonist) initiates the channel's pore opening and elevated $[Ca^{2+}]_I$ promotes fusion of CGRP containing vesicles which also contains TRPs. This results in the release of CGRP and also the translocation of new channels to the plasma membrane (Fig. 1.4, right) (Ferrandiz-Huertas et al., 2014).

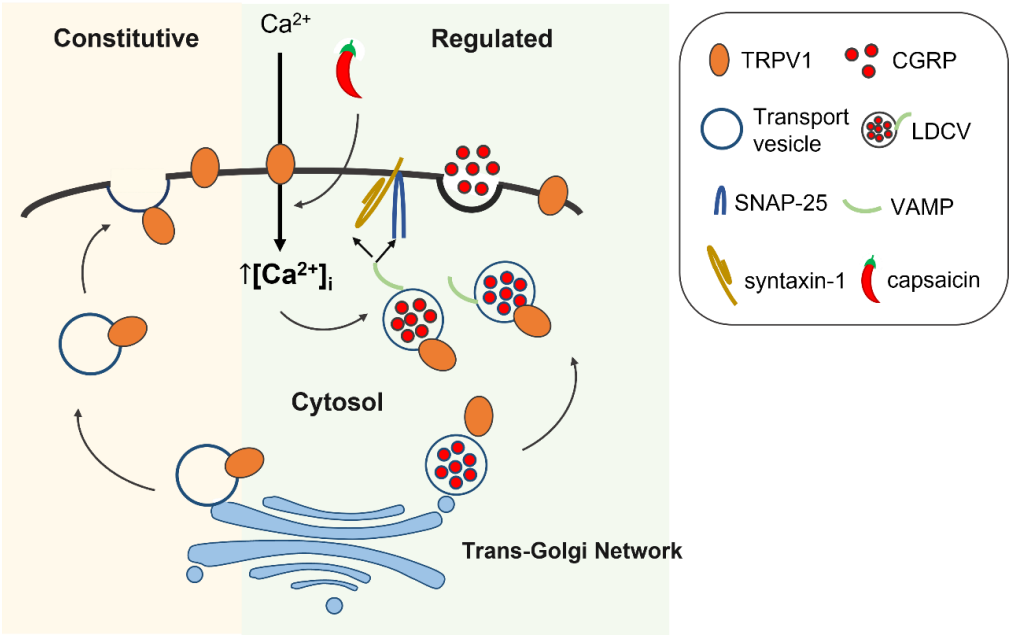

Figure 1.4. TRPV1 channels are delivered to the cell surface by regulated and constitutive exocytosis After synthesis on endoplasmic reticulum and intracellular traffic through the secretory pathway, the channels are sorted into transport or secretory vesicles such as LDCVs at the trans-Golgi-Network (bottom of the illustration). Secretory vesicles might also contain neuropeptides (CGRP). Vesicles traffic to and fuse with the neuronal plasma membrane to deliver TRPV1 to the cell surface. Such fusion can occur constitutively (left side of the illustration), meaning without any external stimulus, or by regulated exocytosis in response to elevated intracellular concentrations of Ca^{2+}; for example, activation of TRPV1 by CAP (red pepper) (right side of the illustration). In regulated exocytosis the fusion of the vesicle with membrane is facilitated by SNAREs. The illustration reproduced from (Ferrandiz-Huertas et al., 2014).

1.1.5 Pro-inflammatory mediators potentiate the activity of TRPV1 and stimulate the trafficking of additional channels to the plasma membrane

Pro-inflammatory compounds such as nerve growth factor (NGF) and tumour necrosis factor-alpha (TNFα) are released after tissue damage, primarily from immune cells but also from non-immune cells. Numerous studies in rodents and humans demonstrated that subcutaneous injection of these compounds induces hypersensitivity to thermal, mechanical, and chemical stimulation (Khan et al., 2008), (Denk et al., 2017). Moreover, their levels are elevated in chronic migraine patients in blood and cerebrospinal fluid (Rozen and Swidan, 2007), (Martins et al., 2015) evidencing their critical role in pain signalling (Denk et al., 2017), (Kalliolias and Ivashkiv, 2016).

1.1.5.1 TNFα signalling cascade

TNFα exerts its effects as homotrimers through binding and activation of two distinct receptors: the TNF receptor-1 (TNFR1) and the TNF receptor-2 (TNFR2). These receptors have distinct structures and functions. TNFR1 is primarily involved in pro-inflammatory signalling and TNFR2 is involved in promoting cell survival and proliferation. TNFR1 is widely expressed in many cell types, including immune cells, endothelial cells, and sensory neurons. TNFR2, on the other hand, is expressed mainly on immune cells, such as T cells, B cells, and macrophages (Webster and Vucic, 2020). Binding of TNFα to TNFR1 initiates trimerisation of the receptor and assembly of distinct signalling complexes termed complex I, IIa, IIb, and IIc which lead to distinct functional outcomes. In inflammation the important role is attributed to TNFR1-complex I signalling which activates nuclear factor κB and p38 mitogen-activated protein kinase (MAPK) (Kalliolias and Ivashkiv, 2016). TNFα upregulates the expression of a variety of inflammatory mediators (CGRP) and pain-related channels such as TRPV1 (Bowen et al., 2006), (Hensellek et al., 2007). However, the cytokine also regulates pain signalling via non-genomic mechanisms. For instance, it rapidly increases tetrodotoxin-resistant sodium channel and acid-sensing ion channel currents in DRGNs neurons (Gudes et al., 2015, Wei et al., 2021). Moreover, it enhances sensitivity of TGNs to CAP (Khan et al., 2008) and AITC via delivery of new channels to the cell surface (Meng et al., 2016). Both genomic and non-genomic mechanisms can involve p38 MAPK pathway (Wei et al., 2021), (Hensellek et al., 2007).

1.1.5.2 NGF/TrkA signalling cascade

NGF has two receptors: the higher affinity tropomyosin receptor kinase A (TrkA) and lower affinity p75 neurotrophin receptor (p75NR) (Denk et al., 2017), (Barker et al., 2020). TrkA is a member of Trk family, which also includes TrkB and TrkC. These are all receptors for members of the neurotrophin family: brain-derived neurotrophic factor (BDNF) and neurotrophin 3 which activate TrkB and TrkC, respectively (Huang and Reichardt, 2003). TrkA is expressed predominantly in nociceptors: it has been detected in cutaneous, muscle, and visceral fibres of the sensory neurons (McMahon et al., 1994). Transgenic mice with KO of genes encoding either NGF or TrkA display a loss compared to wild-type of over 70% of the small-diameter neurons of the TG and DRG, which are considered to be nociceptors. These KO animals also had a reduced sensitivity to noxious heat and mechanical insults (Crowley et al., 1994), (Smeyne et al., 1994), providing solid

evidence of a critical role for NGF in pain perception. Unlike in TrkA-KO mice, p75NR-KO mice still develop acute mechanical and heat hyperalgesia after subcutaneous administration of NGF (Bergmann et al., 1998), indicating that TrkA-mediated signalling is more important in nociceptor sensitisation.

When NGF binds to TrkA, it causes dimerisation of the receptor and promotes autophosphorylation of several of its tyrosine (Y) residues. Consequently, the following intracellular signalling pathways are activated: (1) phosphorylation of human Y490 triggers the MAPK (extracellular signal-regulated kinases 1/2 [ERK1/2]) cascade, which upregulates neuronal differentiation and neurite outgrowth; (2) phosphorylation of Y785 activates phospholipase C-gamma (PLCγ), leading to generation of inositol 3-phosphate (IP3) and diacylglycerol (DAG), which results in the release of intracellular Ca^{2+} and activation of a protein kinase C (PKC)-regulated pathway that promotes synaptic plasticity; (3) phosphorylation at Y751 activates phosphatidylinositol 3-phosphate kinase (PI3K) and the Akt protein kinase, which promotes neuronal survival and its growth (Marlin and Li, 2015). Long-term activation of TrkA signalling via the ERK1/2 pathway upregulates the expression of multiple proteins and peptides implicated in pain, including receptors (TRPV1, P_2X_3, TrkA), neuropeptides (CGRP, SP), sodium ion channels subtype 1.8 or VGCC subtypes 3.2 and 3.3, which are transported to the peripheral terminals leading to enhanced excitability of the neuron fibres in peripheral sensory fields (Ji et al., 2002) (Mantyh et al., 2011). In contrast to ERK1/2, activation of PI3K and PLC cascades by NGF elicits a more immediate and local modulation of nociceptors (see 4.1.3) i.e., enhanced sensitivity to noxious stimuli. *In vitro*, neurotrophin-induced sensitisation of sensory neurons to CAP involves the delivery of newly TRPV1 from intracellular reserves to the cell surface and, to a lesser extent, by modulation of channels activity already located on the plasma membrane (Zhang et al., 2005) (detailed in Chapter 4). Accordingly, pre-treating sensory neurons with inflammation mediators such as TNFα or NGF enhances the currents elicited by CAP and intensifies the resultant increases of $[Ca^{2+}]_i$ (Meng et al., 2016), (Nugent et al., 2018), (Bonnington and McNaughton, 2003), (Zhang et al., 2005) and CGRP release. The neuropeptide interacts with adjacent immune cells, prompting them to release even more pro-inflammatory compounds that further enhance the activity of TRPV1 and other pain channels resulting in the amplification of nociceptive signals. Such enhanced excitability of the sensory neurons underlies the

phenomenon named peripheral sensitisation (Bingham et al., 2009), (Campbell and Meyer, 2006) (Iyengar et al., 2017).

Continuous activation of the sensory neurons also increases neurotransmission to second-order neurons in the dorsal horn causing central sensitisation, a state in which the activation threshold of the neurons in the spinal cord is decreased. This results in an enhanced sensitivity in both injured and non-injured regions (Iyengar et al., 2017). Attenuation of inflammation-induced peripheral sensitisation may be tractable for analgesic intervention if selective inhibitors of these pathways can be developed. Several *in vivo* and preclinical studies investigated antagonising effect of NGF or its receptors to attenuate the neuronal sensitisation. Such treatment showed positive effect on pain relief; however, serious side effects were also documented. Limitations and suggestions for alternatives to this approach are described in Chapter 4.

1.2 CGRP is a pain mediator

1.2.1 CGRP and its receptor

CGRP is a neuropeptide consisting of 37 amino acids that plays a vital role in cardiovascular, digestive, and sensory functions. It has two isoforms, α and β, with comparable biological activity and small differences in potency. α-CGRP is found primarily in the PNS, specifically in small- and medium-diameter cells of the TG (and DRG), which are considered as nociceptors. β-CGRP is mostly synthesised in the enteric nervous system, pituitary gland, and immune cells (Russell et al., 2014), (Iyengar et al., 2017). In the cell bodies of sensory neurons, CGRP is synthesised as part of a larger pro-peptide that is cleaved into the active α or β form and packed into LDCVs where it is stored (Carmine Belin et al., 2020). Upon stimulation of sensory fibres (for example, activation of TRPV1 channels or depolarisation) the neuropeptide is released from its storage by regulated exocytosis (Meng et al., 2007), (Meng et al., 2009). In addition, it can be released through a Ca^{2+}-independent mechanism, which is mediated by the activation of acid-sensitive ion channels (Durham and Masterson, 2013), or by secretion from the cell body to auto-amplify CGRP signalling and activate surrounding neurons and glia.

CGRP acts on a group of G protein-coupled receptors that are composed of three subunits and interact with $G\alpha_s$(Fig. 1.5); (i) a seven transmembrane domains calcitonin receptor-like receptor (CLR), which directly interacts with the $G\alpha_s$ subunit (Iyengar et

al., 2017), (ii) a single transmembrane domain protein called the receptor activity-modifying protein 1 (RAMP1) that is involved in the translocation of the receptor complex to the plasma membrane and facilitates specificity for binding with CGRP, and (iii) receptor component protein (RCP), that interacts with both CLR and RAMP1 to facilitate CGRP binding and signal transduction. Note that CLR can also dimerise with RAMP2 or RAMP3, producing receptors for amylin and adrenomedullin, respectively, but the complex CLR/RAMP1 has the highest affinity for CGRP.

The binding of CGRP with its receptor activates adenylate cyclase and results in elevated intracellular levels of cyclic adenosine monophosphate (cAMP), which in turn activates protein kinase A (PKA). This leads to a phosphorylation of multiple downstream targets and physiological responses, such as neuronal excitability, neurotransmitter release, relaxation of vascular smooth muscle and vasodilation. In addition, CGRP promotes mast cells degranulation (in rats), and activation of glial satellite cells, resulting in the release of nitric oxide, and sensitisation of nociceptors. Collectively, these effects all contribute to neurogenic inflammation and peripheral sensitisation (Iyengar et al., 2017). The neuropeptide is also secreted at the spinal synapse between peripheral nociceptors and second-order neurons, thereby exciting them and promoting central sensitisation.

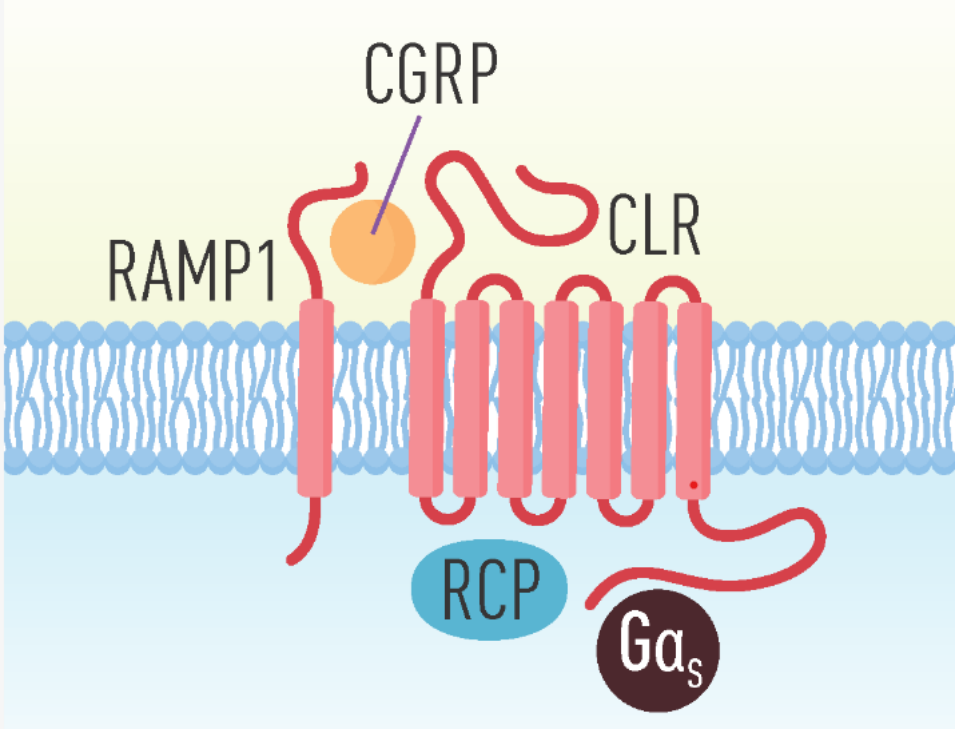

Figure 1.5 Schematic representation of a CGRP receptor

The CGRP receptor complex is comprised of three components: (1) RAMP1 with a single transmembrane domain, which confers specificity for binding with CGRP, (2) CLR with seven transmembrane domains and coupled to $G\alpha_s$ protein, and (3) RCP, which plays a crucial role in signal transduction by enhancing the effective coupling to the $G\alpha_s$ protein. The illustration is taken from (Carmine Belin et al., 2020).

1.2.2 The role of CGRP in pain signalling and migraine pathogenesis

The wide expression of CGRP in nociceptors suggested a role in pain signalling. Interestingly, in rodents and humans, subcutaneous injection of CGRP alone induces minor changes in the sensitivity to mechanical or thermal stimulation (reviewed in (Russell et al., 2014)). However, under conditions of abnormal pain processing, such as those that occur during inflammatory or neuropathic pain states, the role of CGRP in pain becomes more significant. For example, in the carrageenan inflammatory pain model, CGRP-KO mice exhibit a reduced sensitivity to noxious heat and mechanical stimulation compared to wild type animals (Zhang et al., 2001). Moreover, CGRP-KO rodents have been found to exhibit reduced sensitisation of spinal cord neurons in response to nociceptive stimuli suggesting that CGRP modulates synaptic plasticity in the CNS that contributes to pain processing [reviewed in (Russell et al., 2014), (Iyengar et al., 2017)]. Finally, CGRP antagonists inhibited hyperalgesia in rodents caused by intraplantar injection of capsaicin and carrageenan, suggesting that CGRP is involved in the development of inflammation-induced thermal and mechanical hyperalgesia (Russell et al., 2014).

Based on the abundance of CGRP in the sensory fibres of the trigeminovascular system, especially in those innervating the meninges (which comprise three layers of membranes that cover and protect the brain and spinal cord), it has been suggested that this neuropeptide is implicated in migraines and other primary headaches. The mechanism of action of the neuropeptide in the disease pathogenesis is not fully understood, but it is proposed that CGRP causes dilation of meningeal blood vessels, promotes neurogenic inflammation, and sensitises nerve fibres. All these factors can contribute to the development of a migraine headache. Clinical studies have demonstrated that CGRP levels are increased in blood, saliva, and cerebrospinal fluid during migraine attacks. Moreover, infusion of CGRP into rats and humans induced migraine-like behaviour and symptoms, respectively. On the other hand, anti-CGRP treatments, such as monoclonal antibodies to the neuropeptide (Fremanezumab, Galcanezumab) or its receptor (Erenumab), and CGRP receptor antagonists (Ubrogepant), have proven

efficacy in migraine prophylaxis and treatment. However, because CGRP and its receptors are expressed widely throughout the body, long-term antagonism can lead to serious side effects [reviewed in (Ray et al., 2021), (Edvinsson et al., 2018)].

1.3 Botulinum neurotoxins enter sensory as well as cholinergic neurons and block neurotransmitter release

1.3.1 Botulinum neurotoxins: structure and mechanism of action

Regulated exocytosis is sensitive to the botulinum neurotoxins (BoNTs) - bacterial di-chain proteins produced by bacteria called *Clostridium botulinum*. By immunogenicity, these were originally classified into seven serotypes, termed A-G. Thanks to modern sequencing techniques, it has been realised that each serotype class contains multiple sub-types. Chimeras (or mosaic) toxins composed of sequences derived from two different serotypes and new variants, such as BoNT/X, have also been discovered (Zhang et al., 2017). Each BoNT is comprised of a light chain (LC, 50 kDa), having a Zn^{2+} dependent-proteolytic activity, which is linked by a disulphide and non-covalent bonds to a heavy chain (HC, 100 kDa) (Fig. 1.6 A, B). The C terminus of the HC (H_C) consists of two sub-domains, H_{CN} and H_{CC} (both ~25 kDA each), involved in the binding to receptor components on susceptible cells. The N terminus of the HC (H_N, 50 kDa) is referred to the translocation domain (Fig. 1.6 A, B) because it is required for the delivery of the enzymic LC to the cytosol where its substrates are located (Rossetto et al., 2014).

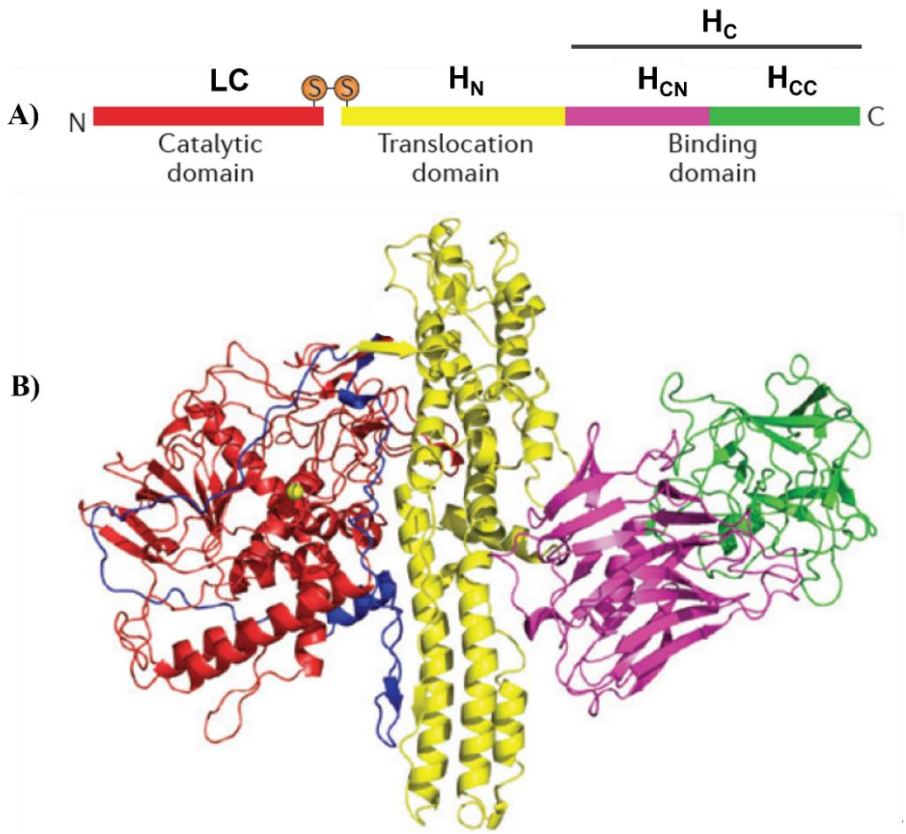

Figure 1.6 Structure of BoNT/A

(A) Schematic representation and (B) crystal structure of BoNT/A (PDBcode; 3BTA). The same colour scheme applies to both (A) and (B). The proteolytic LC is shown in red, the binding subdomain H_{CC} in green, H_{CN} (function is unknown) in pink, and translocation domain H_N in yellow constitute the toxin's HC. The LC is linked to the H_N by a disulphide bond represented by the S-S symbol. The illustration is taken and modified from (Rossetto et al., 2014)

H_C of BoNTs binds to high-affinity acceptors: bipartite entities composed from polysialogangliosides and luminal domains of synaptic vesicle proteins, synaptic vesicle protein 2 (SV2) or synaptotagmin (Fig. 1.7 (1)). After binding to the presynaptic membrane, the BoNTs are endocytosed into a vesicle (Fig. 1.7 (2)). When endocytotic vesicles are formed in this way, a proton pump acidifies the lumen. The resulting disequilibrium in H^+ concentrations across the vesicular membrane creates a proton motive force that is exploited by molecular transporter proteins to load the vesicle with neurotransmitters. However, the acidic interior of the vesicle also elicits changes in the conformation of the H_N. Thus activated, the H_N embeds into the synaptic vesicle membrane, and forms a pore (Fig. 1.7 (3)) through which the LC is translocated into neuronal cytosol where it can access and cleave its substrate (Fig. 1.7 (4)); hence, the H_N is often referred to as the translocation domain. Substrates of various BoNT serotype LC proteases are illustrated in Fig. 1.7 B (Breidenbach and Brunger, 2005).

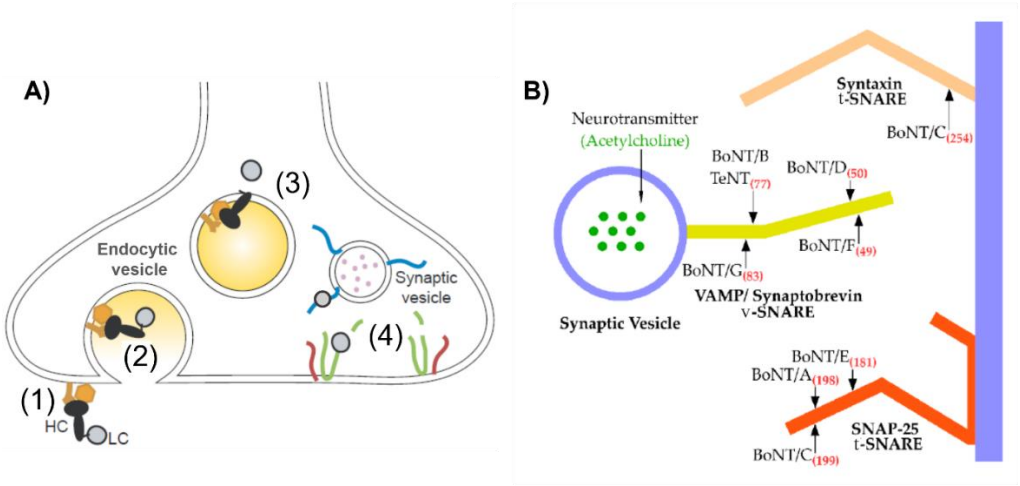

Figure 1.7 Proposed mechanism for the internalisation of BoNTs, and identities of their LC targets in neurons

(A) (1) BoNT, comprised of LC and HC, binds to acceptors on the surface of nerve terminals and enters (2) the neurons by endocytosis. The endosome lumen is acidified by a proton pump and this internal environment promotes translocation of the proteolytic LC to the cytosol. (3) In the neutral pH of the cell cytosol, the LC de-taches from the HC by reduction of disulfide bound. This releases and activates the LC metalloprotease activity. (4) The liberated LCs target and very specifically cleave their SNARE substrates, as indicated in (B). SNAP-25 is cleaved by BoNT/A, /C, and /E at different peptide bonds. In addition to SNAP-25, /C also cleaves syntaxin-1. Both syntaxin-1 and SNAP-25 are located on plasmalemma and are often referred to as target SNAREs (t-SNARE). Serotypes /B, /D, F, and /G cleave VAMP1/2 which is present on synaptic vesicles, and is therefore known as a vesicle SNARE (v-SNARE). Red digits in brackets indicate the amino acid number of the P' scissile bond cleavage by the indicated BoNT serotype. The illustration in (A) was taken and modified from (Breidenbach and Brunger, 2005) and (B) is taken from (Gardner and Barbieri, 2018).

1.3.2 BoNTs are candidates for chronic pain treatment

The ability of the BoNTs to block exocytosis has been exploited for therapeutic benefit in movement disorders, primary hyperhidrosis, and detrusor overactivity. However, it was noticed by clinicians that patients who received an intramuscular injection of the toxin to treat cranio-facial dystonia experienced pain relief too. This could even occur before the muscle relaxation, suggesting that BoNT/A might have an additional independent analgesic effect. Based on the efficacy of BoNT/A for suppressing excessive acetylcholine release at overactive neuromuscular junctions, it was suggested that it might also reduce the release of neuropeptides and neurotransmitters that are increased in chronic pain conditions.

In large, double-blind randomised, placebo-controlled clinical studies, injections around the forehead of onabotulinumtoxinA (a complex of BoNT/A and haemagglutinins; trade name BOTOX®) was demonstrated to reduce the frequency of headaches for chronic migraine patients [reviewed by (Burstein et al., 2020)]. (Aurora et

al., 2010), (Diener et al., 2010), (Dodick et al., 2010). The FDA approved the use of onabotulinumtoxinA for chronic migraine in patients experiencing the symptoms for more than 15 days per month. Follow up studies reported that patients who respond well to BOTOX® display higher serum levels of CGRP prior to treatment than non-responders, and after the treatment serum levels were significantly reduced in responders only (Cernuda-Morollón et al., 2015). However, even in responders, the frequency and severity of migraine attacks are only partially reduced (Dominguez et al., 2018), (Khalil et al., 2014).

1.3.3 BoNT chimeras developed in ICNT

The limited effectiveness of BoNT/A in pain attenuation in some patients is still not understood. One theory arose from observations that BoNT/A was unable to abolish CGRP release from TGNs *in vitro* if it was stimulated by activation of TRPV1 channels by 1 μM CAP (Meng et al., 2007), which induces a large and sustained elevation of $[Ca^{2+}]_i$. The product of SNAP-25 proteolysis by BoNT/A ($SNAP\text{-}25_A$) retains the ability to form stable SNARE complexes and facilitate the release of CGRP (Meng et al., 2009). Thus, it is possible that severe migraine attacks could be refractory to BoNT/A if the excessive stimulation of sensory fibres during migraine attacks can induce such large and sustained increases in $[Ca^{2+}]_i$ *in vivo*.

Advantageously, another serotype, BoNT/E, removes a larger peptide fragment from the C-terminus of SNAP-25 (26 residues, whereas BoNT/A cleaves off only 9). Moreover, LC/E is more potent and cleaves its substrate faster than LC/A (Wang et al., 2008a). However, TGNs are insensitive to BoNT/E, probably because of the lack of acceptors for this toxin (Wang et al., 2008a). To overcome this inability of BoNT/E to bind and enter sensory neurons, a chimera BoNT/EA was developed in ICNT by fusing protease (LC) and translocation (H_N) domains of /E to the receptor-binding (H_C) domain of /A (Fig. 1.8). Despite only cleaving a similar fraction of SNAP-25 as /A, BoNT/EA effectively blocked 1 μM CAP-evoked CGRP release (Meng et al., 2009). Unfortunately, the proteolytic activity of /EA appeared to be very short-lived compared to that of BoNT/A (Wang et al., 2008a). Thus, a variant LC/E-BoNT/A was created in which the powerful LC/E protease was stabilised by attachment to full length BoNT/A (Fig. 1.8). Importantly, this LC/E-BoNT/A chimera was effective in inhibiting CAP-induced CGRP exocytosis *in vitro* and also proved more successful than BoNT/A for attenuation of

mechanical and cold hypersensitivity in a model of neuropathic pain in rats (Wang et al., 2017). Importantly, a single injection produced a long-lasting reduction in hypersensitivity, and was prolonged even further (up to 20 days) by a second intraplantar administration of LC/E-BoNT/A (Wang et al., 2017).

BoNT/D cleaves another member of the SNARE complex, VAMP1/2/3, and inhibits CGRP release evoked by high K^+ and CAP (Meng et al., 2007). Despite the toxin's acceptor SV2 are also found in humans, the studies in human muscles showed no effect of the toxin on neuromuscular transmission (Coffield et al., 1997), (Eleopra et al., 2013); therefore, chimera BoNT/DA, comprised of proteolytic and translocation domain from /D and acceptor binding domain of /A (Fig. 1.8), was created for pre-clinical evaluation of its therapeutic potential.

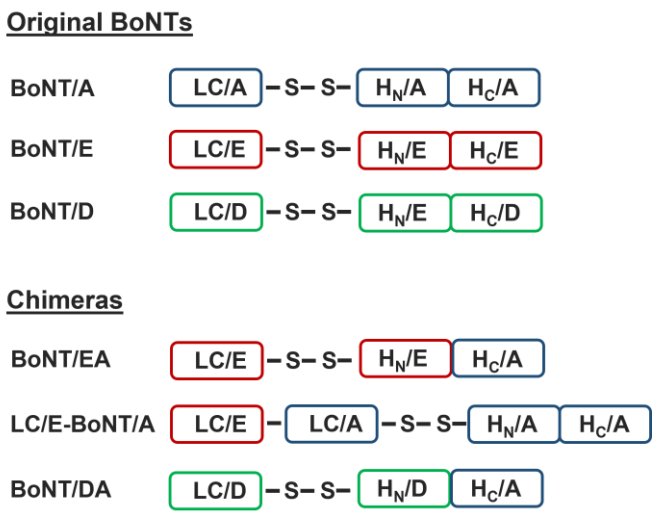

Figure 1.8. Diagram of BoNT/A, BoNT/E, BoNT/D, and chimeras created by gene recombination and expression in *E. coli.*
Rectangles represent light chain (LC), binding (H_C) and translocation (H_N) domains of toxins; S-S indicates di-sulphide bonds between LC and H_N.

1.4 Project aims and objectives

A better understanding of the link between the intensity of nociceptors' excitation by activation of TRP channels, changes in intracellular $[Ca^{2+}]_i$, and evoked CGRP release could aid the development of more effective BoNT-based analgesic therapeutics. To this purpose, the major aim of the study was to investigate *in vitro* the inhibitory effect of BoNT variants on CGRP regulated exocytosis evoked from sensory neurons by concentration ranges of agonists of TRPV1 and TRPA1, representing noxious stimulation of distinct intensities. Moreover, these channels can be potentiated by pro-inflammatory

compounds such as NGF and deciphering the role of SNAREs in this process will bring awareness of the molecular basis of nociceptor sensitisation.

To achieve these aims, the following facets needed to be explored. First, in a view of the partial analgesic effect of BoNT/A in patients with CM, it was necessary to investigate the efficacy of BoNT/A for reducing the amounts of CGRP released in response to a range of [CAP] or [AITC]. Taking advantage of cultured sensory neurons facilitated the quantification of released neuropeptide by ELISA and the monitoring of $[Ca^{2+}]_i$ by confocal microscopy in control cells and in those pre-treated with BoNT/A. Use of LC/E chimeras that truncate a larger SNAP-25 C-terminal fragment than /A, or BoNT/DA which proteolyses VAMP1/2/3, facilitated investigations into the involvement of SNARE-dependent exocytosis in the acute potentiation of TRPV1 and TRPA1 by pro-inflammatory factors, and the effectiveness of inactivating different SNAREs for blockade of these processes. NGF was chosen as an example pro-inflammatory factor because of its well established and important role in inflammatory pain development. Also, its acute effect on potentiation of TRPV1 has been established by electrophysiology and Ca^{2+} imaging in cultured DRGNs but whether it has similar effects on TRPA1 is poorly defined. The ultimate goal of the study is to identify the optimum properties for incorporation into BoNT/A-based chimeras for the alleviation of nociceptor sensitisation and attenuation of pain signalling.

2 Materials and Methods

2.1 Materials

2.1.1 2.1.1 Animals

Sprague Dawley rats were purchased from Envigo (formerly Harlan) and bred in an approved Bio-resources Unit in DCU. The experiments, maintenance and care of the rodents complied with the European Communities (Amendment of Cruelty to Animals Act 1876) Regulations 2002 and 2005. Experimental procedures had been approved on 1 May 2018 by the Research Ethics Committee of Dublin City University (DCUREC/2018/091).

2.1.2 Cell culture and related materials

Ca^{2+} and Mg^{2+}-free Hanks' balanced salt solution (CMF-HBSS), Dulbecco's Modified Eagle's Medium (DMEM), Percoll®, penicillin-streptomycin, poly-L-lysine, laminin, foetal bovine serum (FBS), cytosine arabinoside (ARA-C), Benzonase® nuclease (Merck Millipore) and bovine serum albumin (BSA) were purchased from Sigma-Aldrich. Bio-Sciences supplied collagenase I, Dispase®, B-27™ Supplement, 2.5S NGF, and 24 and 48-wells plates.

2.1.3 Antibodies

Table 2.1 List of primary antibodies

Antibody target	**Catalog number**	**Monoclonal (Mab) or polyclonal (Pab), raised in species indicated (immunogen epitope)**	**Supplier**	**Dilution (v/v) / concentration used**	
				Western blotting	**Immuno-fluorescence**
TRPV1	AB5566	Pab, guinea pig (C-terminus)	Millipore		1:500
TRPA1	ACC-037	Pab, rabbit (747-760 amino acids of human TRPA1)	Alonome		1:200

CGRP	ab81887	Pab, mouse (full length of the peptide)	Abcam		1:250
CGRP	C8198	Pab, rabbit	Sigma		1:500
Neurofilament 200 (NF200)	N4142	Pab, rabbit	Sigma		1:500
Neurofilament 200 (NF200)	N5389	Mab (clone NE14), mouse	Sigma		1:250
SNAP-25	SMI-81	Mab, mouse, binds to the full-length SNAP-25	Covance	1:3000	1:250
TrkA	06-574	Rabbit	Merck		1:500
Syntaxin-1	S0664	Monoclonal (clone HPC-1), mouse	Merck	1:2000	
phospo-ERK1/2	9101	Rabbit	Cell Signalling Technology	1:3000	
total ERK1/2	9102	Rabbit			
VAMP1/2/3	104102	Rabbit	Synaptic Systems	1:1000	
NGF	AN-240	Pab, rabbit (2.5 S mouse NGF)	Alomone	500 ng/ml (used for NGF deprivation from TGNs cultures)	

Anti-species secondary antibodies conjugated with:

- Alexa Fluor® (488, 555 or 633) were obtained from Invitrogen and used at 1:1000 dilution

- Alkaline phosphatase (AP) was purchased from Sigma and used at 1:10,000 dilution

2.1.4 Other reagents

Enzyme-linked immunosorbent assay (ELISA) plates were obtained from Bertin Technologies. Reagents for electrophoresis and Western blotting: lithium dodecyl sulphate (LDS) sample buffer, 12% Bolt™ Bis-Tris polyacrylamide gels, 3-(n-morpholino)propanesulfonic acid (MOPs) running buffer; pluronic F-127 acid, Fluo-4 AM were obtained from Bio-Sciences. Polyvinylidene fluoride (PVDF) membrane and Bio-Rad protein standards were bought from AccuScience.

2.2 Methods

2.2.1 Culturing of rat trigeminal ganglia neurons (TGNs)

2.2.1.1 Isolation and dissociation of TGNs

TG were dissected from 3 to 7 day-old Sprague Dawley rat neonates as described in (Malin et al., 2007) and kept in ice-cold CMF-HBSS. Before digestion, TGs were chopped into small pieces and spun at 170 x g for 5 min. at room temperature to pellet the ganglia pieces. Tissue was digested for 30 min. at 37 °C in 1:1 (v/v) mixture containing 1275 U collagenase I and 17.6 U Dispase®. 12.5 U of Benzonase® nuclease were added to the digesting solution to reduce clumping of the tissue, cells were gently agitated with a 2.5 ml Pasteur pipette, and then incubated at 37 °C for 15 min. After enzymatic digestion, the cell suspension was diluted with 10 ml of DMEM and centrifuged for 5 min. at 170 x g at room temperature. Pellets were re-suspended in 4 ml of DMEM and gently triturated through a 10 ml serological pipette until all tissue chunks were dissociated entirely. If some chunks remained upon visual inspection of the suspension, they were triturated several times through a 1 ml disposable plastic pipette tip (P1000).

2.2.1.2 Purification of TGNs using Percoll®

To separate neurons from non-neuronal cells, myelin and nerve debris, the dissociated cell suspension was centrifuged through a discontinuous Percoll® gradient, as described in (Eckert et al., 1997). The ionic strength of Percoll® stock solution was increased (to ~330 mOsm/kg, suitable for isolation of living cells) by the addition NaCl to a final concentration of 150 mM in Percoll® stock solution before being diluted with DMEM to make 30% and 60% (v/v) Percoll® solution. A 60/30 step gradient of Percoll® was prepared in two 15 ml conical tubes by layering 4 ml of 30% solution over 4 ml of 60%. Approximately 4 ml of dissociated cell suspension was layered on the top of the

Percoll® gradient and centrifuged at 1800 x g for 10 min. at room temperature. A mat of cellular debris formed above the 30% layer was carefully removed and set aside for further processing Before harvesting the 60/30 interface and 30% layer where most of the TGNs were enriched. However, a large minority of TG neurons were entrapped in the above-noted mat of debris, so to recover these this layer was dispersed in 4 ml DMEM and subjected to another round of centrifugation for 10 min. through a second Percoll® gradient. This time the mat of debris above the 30 % Percoll® layer was removed and discarded before harvesting the 60/30 interface and 30% layers. These were combined with the corresponding layers collected after the first round and the aggregate sample was then diluted and thoroughly mixed with DMEM to reduce the Percoll® concentration to ~10% before further centrifugation at 1800 x g for 5 min. The supernatant was discarded and the pelleted cells were retained.

2.2.1.3 Plating

After purification through Percoll® gradient, cell pellets were re-suspended in normal culture medium (Table 2.2). TGNs were seeded at a density of 20,000-30,000 neurons per well in 48-wells plates or 30,000-35,000 per glass coverslip (see 2.2.7) that had been pre-coated with poly-L-lysine (0.1 mg/ml) and laminin (20 µg/ml). An anti-mitotic drug, 10 µM of ARA-C, was added from day 1 to 5 in culture to suppress the growth of dividing (i.e., non-neuronal) cells. The medium was exchanged every day unless otherwise specified.

2.2.2 Treatment of cultured TGNs

2.2.2.1 NGF withdrawal from cultured TGNs

After two days *in vitro* (DIV), cells were washed 3 x with 0.5 ml per well with NGF-free medium (Table 2.2) and for the next two days, TGNs were maintained in starvation medium (Table 2.2). On DIV 4 cells were utilised to quantify resting and stimulated CGRP release under different experimental conditions.

Table 2.2 DMEM-based media used in TGNs culturing

Medium	Supplemented with:
Normal	10% (v/v) FBS, 1% (v/v) penicillin-streptomycin, 1% (v/v) B-27™ Supplement, and 50 ng/ml 2.5S NGF

NGF-free	10% (v/v) FBS, 1% (v/v) penicillin-streptomycin, 1% (v/v) B-27^{TM} Supplement, 10 μM ARA-C
Starvation	10% (v/v) FBS, 1% (v/v) penicillin-streptomycin, 1% (v/v) B-27^{TM} Supplement, 10 μM ARA-C, 500 ng/ml anti-NGF antibodies

2.2.2.2 Treatment of cultured TGNs with BoNTs

After 2-6 DIV, cultured TGNs were exposed for 24 or 48 h at 37 °C to BoNT/A, BoNT/EA, LC/E-BoNT/A or BoNT/DA in 0.2-0.25 ml normal culture medium or starvation medium (2.2.1.3 and 2.2.2.1 respectively), at concentrations indicated on Figure legends. When experiments involved incubation with the toxins for 48 h, rather than replacing the medium as usual after the first 24 h an additional 0.3 ml of normal medium (lacking BoNT) was added to the wells and the cells were returned to 37 °C for the remaining 24 h. Thus, the concentration of BoNT was reduced ~3-fold for the second 24 h of these experiments but the original concentrations applied are the values described in Figures and text. Control cells were exposed to normal medium lacking BoNT, but were otherwise treated in the same way. Before release experiments, the unbound BoNTs were removed by subsequent washing with 3 x 0.5 ml HEPES buffered saline (HBS) (see below). After release assay (described in 2.2.2.3), treated and control cells (one well per group) were lysed in 0.06 ml of 1x sulphate LDS sample buffer, heated at 95°C for 5 min. and subjected to sodium dodecyl sulphate-polyacrylamide gel electrophoresis (SDS-PAGE) and Western blotting as described in 2.2.4 to quantify the % of SNAP-25 cleavage.

2.2.2.3 Incubation of TGNs to monitor CGRP release

After 4-7 DIV the medium was gently aspirated from TGNs, and 0.25 ml of HBS (mM: 22.5 HEPES, 135 NaCl, 3.5 KCl, 1 $MgCl_2$, 2.5 $CaCl_2$, 3.3 glucose, and 0.1% (w/v) BSA, pH 7.4) was added into each well, followed by 30 min. incubation at 37 °C. The sequence of incubations included a first 30 min. period with HBS for the quantification of spontaneous release and a subsequent 30 min. incubation with CAP, AITC or 60 mM KCl modified HBS (HBS-HK, mM: 22.5 HEPES, 78.5 NaCl, 60 KCl, 1 $MgCl_2$, 2.5 $CaCl_2$, 3.3 glucose, and 0.1% (w/v) BSA, pH 7.4). Some experiments involved more complex multi-step experimental manipulations and these are indicated schematically in the relevant figures and detailed in the associated legends.

For stimulation of TRPV1 or TRPA1, 1000x working concentration stocks of the requisite agonists, CAP and AITC were prepared in ethanol and dimethyl sulfoxide (DMSO), respectively. Working solutions were prepared by 1000-fold dilution of the latter stocks into HBS. For solvent control purposes, 0.1% (v/v) ethanol or DMSO was added to HBS lacking CAP or AITC, respectively, and used for the estimation of spontaneous release. In experiments that included a period of incubation with NGF, it was added to HBS from a 0.1 mg/ml stock solution of the neurotrophin in DMEM. For the quantitation of Ca^{2+}-independent release evoked by NGF, CAP or AITC, a modified HBS was used with $CaCl_2$ being replaced by 2 mM EGTA. After the requisite incubation periods, all the cell-bathing solution was aspirated from the cells and centrifuged for 1 min. 20,000 × g at 4 °C to remove non-solubilised matter, and the supernatant fractions were stored frozen (-20 °C) until being assayed for CGRP content. To measure intracellular CGRP, at the end of each experiment the cells were lysed with a solution of 1% Triton X-100 in HBS on ice for 10-15 min. and triturated through a 1 ml pipette (P1000) 3-4 times. The lysates were centrifuged for 1 min. 20,000 × g at 4 °C to remove non-solubilised matter. The supernatants (soluble cell lysates) were stored at -20 °C before CGRP quantification by ELISA.

2.2.3 Quantification of CGRP release by ELISA

To determine the amounts of CGRP released from the TGNs and that present in soluble cell lysates, 0.1 ml sample aliquots or standards were subjected to ELISA using commercially available kits (Bertin Technologies, A05482). The assay is based on the double-antibody sandwich technique and detects CGRP in the range of 8-500 pg/ml. The 96-wells plate provided with the kit are coated with monoclonal antibodies specific for CGRP. These antibodies bind to CGRP in the samples, trapping the neuropeptide on the plate. Some wells are incubated with known amounts of a standard CGRP sample (provided with the kit) so that a standard curve can be plotted that enables the determination of the amounts of CGRP in test samples. CGRP trapped on the plates is detected by a second antibody that binds to a different epitope of the neuropeptide and is conjugated with acetylcholinesterase (AchE). After dilution to working concentration, the solution of conjugated-antibody was added to each well before overnight incubation 4 °C. The next day the solution containing unbound antibodies was removed and wells extensively washed before the amount of immobilised CGRP was determined by adding an AchE substrate (Ellman's reagent) that develops into a colourimetric product in the

presence of the enzyme. For this, the plate was incubated in the dark with gentle agitation in an orbital shaker. Importantly, the assay is temperature-sensitive, so all manipulations were performed at 20-23 °C. The final product of the enzymic reaction is 5-thio-2-nitrobenzoic acid, which is bright yellow colour that can be quantified by measuring the absorbance at 405-420 nm. Readings were performed using a Techan microplate reader at 405 nm after 30-90 min. incubation until the readings of the highest standard (500 pg/ml) reached 1 absorbance unit. The intensity of the yellow colour, which was determined spectrophotometrically, is proportional to the amount of the CGRP present in the well. Every time the assay was performed, a standard curve was plotted for the known CGRP samples and a best-fit line through the points drawn using GraphPad Prism 9 (GraphPad Software, San Diego, CA, USA) software; this was used to determine the concentration of CGRP in experimental samples. If samples produced readings that were out of the standard curve range, they were re-analysed by repeating the ELISA after appropriate dilutions.

2.2.4 SDS-PAGE and Western blotting

2.2.4.1 SDS-PAGE

Protein samples were mixed with Bolt™ 1x LDS sample loading buffer (Novex, B008) and heated at 95 °C for 5 min. Prepared samples were loaded onto precast 12% Bolt™ Bis-Tris sodium dodecyl sulphate-polyacrylamide gels (Novex, NW0012A). Proteins were separated by electrophoresis run at 180 volts at room temperature using MOPS running buffer (Novex, B0001) until proteins were separated according to their molecular masses, as indicated by loading a control lane with pre-stained protein markers (BioRad, 161-0373).

2.2.4.2 Western blotting

Proteins to be subjected to Western blotting were resolved by SDS-PAGE (described in 2.2.4.1) before electrophoretic transfer to PVDF membranes by the semi-dry method, using a Pierce™ power blotter (Thermofisher). Prior to transfer, the PVDF membranes were pre-wetted in methanol and equilibrated in a 1-step transfer buffer (Thermofisher, 84731). The transfer was performed according to the manufacturer's prescribed protocol. Then, non-specific binding sites on membranes were blocked by incubation for 60 min. in TBST buffer (50 mM Tris, 150 mM NaCl, 0.1% (v/v) Tween-20, pH 7.6) containing 3% (w/v) BSA. The membrane was then exposed to specific

primary antibodies diluted (see Section 2.1.3) in the same TBST containing 3% (w/v) BSA for either 1 h at room temperature or overnight at 4 °C with gentle agitation. Unbound primary antibodies were removed by 3 x 10 min. wash periods with TBST. Membranes were exposed to the species-specific secondary antibodies conjugated with alkaline phosphatase (AP, see section 2.1.3) in TBST for 1 h at room temperature with agitation. Unbound secondary antibodies were removed and the PVDF subjected to 3 x 10 min. washes with TBST, then membranes were equilibrated for 5 min. in AP buffer (mM: 100 Tris, 100 NaCl, 5 $MgCl_2$, pH 9.5). To reveal bound antibodies, the PVDF membranes were then exposed to AP buffer containing the AP substrates 5-bromo-4-chloro-3-indolyl-phosphate (50 mg/ml) and nitroblue tetrazolium chloride (10 mg/ml) to develop a colour product. Digital images of immuno-labelled bands were photographed using a G: BOX Chemi-16 digital camera and saved as TIFF or JPEG files.

2.2.4.3 Densitometric quantification

Densitometric analysis of digitised images following Western blotting was performed using Image J software. Pixel intensities were calculated using the gel analysis tool. Data collected from several independent experiments were processed and plotted using GraphPad Prism 9.

2.2.5 Immuno-cytochemistry

TGNs were grown for the periods indicated in Figure legends on round glass coverslips (diameter 9 or 13 mm) coated with poly-l-lysine and laminin as in 2.2.1.3. Prior to immuno-labelling, the cells were washed once with 1 ml of pre-heated Dulbecco's phosphate-buffered saline (DPBS) for 1 min. All subsequent procedures were performed at room temperature, unless otherwise specified. The samples were fixed for 30 min. with 3.7% paraformaldehyde in DPBS. The cells were then washed with DPBS three times (for 1 min. each time), and then permeabilised with Triton X-100 detergent by incubation in antibodies dilution buffer [AbD: 0.5% (v/v) Triton X-100, 0.1% (w/v) BSA in DPBS] for 15 min. before blocking non-specific binding sites by incubation with 10% (v/v) normal donkey serum (Sigma) in AbD for another 30 min. Primary antibodies were applied in AbD at concentrations indicated in section 2.1.3 and left for 2 h. Some coverslips were exposed to AbD only (to serve later as control samples for testing the specificity of the secondary antibodies). Unbound primary antibodies were removed by 5 times washing with antibodies wash buffer (AbW: 0.1% (v/v) Triton X-100 in DPBS)

prior to being exposed to species-specific immunoglobulin binding secondary antibodies conjugated with Alexa Fluor® (see section 2.1.3) in AbD for 1 h. After the latter period, the cells were extensively washed (5 times for 2 min. with AbW and then once with water). To stain nuclei, Hoechst 33342 (1:1,000 v/v in water) was applied for 1 min. and then cells were rinsed again with water for another minute. Stained coverslips were mounted with ProLong™ Glass Antifade Mountant (Thermo Fisher Scientific) and imaged on a confocal microscope (Zeiss Observer Z1-LSM710). Images were acquired through 20 or 40X oil objectives (EC Plan-NEOFLUAR20x/0.5 NA or EC Plan-NEOFLUAR40x/1.3 NA, respectively) using Zen Black 2.3 software (Carl Zeiss, Oberkochen, Germany). Before recording, confocal settings were adjusted such that no Alexa Fluor® signal was observable in control coverslips (i.e., in cells exposed only to the secondary antibodies). The images were recorded in phase contrast and fluorescence mode, where fluorophore of the secondary antibodies was excited by laser at wavelength appropriate for the conjugated fluorophore(s). Emitted fluorescence was captured by a photomultiplier. Micrographic images were constructed for analysis using software supplied by the microscope manufacturer and were saved as a separate TIFF.

2.2.6 Protein quantification by bicinchoninic acid assay

Protein concentrations were determined using a bicinchoninic acid (BCA) protein assay kit, by reference to standard solutions of BSA. TGNs were lysed in 0.25 ml HBS supplemented with 1% (v/v) Triton X-100 on ice for 10-15 min. and 0.25 ml of each sample or BSA standard were applied to a 96 microplate; 0.2 ml mixture of reagent A and B (50:1) prepared on the day of use supplied in the kit were added to each well. The plate was mixed thoroughly and incubated for 30 min. at 37°C before absorbance at 562 nm was read on a spectrophotometer. Concentrations in test samples were calculated by reference to a best-fit line (generated in GraphPad Prism 9) through the readings for different amounts of BSA standard.

2.2.7 Intracellular Ca^{2+} imaging and analysis of fluorescence intensities

TGNs prepared and cultured as described in 2.2.1 were plated on 13 mm diameter round glass coverslips coated with poly-L-lysine and laminin as described in 2.2.1.3. After 4 DIV, cells were washed with HBS supplemented with a low concentration of BSA (10 µg/ml, HBS-LB) and loaded with 3 µM Fluo-4 acetoxymethyl ester (Fluo-4 AM) in the presence of 0.02% pluronic F-127 acid (facilitates the solubilisation of the

dye in aqueous solutions) for 20-30 min. at 37 °C. Cells were then placed in a superfusion chamber [90 µl/mm (volume per depth), RC-25; Warner Instruments, Holliston, MA, USA] mounted on the stage of a Zeiss LSM710 confocal microscope and left for 10 min. with 2 ml/min continuous perfusion with HBS-LB to equilibrate. Confocal imaging was performed at ambient temperature (22-26 °C) using a 488 nm argon laser and 20x magnification objective (EC Plan-NEOFLUAR20x/0.5 NA) at 0.33 Hz frame rate. Baseline fluorescence was recorded for 5-6 min. before switching to HBS-LB containing CAP or AITC, which was added from 1,000x stock solutions prepared in ethanol or DMSO on the day of use. Recordings were continued in the presence of agonist for 30 min. In some experiments control recordings were performed with a vehicle (HBS-LB containing 0.1% (v/v) ethanol, specified in the Figure legend). At the end of each experiment, after washing out the AITC or CAP, TGNs were stimulated with 100 mM KCl in HBS-LB (mM: 22.5 HEPES, 38.5 NaCl, 100 KCl, 1 $MgCl_2$, 2.5 $CaCl_2$, 3.3 glucose, and 10 µg/ml BSA, pH 7.4) to determine the total number of excitable Fluo-4 AM loaded TGNs in the image field. The intensities of recorded fluorescence signals (F) were analysed offline. Regions of interest (ROIs) were applied to individual TGN somata, and F was measured for each ROI in every frame of the video recordings using the average pixel intensity tool in Image J (version 1.53e, National Institutes of Health, USA). Values were exported to Microsoft Excel® (Office 365, Microsoft Corporation, St Redmond, WA, USA) for further analysis. Measurements for time points recorded during the first 5-6 min. were averaged to determine initial fluorescence intensity (F_0) and the standard deviation (s.d.) in this baseline signal over this period. Changes in fluorescence intensity (F) relative to initial values (F_0) were calculated for every time point using the formula $(F-F_0)/F_0$. ROIs that exhibited an increase of fluorescence such that $(F-F_0)/F_0$ was greater than F_0 plus 10x s.d. were considered to be responders. Mean $(F-F_0)/F_0$ values and the standard error of the mean (s.e.m.) were determined for each time point by averaging of the signals from all responders and plotted against elapsed time using GraphPad Prism 9. The area under the curve (AUC) of traces generated for each [AITC] or [CAP]/vehicle were determined using the tool available in the GraphPad program (Belinskaia et al., 2022).

2.2.8 Recombinant BoNTs production

Recombinant BoNTs were created by Dr. Jiafu Wang, expressed and purified by Dr. Seshu Kumar Kaza (LC/E-BoNT/A) or Dr. Wang (BoNT/DA and /EA). A detailed

description of the production process is given in (Wang et al., 2008a), (Wang et al., 2017). Briefly, the steps involved were:

2.2.8.1 Gene cloning

To create an expression vector containing the nucleotide sequence encoding LC/E-BoNT/A, genes for LC/E and BoNT/A were cloned into the pET29a vector that contains a C-terminal sequence of six histidine (His) named $(His)_6$-tag that is fused to the novel protein (Fig. 2.1). Likewise, to create $(His)_6$-tagged BoNT/EA or /DA, a DNA fragment encoding the binding domain of BoNT/A (Hc/A) was ligated to a sequence encoding either the LC plus the translocation domain of BoNT/E (LC-H_N/E) or /D (LC-H_N/D), respectively, and cloned into the pET29a vector. Note that DNA encoding short peptides for binding and cleavage by human thrombin were inserted into the coding sequences for LC/E-BoNT/A and BoNT/EA; in both cases, two thrombin consensus sequences were inserted, one of them in an exposed loop to facilitate nicking (see below) and the other just before the $(His)_6$-tag to facilitate its removal from the purified protein.

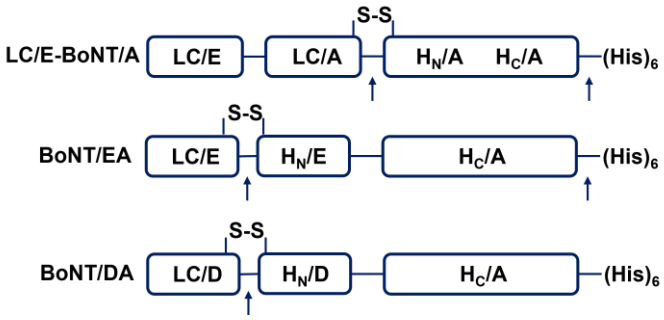

Figure 2.1 Schematic representation of engineered BoNT chimeras LC/E-BoNT/A, BoNT/EA, and BoNT/DA

Rectangles represent light chain (LC), binding (H_C) and translocation (H_N) domains of toxins; S-S and arrows indicate the inter-chain disulphide bond and consensus sites for thrombin (LC/E-BoNT/A) or trypsin (/EA and /DA) cleavage, respectively; $(His)_6$ represent sequence of six histidine. The illustration modified from (Wang et al., 2017), (Wang et al., 2008a), and (Belinskaia et al., submitted to Intl J Mol Sci).

2.2.8.2 Bacterial expression

Sequence-verified plasmids were transformed into *E.coli* for the expression of the $(His)_6$-tagged proteins as single-chain (SC) polypeptides., Transformed bacteria were grown initially at 37 °C in an auto-induction medium (Studier, 2005) so that transgene expression is induced automatically when glucose levels expire; when the optical density of the culture at 600 nm (OD_{600}) reached 1 absorbance unit, the temperature was reduced to ~22 °C, which proved optimal for the expression of functional recombinant protein.

After a suitable expression period (usually 16-20 h), when the OD_{600} stopped rising, bacteria were harvested by centrifugation. The pelleted cells were resuspended in lysis buffer (20 mM HEPES, 300 mM NaCl, pH 8) then were ruptured with lysozyme and 1 to 2 freeze-thaw cycles. The crude lysate was centrifugated again to remove insoluble matter and a DNAse (Benzonase®) was added to break down DNA, which interferes with the process for purification of the recombinant protein (see below).

2.2.8.3 Protein purification

Tagged BoNTs were purified from the clarified soluble cell lysates by immobilised metal-ion affinity chromatography (IMAC) on Talon® resin charged with Co^{2+}, which takes advantage of a strong interaction between the $(His)_6$-tag and cobalt ions to retain the SC in the column. After passing the lysate through the column by gravity-induced flow, the resin was washed with a low concentration of imidazole (5-10 mM in lysis buffer) to dislodge weakly bound proteins from the resin. Then the protein of interest was eluted with a higher concentration of imidazole (250 or 500 mM imidazole in lysis buffer) and collected in fractions. The protein amounts in each fraction were quantified by BCA assay and the fractions containing protein were analysed by SDS-PAGE followed by Coomassie staining. Those fractions containing the recombinant protein of interest were pooled, buffer exchanged using gel-filtration columns. If necessary, proteins were subjected to ion-exchange chromatography (IEX) to remove impurities (Wang et al., 2017), (Wang et al., 2008a).

2.2.8.4 Nicking

As stated before, the recombinant BoNTs were expressed as SC polypeptides. These are pre-proenzymes and the first step of their activation requires the restricted proteolysis (or 'nicking') of one or more peptide bonds in an exposed loop between two cysteine residues that are directly linked to each other by a disulphide bond. Hence, such nicking creates a di-chain (DC) structure of two polypeptides linked by a disulphide bridge. These DCs are fully activity in terms of neurotoxicity. Nicking was achieved by limited exposure to trypsin (BoNT/EA) or thrombin (that cleaved at two engineered sites, as described above). Conversion from SC to DC was monitored by SDS-PAGE in the presence of reducing agent (50 mM dithiothreitol), which severs the disulphide bond, followed by protein staining with Coomassie Blue dye; if necessary, incubation periods with trypsin or thrombin were extended until at least 99% of the SC had been converted to DC. Removal of $(His)_6$-tags was confirmed by SDS-PAGE followed by electro-

transfer of separated proteins to PVDF membrane and Western blotting with anti-$(His)_6$-tag antibodies followed by alkaline phosphatase conjugated secondary antibodies; a sample of un-nicked SC was used as a $(His)_6$ containing control and bound antibodies were detected by the development of a coloured product (see 2.2.4).

2.2.9 Data analysis

Data calculations were performed in Microsoft Excel and graphs generated in GraphPad Prism 9; each point represents a mean±s.e.m. or s.d. as indicated in Figure legends. CAP and AITC dose-dependent relationships were fitted using the formula: Y=min+(max-min)/(1+10^((LogEC_{50}-X)*Hill Slope)). Welch unpaired t-test, one- or two-way analysis of variance (ANOVA) was used to evaluate the significance of changes. Statistical significance was attributed between groups when $p<0.05$. Asterisks or hashtags indicate p values; **** or ####, $p<0.0001$, *** or ###, $p<0.001$, ** or ##, $p<0.01$, * or #, $p<0.05$.

3 The extent to which BoNT/A reduces capsaicin-evoked CGRP release from TGNs depends on the concentration of the TRPV1 agonist applied to the neurons

3.1 Overview

Current theory of migraine pathophysiology proposes that migraine attacks are initiated in the hypothalamus, following by descending activation of the TNC and TG. This results in the release of endogenous compounds (for example, H^+ or NO) that stimulate TRPV1 channels to open. Consequently, Ca^{2+} floods into the neurons and triggers the secretion of CGRP (and other neurotransmitters), which promotes neurogenic inflammation and peripheral sensitisation (Haanes and Edvinsson, 2019), (Iyengar et al., 2017). By immuno-cytochemistry, it was confirmed that TRPV1 is present on the trigeminal sensory fibres that innervate the meninges and that its expression is increased in patients with chronic migraine compared to healthy controls. On this basis, TRPV1-targetted therapies are used in the treatment of migraines. For example, a strategy for desensitisation of this channel by intranasal delivery of CAP or Civamide (a synthetic TRPV1 agonist) has been employed with some success. TRPV1-antagonists also showed some effect in pre-clinical studies. Unfortunately, modulation of TRPV1 activity by agonists or antagonists can also cause undesirable side effects resulting in high rates of discontinuation with these treatments [reviewed in (Meents et al., 2010), (Dussor et al., 2014), (Benemei and Dussor, 2019)].

The inhibition of CGRP release evoked by TRPV1 is used as an alternative treatment for chronic migraines (see General Introduction). A potent inhibitor of regulated exocytosis, BoNT/A has been used for some years for prophylaxis and treatment of chronic migraine. Large scale clinical studies demonstrated that intracranial injections of the toxin reduced the duration and severity of migraine headaches (Dodick et al., 2010) and its positive effect was associated with the reduction of CGRP levels in blood samples (Cernuda-Morollón et al., 2015). However, a reduction of migraine symptoms was not observed in all patients. BoNT/A has also been tested in humans in a CAP-induced pain model, which mimics trigeminal-mediated vasodilation, to investigate the toxin's putative anti-nociceptive effect. In this model, subcutaneous or topical application of CAP promotes the local release of vasoactive neuropeptides resulting in neurogenic inflammation and the sensitisation of the affected area. It was found that BoNT/A pre-injection into forehead or forearm reduced flare, vasodilation, skin temperature, pain, and secondary hyperalgesia (Gazerani et al., 2006), (Gazerani et al., 2009), (Tugnoli et al., 2007) and the effect lasted up to one week. On the other hand, (Voller et al., 2003) and (Schulte-Mattler et al., 2007) reported that /A had no effect on

CAP-induced pain in human skin, and the reason for such contrary outcomes has not been pinpointed.

Thus, the processes involved in the analgesic effects of BoNTs are still unclear and proposed mechanisms are controversial. Despite *in vitro* studies demonstrating its inhibition of neuropeptide release evoked by depolarisation or bradykinin (Welch et al., 2000), (Meng et al., 2007), BoNT/A proved to be a feeble inhibitor of CGRP exocytosis elicited from rat TGNs by activation of TRPV1 with CAP (Meng et al., 2007). Based on these studies, it was hypothesised that the efficacy of the toxin may depend on the level of TRPV1 activation. In this regard, LC/E-containing chimeras that remove a larger fragment of SNAP-25 (see 1.3.3) were tested herein in comparison to BoNT/A for inhibition of the CGRP release evoked from TGNs by different [CAP], with the aim of determining whether these chimeras remain effective under conditions that are refractory to BoNT/A, which might translate into an improved therapeutic potential.

3.2 Results

3.2.1 Isolation, cultivation, and morphological plus histochemical characteristics of cultured TGNs

Cultures of sensory neurons from neonatal rodents have been extensively used as a model to study the molecular basis of pain signalling. These preparations have some limitations, such as a dependency on growth factors for neuron survival *in vitro*. However, they allow researchers to examine under controlled conditions events such as exocytosis, the trafficking of receptors or channels and the regulation of signalling cascades. For example, rat TGNs have been used to investigate the effect of pro-inflammatory compounds on CGRP release (Durham et al., 2004), (Meng et al., 2007) and sensitisation of pain-related channels (Meng et al., 2016), (Nugent et al., 2018). Another advantage of neonatal sensory neurons when compared to neurons from adult animals is their relatively easy isolation and cultivation at high density. Moreover, a substantial number of these neurons in culture express pertinent proteins: SNAP-25, TRPV1, and CGRP (Meng et al., 2007). Therefore, cultured sensory neurons from neonatal rats were chosen as a suitable model to investigate the efficacy of BoNT/A and chimeric toxins created in ICNT for the inhibition of CGRP exocytosis evoked by activation of TRPV1 (Chapter 3) or TRPA1 (Chapter 5).

TGNs were dissected and dissociated using an established protocol already employed within ICNT. To improve the quality of cultures in terms of their purity (i.e., absence of non-neuronal cells or unwanted tissue fragments), health and survival, was introduced an additional preparatory step comprising the centrifugation of crude tissue digests through a discontinuous 60/30% Percoll® gradient before plating the purified neurons (see 2.2.1.2). In healthy TGN cultures, most of the cells had a bright and round-shaped soma with fine fibres (Fig. 3.1). After one day *in vitro* (DIV) in the presence of NGF, cells had already started to establish a neuropil (Fig. 3.1 A); by DIV 4 and thereafter TGNs had elaborated an extensive network of fibres (Fig. 3.1 B, C).

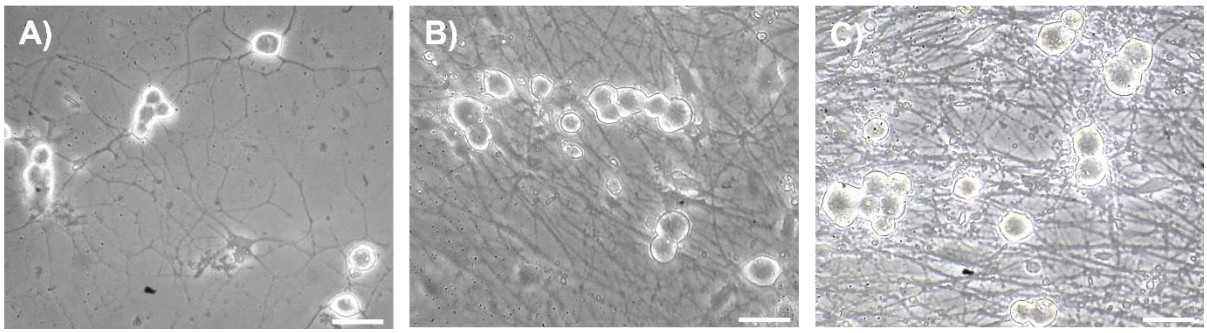

Figure 3.1 Representative images of cultured TGNs at 1, 4, and 9 DIV
TGNs were dissected from neonatal rats (P3-6), seeded ~25,000 neurons per well and maintained in the presence of 50 ng/ml NGF for up to 9 days. (A) After 24 h of plating (1 DIV) cells had already grown processes, and this nascent neuropil continues to grow in density and complexity as shown here at DIV 4 (B) and DIV 9 (C). Photographs were taken with a digital camera attached to an Olympus IX71 light microscope operated in phase-contrast mode. Scale bar 25 µm.

Immuno-cytochemistry with fluorescence microscope imaging was chosen as an assay to confirm that the cultures express neuropeptides and the proteins of interest: CGRP, TRPV1, and SNAP-25. Cultured TGNs were processed as described in section 2.2.5 in collaboration with Dr Tomas Zurawski, DCU. Labelling of cell cultures with antibodies specific for a broadly expressed pan-neuronal marker called neurofilament 200 (NF-200) demonstrated that the preparations are enriched with TGNs (Fig. 3.2 A) expressing several relevant proteins as expected (Meng et al., 2007). A substantial fraction of neurons express CGRP (Fig. 3.2 B, C; yellow colour in C indicates expression of both antigens) and all of those also contained SNAP-25, which is required for fusion of LDCVs with plasmalemma and neuropeptide release (see 1.1.3, Fig. 3.2 D-F) and is the substrate of BoNT/A and /E proteases. Antibodies specific to TRPV1 revealed the expression of this protein in all CGRP-positive cell bodies and neuronal fibres (Fig. 3.2

G-I). Thus, a suitable *in vitro* platform was established for the investigation of BoNTs' inhibition of CGRP release evoked by a range of [CAP].

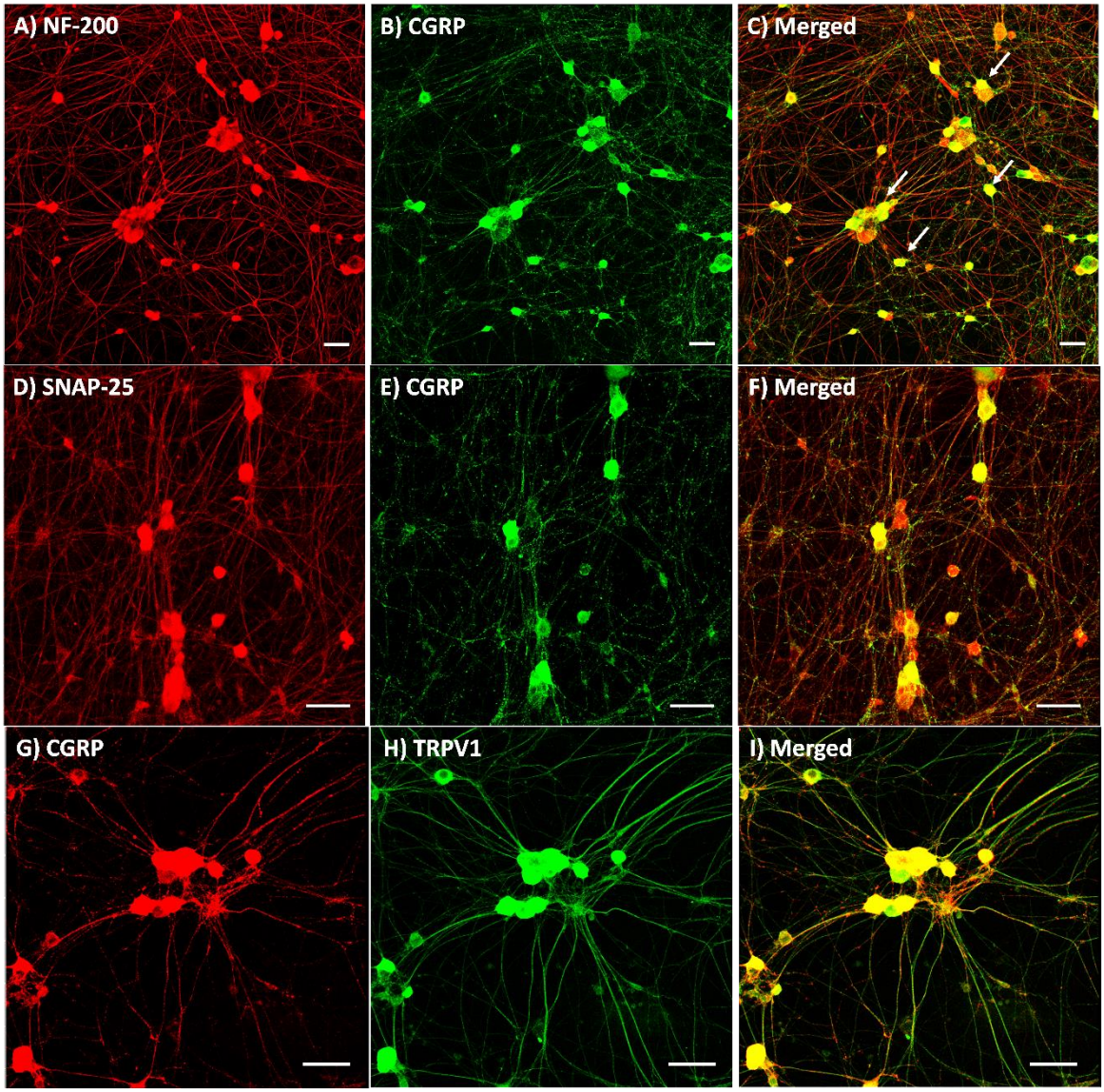

Figure 3.2 Established TGNs cultures from neonatal rats are enriched with CGRP-expressing neurons which also contained TRPV1 and SNAP-25
Neurons were isolated from neonatal rats and grown on coverslips for 9 DIV before being fixed, permeabilized, and labeled, as detailed in 2.2.5, with primary antibodies specific for (A) NF-200, (B, E, G) CGRP, (D) SNAP-25, (H) TRPV1. After washing, cultures were exposed to the secondary antibodies conjugated to Alexa Fluor® 488 (green) or Alexa Fluor® 633 (red). Primary and secondary antibodies, the host species in which they were produced, and the dilutions used are described in section 2.1.3. (C, F, I) Merged images demonstrate co-localisation of indicated proteins. Scale bar 50 µm. Labeling and confocal imaging was performed by Dr Tomas Zurawski.

Interestingly, imaging at a higher magnification revealed a CGPR-positive punctate staining along neuronal fibres (Fig. 3.3 A), which is consistent with the expected localisation of this neuropeptide inside intracellular vesicles. However, note that vesicles

are smaller than the light microscope resolution limit, so the precise location cannot be confirmed by this method, and single neuropeptide-containing vesicles cannot be resolved from clusters. TRPV1 labelling was brightest in cell bodies and in fibres (Fig. 3.3 B), whilst SNAP-25 immuno-signal was present relatively strong in neuronal fibres and less intense in cell bodies (Fig. 3.3 C).

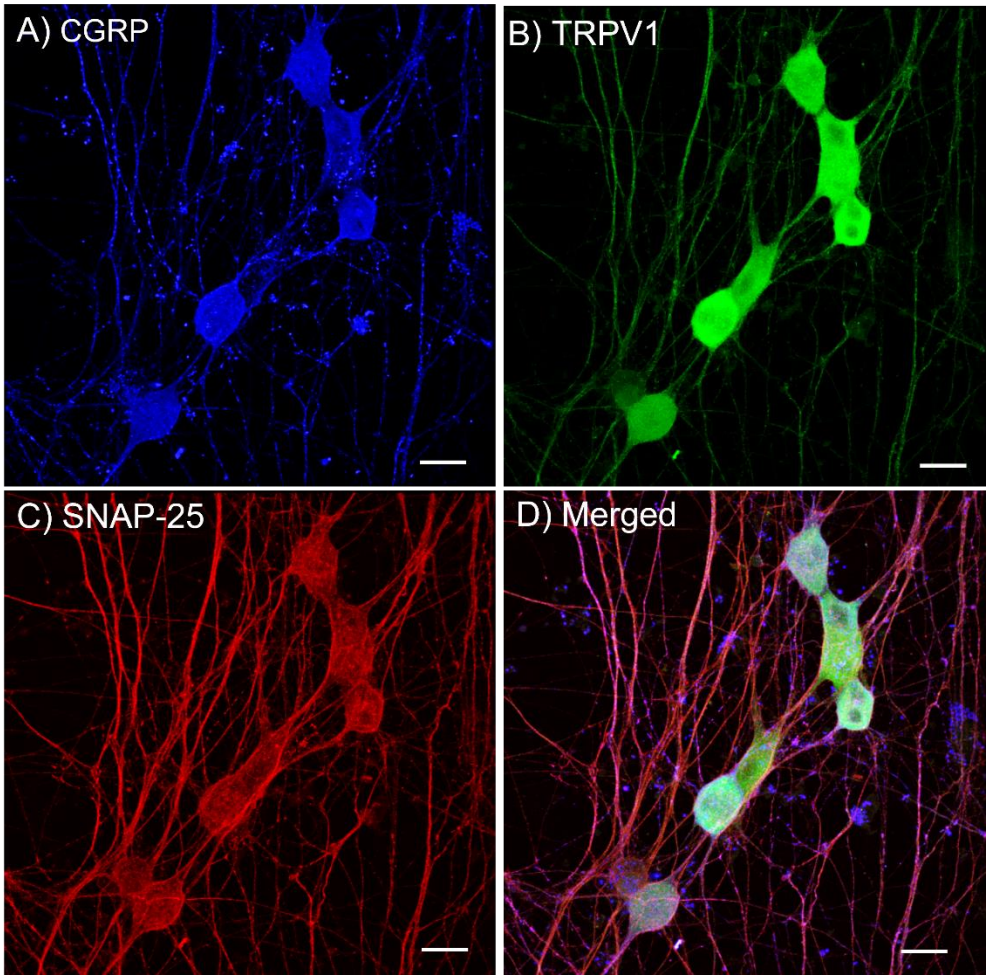

Figure 3.3 In TGNs cultures, SNAP-25 is present in neurons which co-express CGRP and TRPV1
TGN cultures at 9 DIV were counterstained with (A) anti-CGRP and (B) anti-TRPV1, and (C) anti-SNAP-25 antibodies. Cells were washed and incubated with host-specific secondary antibodies (A) Alexa-Fluor® 633 (blue), (B) Alexa-Fluor® 488 (green) and (C) Alexa-Fluor® 555 (red). The merger of these three images (D) demonstrates that most of CGRP-positive cells contain both TRPV1 and SNAP-25. Scale bar 20 µm. Labeling and confocal imaging was performed by Dr Tomas Zurawski

3.2.2 Concentration-dependent stimulation of Ca^{2+} influx by CAP in cultured TGNs

To establish the sensitivity of cultured TGNs to CAP, cells at 4 DIV were loaded with a Ca^{2+}-sensitive fluorescent indicator Fluo-4 AM, which because of its neutral charge crosses the cell membrane. In the cytosol, the AM group is cleaved off by cell esterases, trapping the sensor inside the cell cytosol. In the presence of elevated

concentrations of free Ca^{2+}, the ion binds to the sensor and the latter fluoresces when excited at ~494 nm; hence, increases in fluorescence intensity indicate raised concentrations of intracellular Ca^{2+} $[Ca^{2+}]_i$. TGNs were loaded with the dye for 20-30 min. then washed extensively with recording buffer to remove non-incorporated sensor prior to confocal imaging as described in 2.2.7 of Materials and Methods. Before fluorescence recordings, images of the cells were captured in the phase-contrast mode to enable estimation of ROI (see later) (Fig. 3.4 A). Baseline fluorescence was recorded for 6 min. before 30 min. of exposure to 0.01-1 µM CAP (or 0.1% ethanol, which served as a vehicle). At the end of each experiment, to identify all excitable cells, cultures were exposed for 1 min. to a modified recording buffer (HBS-HK) containing an elevated concentration of potassium ions (100 mM K^+) with the sodium ion concentration reduced to maintain tonicity equivalent to unmodified recording buffer. Representative images of fluorescence intensities during recordings of baseline, 1 µM CAP-stimulation, and HBS-HK recordings are shown in Fig. 3.4 panels B, C, and D, respectively. A new sample of cells was used for recording responses to each [CAP] to avoid the results being confounded by agonist-induced desensitisation of TRPV1 (Koplas et al., 1997).

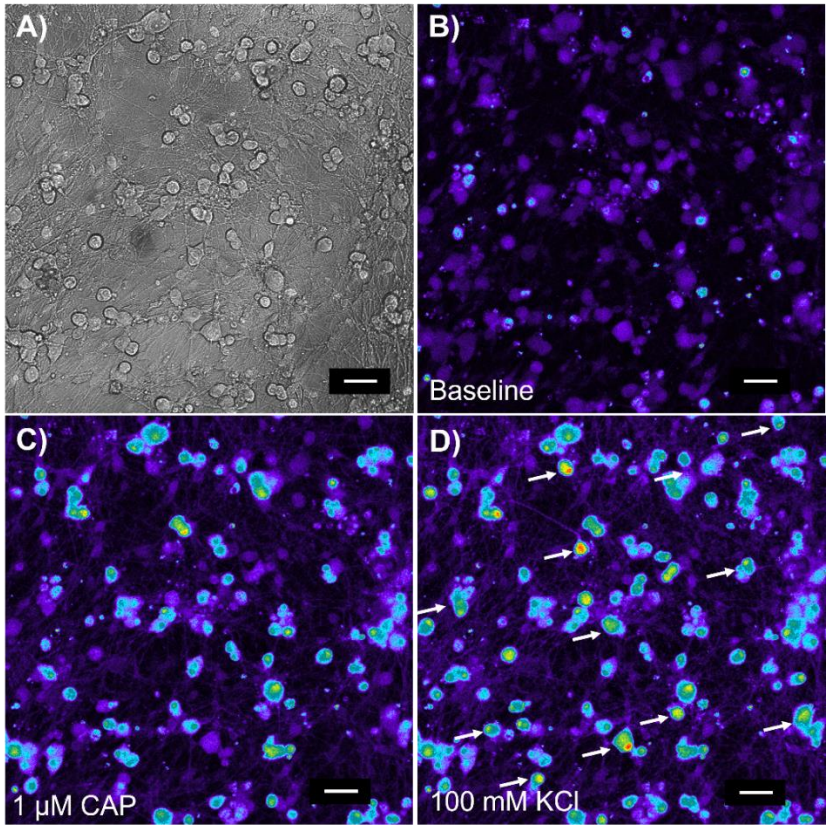

Figure 3.4 Stimulation with 1 µM CAP or 100 mM K^+ provokes increased fluorescence in cultured TGNs pre-loaded with a Ca^{2+}-sensitive dye, Fluo-4 AM

(A) Prior to recording in fluorescence mode, images of the cells were captured by phase-contrast to identify ROI. (B-D) Fluorescence imaging was performed using the Zen rainbow 2 colour channel, which applies a false colour spectrum according to fluorescence signal intensity. Purple indicates low intensity and blue, green, yellow, and red colours represent signals of increasing strength. (B) During a 6 min. period without any stimulus, cells did not display changes in fluorescence as most of them are purple. (C) 30 min. application of 1 µM CAP activated a large number of TGNs (cells with blue and orange colours), but not all of them. The image shows signals of various intensity recorded after 1 min. of exposure to CAP. (D) A 1-min. application of HBS-HK activated more cells than 1 µM CAP as it additionally excited those that did not respond to CAP (white arrows). Scale bar 50 µm.

The intensities (F) of fluorescence signals observed in video micrograph recordings were measured and selection criteria to determine responding cells are described in 2.2.7. The number of cells that were excited by CAP increased as the cultures were exposed to higher concentrations of this TRPV1 agonist. In cultures exposed to 0.01 and 0.02 µM CAP, respectively, 60% and 68% of the cells responded with increased fluorescence. At 0.05 µM CAP, the number of responders rose to 85% but increases in CAP concentration above 0.1 µM did not raise the proportion any higher (Fig. 3.5 A). It appears that [CAP] from 0.05-1 µM was sufficient to activate all the neurons that express TRPV1. To compare the increases of $[Ca^{2+}]_i$ during stimulation with different [CAP] or vehicle (0.1% ethanol), $(F-F_0)/F_0$ was estimated for each ROI; then the mean increase (±s.e.m.) at each time point was calculated and plotted against time (Fig. 3.5 B). Notably, raising [CAP] caused faster and larger increases in normalised fluorescence. To quantify and compare sustained responses to different [CAP], AUC of the latter plots was calculated for each individual cell and mean values plus s.e.m. for responses to each [CAP] are demonstrated on the bar chart (Fig. 3.5 C). A fraction of cells (~17%) had a very low level of spontaneous cell excitability during 30 min. exposure to the vehicle; however, the average AUC for this group was tiny (1.8±0.6 arbitrary units) when compared to mean fluorescence recorded during CAP application (see below). Upon increasing [CAP], the mean AUC of curves plotted for CAP responders grew to 10±3.1, 15.8±2.8, 39±3.7, 45.7±3.5, 51.7±3.7, and 72.9±3.9 arbitrary units for 0.01, 0.02, 0.05, 0.1, 0.3, and 1 µM CAP respectively. Thus, a dose-dependent relationship between [CAP] and stimulated increases of $[Ca^{2+}]_i$ is clearly demonstrated (Fig. 3.5 C).

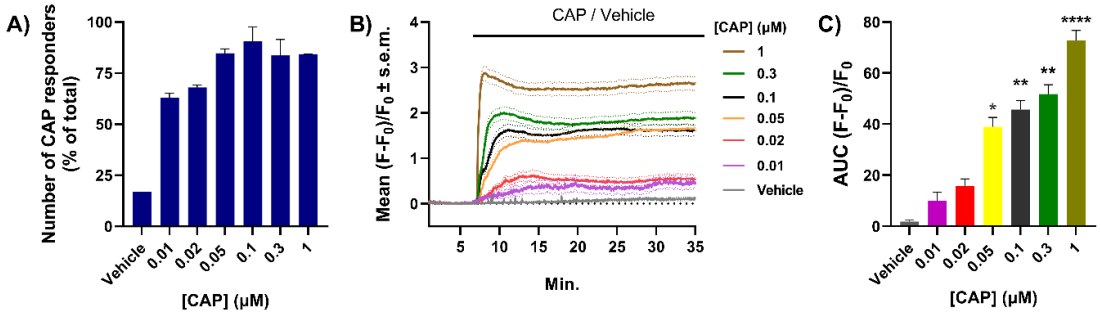

Figure 3.5 CAP causes dose-dependent increases in the fraction of responding cells and $[Ca^{2+}]_i$ in cultured TGNs

TGNs 4 DIV were loaded with Fluo-4 AM and F was recorded by serial time-lapse confocal microscopy before and during 30 min. stimulation with the indicated [CAP]. (A) Histogram showing the proportion of CAP-responding cells from a total number of excitable cells (sum of CAP and 100 mM KCl responders). (B) The mean normalised increase in fluorescence in cells identified as responders and plotted against time. The solid lines indicate mean values and broken lines represent s.e.m. (C) AUC of the fluorescence traces shown in (B). Column heights and error bars represent the mean of AUC plus s.e.m. Asterisks show a significant difference in mean fluorescence induced by CAP compared to the mean of vehicle-treated cells; * $p<0.05$, ** $p<0.01$, *** $p<0.001$, **** $p<0.0001$, ordinary one-way ANOVA followed by Bonferroni's *post hoc* test. N=2, n>100. This figure was modified from (Belinskaia et al., 2022).

3.2.3 Quantification of spontaneous and stimulated CGRP exocytosis from cultured TGNs

As the increase of $[Ca^{2+}]_i$ triggers regulated exocytosis, it was necessary to set up a protocol for measuring CGRP release from cultured TGNs. Such an assay was previously established in host laboratory (Meng et al., 2007). It consisted of culturing TGNs 7-10 DIV in the presence of NGF prior to sequential incubation with HBS to measure spontaneous CGRP release, followed by incubation with 1 µM CAP in HBS or HBS-HK to quantify stimulated CGRP exocytosis (Fig. 3.6). At the end of the experiments, cells were lysed with a mixture of 2M acetic acid (A.A) and 0.1% (v/v) trifluoroacetic acid (TFA), with freeze-thaw of the suspension three times to ensure complete rupture of the cells. The liquid in the samples was then evaporated off under vacuum to recover the solid material, which included precipitated CGRP. To quantify the neuropeptide in the resulting powder, it was reconstituted in ELISA buffer. Spontaneous and stimulated CGRP release, plus the neuropeptide cellular content were analysed by ELISA as described in 2.2.3. The amounts of released CGRP were expressed as % of the total content (i.e., the sum of released CGRP and the amount that remained inside the cells). Such an approach facilitates comparisons between experiments performed on neuron cultures prepared at different times and accommodates inevitable variations in cell numbers.

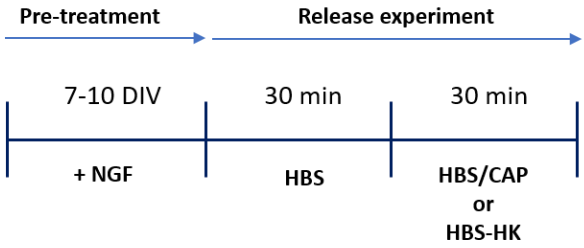

Figure 3.6 Schematic illustrating a protocol established in ICNT for quantification of CGRP release Cultured TGNs were grown in presence of NGF for 7-10 days. The amounts of CGRP release were quantified during sequential 30 min. exposures to HBS only (spontaneous release) and then to CAP in HBS or HBS-HK (stimulated release). At the end of the experiment, cells were lysed as described in 3.2.3 and the amounts of CGRP were quantified by ELISA.

In pilot experiments utilising the protocol described above, unexpectedly, the normalised values of CGRP measured proved to be highly variable (Fig. 3.7 A). To reduce such inconsistency, I introduced a simpler alternative approach involving direct solubilisation of neurons with Triton X-100 in HBS. Notably, this modification made the assay more rapid and improved precision without compromising sensitivity (Fig. 3.7 A). To establish an optimal concentration of Triton X-100 for CGRP protein solubilisation, three concentrations (0.1%, 0.5%, and 1% (v/v)) were tested (Fig. 3.7 B). In the cells solubilised with 0.5% and 1% of Triton X-100, levels of CGRP were significantly higher ($p=0.002$ and $p=0.006$ respectively) than in TGNs, lysed in 0.1%. There was no significant difference in CGRP amounts recovered between 0.5% and 1% Triton X-100, and the higher concentration was used for cell solubilisation in all subsequent experiments.

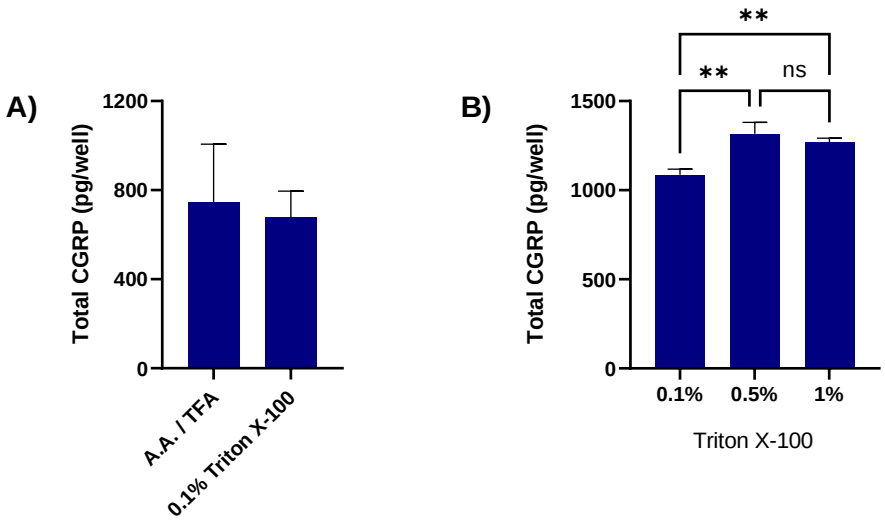

Figure 3.7 Cells solubilised in Triton X-100 with an optimal concentration of 1% (v/v) showed lower variability in detected CGRP levels

(A) Cultured TGNs were scraped in 2M acetic acid (A.A.) in 0.1% TFA, freeze-thaw three times, vacuum dried, and reconstituted in ELISA buffer. Another set of cells were solubilised in HBS, supplemented with 0.1% (v/v) Triton X-100. (B) In a separate experiment, neurons were solubilised in HBS with indicated concentrations of Triton X-100. In (A) and (B) CGRP cell content was quantified by ELISA. Data presented as mean+s.d., n≥6. Statistical significance of differences was determined using ordinary one-way ANOVA, with Bonferroni's multiply comparisons test, ** p<0.01.

Depolarisation with 60 mM K^+ induced a significant (p<0.0001) increase in the fraction of neuropeptide exocytosed, 33% of the total CGRP content (Fig. 3.8 A), compared to spontaneous release of only 1.5%. By contrast, stimulation with 1 µM CAP elicited release of a lesser amount then KCl, 18% of the total (Fig. 3.8 B).

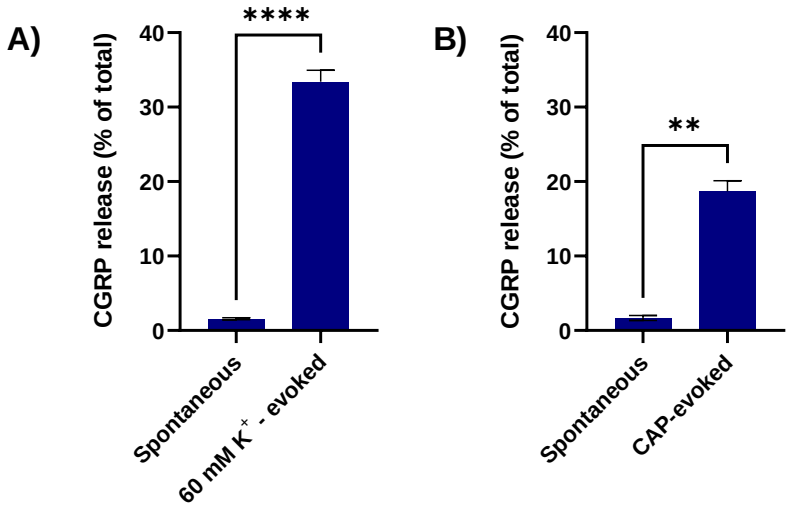

Figure 3.8 Stimulation of cultured TGNs with 60 mM K^+ or 1 µM CAP induces a significant increase of CGRP release

TGNs were maintained in culture for 7-10 days in presence of NGF. The amounts of CGRP released were quantified during sequential 30 min. exposures, firstly to HBS to measure spontaneous release, and then to (A) HBS-HK or (B) 1 µM CAP in HBS. At the end of the experiment, cells were solubilised with 1% Triton X-100. The amounts of CGRP released or retained in the cells were quantified by ELISA and expressed as a % of the total neuropeptide content. Data are presented as mean+s.e.m., n≥3 from one (CAP) or two (60 mM K^+) experiments. Statistical analysis was performed by two-tailed Welch unpaired t-test, ** p<0.01, **** p<0.0001.

To establish a concentration-dependence relationship for stimulation of CGRP release, TGNs were treated with logarithmic (base 10) increments of [CAP] (Fig. 3.9 A). Surprisingly, this revealed a complex relationship between [CAP] and CGRP release. At low [CAP] from 0.001 to 0.1 µM CAP, CGRP increased with each increment in stimulus concentration, until a maximum was reached of ~37% of total CGRP. Interestingly, this amount is comparable to that released in response to depolarisation with high [K^+]. Even

more remarkably, further increases in [CAP] produced no additional CGRP release. In fact, the amounts declined; for example, 1 µM CAP evoked less than half of the response to 0.1 µM (respectively, 15 and 37% of the total available) (Fig. 3.9 A). This was surprising because the Ca^{2+}-imaging assay had demonstrated that increases in $[Ca^{2+}]_i$ corresponded to rising [CAP] up to 1 µM (Fig. 3.5 B, C). This suggests that the decrease in CGRP exocytosis at high [CAP] (i.e., >0.1 µM) is not a result of TRPV1 desensitisation or any other process that could lead to a reduction in channel activity. Importantly, extracellular Ca^{2+} was essential for CGRP release evoked by either 0.1 or 1 µM CAP (Fig. 3.9 B), excluding the possibility of a non-regulated mechanism. To gain further evidence that CGRP release was stimulated by TRPV1 activation, cultured TGNs were pre-treated for 30 min. with 1 µM capsazepine (CPZ), a competitive TRPV1 antagonist. Cells were exposed to 0.1 or 1 µM CAP in presence or absence of the antagonist for another 30 min. Stimulation of CGRP release by 0.1 µM CAP together with CPZ revealed a ~85% reduction of evoked exocytosis (from 24.5% to 3.8% of the total CGRP, p=0.008) (Fig. 3.9 C). In contrast, 1 µM CPZ was unable to abolish CGRP release evoked by high 1 µM [CAP] (data not shown). Unfortunately, increasing the CPZ concentration to 10 and 50 µM revealed an unexpected effect as the antagonist itself stimulated CGRP release, up to 15% of the total neuropeptide content even before CAP application. In this regard, it has been reported that 10 µM CPZ induced the release of Ca^{2+} from intracellular stores, which might explain how it can stimulate CGRP exocytosis (Phillips et al., 2004). Consequently, the range of 0.001-0.1 µM CAP was chosen as optimal for fitting a dose-response curve, which revealed a half-maximum effective concentration (EC_{50}) for CAP of 0.02 µM (Fig. 3.9 A). This [CAP] was used for further experiments to test the acute effect of NGF on TRPV1 sensitisation (Chapter 4).

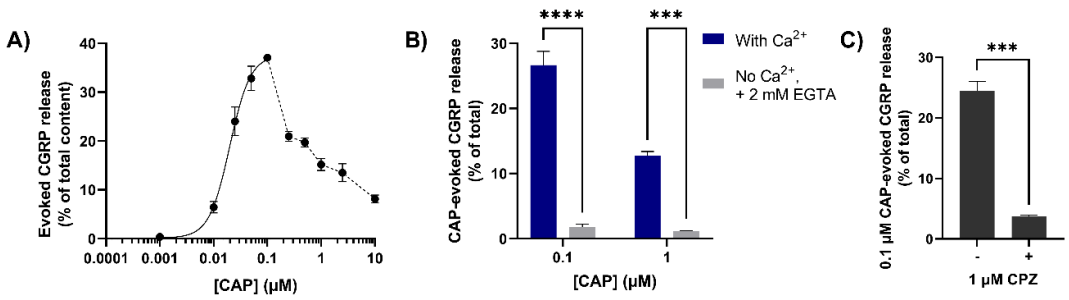

Figure 3.9 CAP elicits Ca^{2+}-dependent CGRP release from cultured TGNs in a dose-dependent manner

(A) TGNs were exposed to various CAP concentrations ([CAP]) for 30 min., and the amount of CGRP released into the bathing solution was quantified and expressed as a % of the total CGRP content (i.e., amount released plus quantity retained inside the cells). The inclining part of the relationship (0.001 to 0.1 μM) was fit with a four-parameter logistic function (see 2.2.9) with R^2=0.884, yielding for CAP EC_{50}=0.02 μM. Individual values for the declining part (0.1 to 10 μM) are connected by a broken line and not included in the fitting. (B) Comparison of CAP-evoked CGRP release in the presence or absence of extracellular Ca^{2+}; in the latter case, 2 mM EGTA was included instead of Ca^{2+}. (C) Histogram displaying the amounts of released CGRP, stimulated by 0.1 μM CAP in presence of 1 μM CPZ. Data are presented as mean±s.e.m., for (A) N≥4, n≥16; for (B) N=1, n=3; for (C) N=1, n=4; error bars are not shown where they are smaller than the associated symbol. Two-way ANOVA followed by Bonferroni's *post hoc* test and unpaired two-tailed Welch test were applied for (B) and (C), respectively. *** p<0.001, **** p<0.0001.

3.2.4 Inhibition of CGRP release and SNAP-25 cleavage by BoNT/A

Next, the extent of SNAP-25 proteolysis by BoNT/A was measured. TGNs were incubated for 48 h with 100 nM BoNT/A, while control cells were exposed to the same volume of toxin-free medium. Then cells were solubilised in 1x LDS sample buffer and subjected to SDS-PAGE prior to electrophoretic transfer to PVDF membrane and Western blotting with an antibody reactive with SNAP-25 epitope that is preserved after its truncation by BoNT/A. The proportion of truncated and intact SNAP-25 was estimated by densitometry (detailed in 2.2.4.3) of the requisite bands revealed upon development of immuno-signals; cleaved SNAP-25 migrates faster during SDS-PAGE and, therefore, develops as a band in a lower position (i.e., farther migration through the PAGE gel) than the intact protein (Fig. 3.10 A). Treatment with 100 nM BoNT/A for 48 h led to cleavage of the SNAP-25 present in the cells (Fig. 3.10 B), as revealed by a reduction in the amount of intact SNAP-25, and the appearance of a faster migrating immuno-reactive band that was not observed in toxin-free control cells (Fig. 3.10 A). Incubation with BoNT/A significantly (p=0.003) reduced spontaneous CGRP release (Fig. 3.10 C) but did not change the total amount of the neuropeptide (p=0.33) (Fig. 3.10 D). As expected, BoNT/A blocked 60 mM K^+ evoked CGRP release (p<0.0001) (32 vs 8% of the total in control and treated cells, respectively), but only slightly reduced 0.3 μM CAP evoked CGRP release (p=0.16) (26 vs 21%, Fig. 3.10 E, F). However, it should be noted that in other experiments (see later) inhibition of 0.3 μM CAP evoked CGRP release did (just) reach significance.

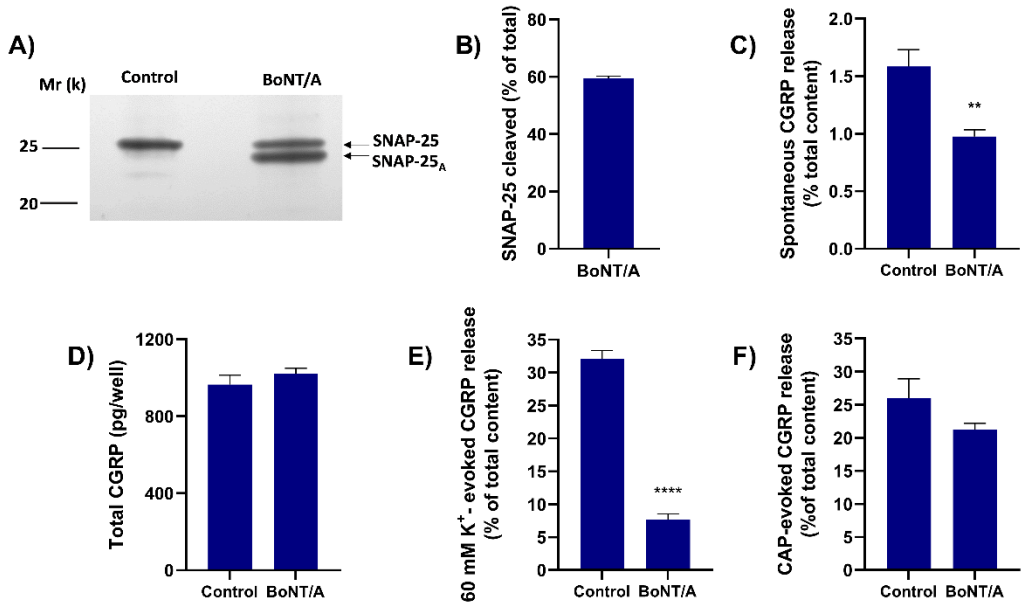

Figure 3.10 100 nM BoNT/A cleaves SNAP-25 in TGNs and blocks their K^+-depolarisation evoked CGRP release, but only partially inhibits the neuropeptide exocytosis stimulated by 0.3 µM CAP
Cultured neurons 7 DIV were pre-treated with 100 nM BoNT/A for 48 h. The release experiment was performed as described in Fig. 3.6, except that cells were solubilised in 0.1% Triton X-100 in HBS. (A) At the end of the release experiment, one well of each of BoNT/A-treated and control cells were solubilised in 1x LDS sample buffer and subjected to Western blotting as described in the Materials and Methods. PDVF membranes were exposed to mouse monoclonal antibodies recognising intact and cleaved SNAP-25. Black lines to the left indicate the migration of 20 and 25 k molecular weight standards. (B) The amount of cleaved SNAP-25 in BoNT/A-treated cells was calculated as a % of total SNAP-25 (sum of intact and cleaved product) (mean+s.e.m., N=2). (C-F) Histograms showing: (C) Spontaneous CGRP release, (D) total CGRP (sum of released and intracellular content); (E-F) CGRP release stimulated by 60 mM KCl or 0.3 µM CAP. Note that spontaneous exocytosis values were subtracted from amounts in the presence of stimulus to calculate the evoked component. N=1, n=3, mean+s.e.m. Unpaired one- (C, E, F) or two-tailed (D) Welch test was applied, N=1, n=3; ** $p<0.01$, **** $p<0.0001$.

3.2.5 E-cleaving chimeras proved to be better inhibitors than BoNT/A of 1 µM CAP-evoked CGPR release

To overcome the aforementioned limitation of BoNT/A in the blockade of 1 µM CAP induced CGRP exocytosis, a chimeric toxin was developed (see 1.3.3), BoNT/EA comprised of LC and translocation domain of BoNT/E (LC-H_NE) attached to H_C of BoNT/A (H_C/A) (Fig. 1.6). After 48 h exposure of TGNs 7 DIV to 100 nM BoNT/EA, toxin-treated and control cells were subjected to Western blotting similar to that above with a slight modification. After separating proteins on SDS-PAGE and their transfer to PVDF membrane, the latter was cut horizontally midway between 25 k and 37 k molecular weight markers. The upper part of the membrane was exposed to antibodies recognising syntaxin-1, serving as a loading control. The lower part of the membrane was

exposed to immunoglobulins that recognise SNAP-25. The /E-product migrates as a band at ~20 k (Fig. 3.11 A), smaller than A-product because /E cleaving toxins remove 26 amino acids from SNAP-25, whereas /A cuts off only 9 (Fig. 1.5 B). Treatment of cultured TGNs with 100 nM BoNT/EA revealed cleavage of 72% of SNAP-25 (Fig. 3.11 B). Interestingly, total CGRP in BoNT/EA treated cells was slightly (although not significantly) higher than in control (p=0.22) (Fig. 3.11 D). Like BoNT/A, the /EA reduced spontaneous CGRP release (p<0.0001) (Fig. 3.11 C), but unlike the former it also significantly (2-fold) reduced neuropeptide exocytosis stimulated by 0.3 µM CAP (from 32% of total CGRP in control to 16% in BoNT/EA treated cells; p=0.002) (Fig. 3.11 E).

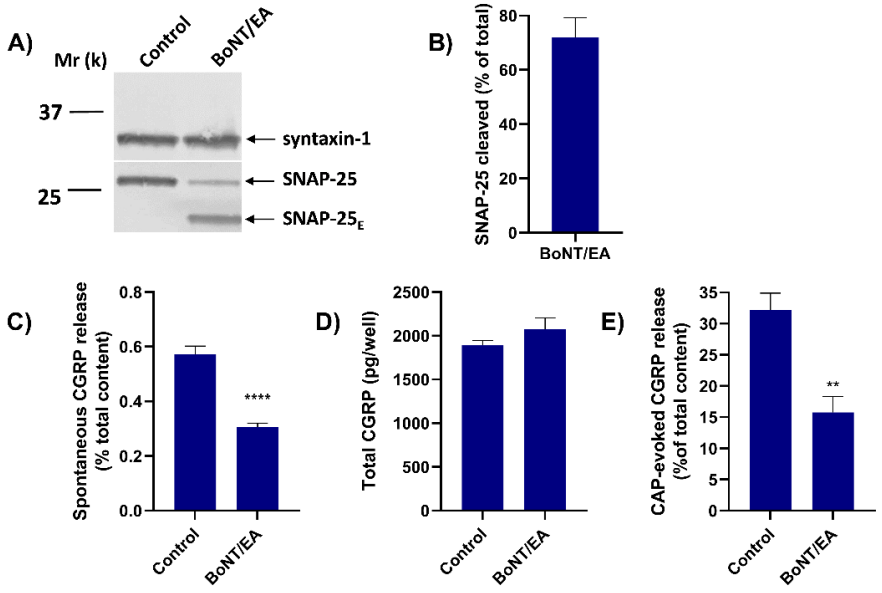

Figure 3.11 Chimeric toxin BoNT/EA extensively cleaves SNAP-25 and effectively blocks CAP-provoked CGRP release

TGNs 7 DIV were pre-treated with 100 nM BoNT/EA for 48 h. The release experiment was performed identically to that described for BoNT/A. (A) One well of intoxicated cells and one of the controls were solubilised in 1x LDS sample buffer and subjected to Western blotting. PVDF membranes were cut horizontally midway between 25 k and 37 k molecular weight markers. The upper part was exposed to mouse monoclonal antibodies recognising syntaxin-1 and the lower portion to mouse anti-SNAP-25 (for details see 2.1.3). (B-E) Histograms show the levels of (B) cleaved SNAP-25, (C) spontaneous CGRP release, (D) total CGRP, and (E) 0.3 µM CAP-evoked CGRP release. Data are presented as mean + s.e.m., N=2, n≥4. Unpaired one- or two-tailed (D) Welch test was applied to data in C, E and D, respectively; ** p<0.01, **** p<0.0001.

To confirm functional properties of another chimera LC/E-BoNT/A, composed of LC/E and BoNT/A (see 1.3.3), cultured TGNs were incubated with the toxin for 24 h according to a published protocol (Wang et al., 2017). Densitometric analysis of Western

blotting digital images revealed 5, 21, 41, and 69% of cleaved SNAP-25 for 0.1, 1, 10, and 100 nM LC/E-BoNT/A (Fig. 3.12 A, B). Notably, LC/E-BoNT/A produced predominantly LC/E-cleaved product, suggesting that LC/E further cleaved the SNAP-25_A product (Fig. 3.12 A). In accord with the observed extents of SNAP-25 cleavage, the chimera blocked 1 µM CAP-evoked CGRP release in a dose-dependent manner (Fig. 3.12 B). Because 100 nM of toxins gave the largest amount of cleaved SNAP-25, this concentration was chosen for further experiments.

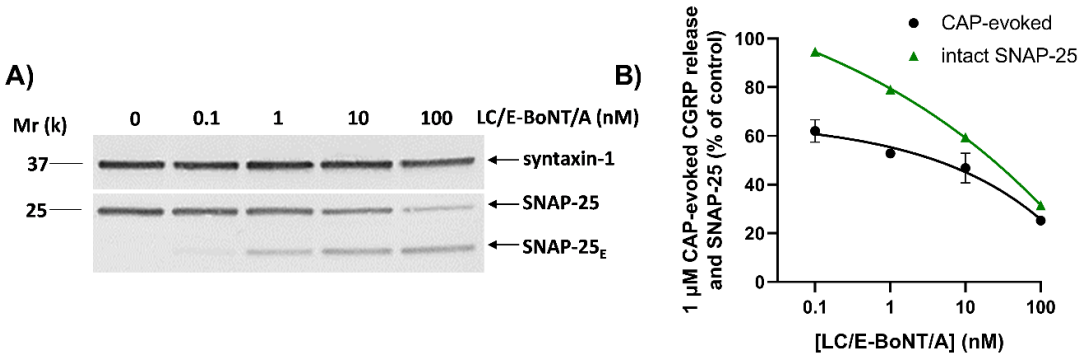

Figure 3.12 Chimera LC/E-BoNT/A cleaves SNAP-25 and effectively blocks 1 µM CAP-evoked CGRP release in a dose-dependent manner
TGNs 7 DIV were treated for 24 h with 0.1, 1, 10, and 100 nM LC/E-BoNT/A before incubation with HBS to evaluate spontaneous CGRP release followed by 1 µM CAP to determine evoked exocytosis of the neuropeptide. (A) Western blotting with anti-SNAP-25 antibodies demonstrates the increase of SNAP-25_E product upon raising the concentration of LC/E-BoNT/A. (B) The chimera dose-dependently cleaved SNAP-25 and reduced CAP-evoked CGRP release. Data are presented as mean+s.e.m., N=1, n≥3.

Because CAP induces a dose-dependent increase in $[Ca^{2+}]_i$ (Fig. 3.5 and (Cholewinski et al., 1993)) and at high $[Ca^{2+}]_i$ SNAP-25_A can form a complex with its SNARE partners, it was interesting to investigate if BoNT/A will be more effective in blocking CGRP exocytosis induced by lower [CAP] that elicit smaller changes in $[Ca^{2+}]_i$. To address this query, cultured TGNs were treated with BoNT/A, BoNT/EA, and LC/E-BoNT/A for 48 h and CGRP release was stimulated by 0.02, 0.1, 0.3, and 1 µM CAP. To readily assess and compare the blockade of CGRP release evoked by CAP, neuropeptide exocytosis at each toxin concentration was plotted as a % of the level obtained for toxin-free control samples (Fig. 3.13). This clarified that the ability of BoNT/A to block CGRP release depends on the vanilloid concentration. In this experiment, BoNT/A cleaved the majority of the SNAP-25 but, as expected, BoNT/A only slightly reduced 1 µM CAP evoked CGRP release (Fig. 3.13 B). However, upon lowering [CAP] the release was significantly inhibited: for BoNT/A-treated cells exposed to 0.02, 0.1, and 0.3 µM CAP,

CGRP exocytosis reached only 37%, 70%, and 82% of control levels, respectively (Fig. 3.13 B). By contrast, /E cleaving toxins cleaved 63 and 77% of SNAP-25 (for LC/E-BoNT/A and BoNT/EA, respectively) and both significantly ($p<0.0001$) blocked CGRP release stimulated by all [CAP] (Fig. 3.13 A, B).

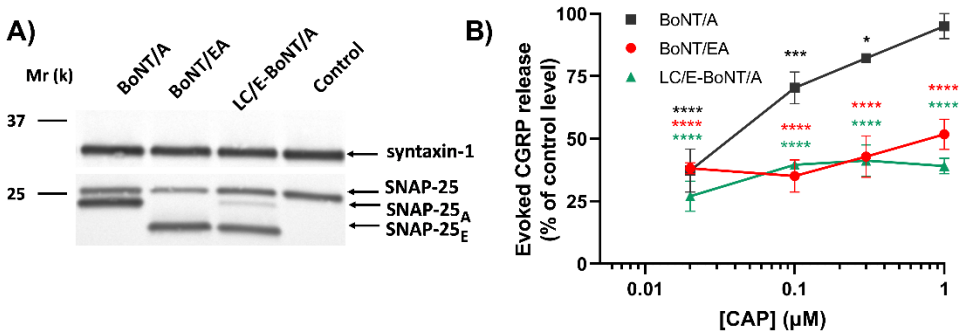

Figure 3.13 BoNT/A, BoNT/EA and LC/E-BoNT/A extensively cleave SNAP-25; the efficacy of BoNT/A in the blockade of CAP-evoked exocytosis declines upon increasing [CAP], while /E-cleaving toxins diminish the neuropeptide exocytosis stimulated by all [CAP]

(A) Western blot of 1x LDS-solubilised lysates of cells that had been pre-incubated for 48 h in the absence (control) or presence of 100 nM of the indicated BoNTs, using an antibody recognising intact SNAP-25 and cleavage products of BoNT/A (SNAP-25_A) or of chimeras containing /E protease (SNAP-25_E). The blot was additionally probed with an antibody to syntaxin-1 to confirm equality of the amount of protein loaded. (B) The amounts of CGRP released, evoked during 30 min. by [CAP] from TGNs pre-treated with the toxins as above, are expressed as % of requisite control values for this experiment (7.3±1.2, 33.6±2.8, 24±3.3, and 13.3±2.1% of total CGRP for 0.02, 0.1, 0.3 and 1 µM CAP, respectively). One-way ANOVA with Bonferroni's *post hoc* test was applied to test the significance of the difference between toxin treated cells and control. * $p<0.05$, *** $p<0.001$, **** $p<0.0001$. This figure was modified from (Antoniazzi et al., 2022).

In summary, these experiments revealed that the efficacy of BoNT/A in blocking CGRP exocytosis from sensory TGNs depends on the level of TRPV1 activation and associated increases in $[Ca^{2+}]_i$.

3.3 Discussion

3.3.1 Cultured TGNs from neonatal rats contain the proteins required for CGRP exocytosis

Trigeminal ganglia play a central role in migraine pathophysiology. Its sensory neurons express pain transducing TRP channels, and when activated release neurotransmitters [reviewed in (Benemei and Dussor, 2019)]. Neonatal rat cultured TG neurons are commonly used to study the molecular mechanisms involved in pain signalling (Kress and Reeh, 1996). Immuno-cytochemistry verified that a substantial

proportion of these neurons expressed CGRP (Fig. 3.2) and all the CGRP-positive cells contained a pain related channel TRPV1. Importantly, a member of the neuronal SNARE complex SNAP-25 (Fig. 3.2), which is critical for membrane fusion and the unique substrate for both BoNT/A and /E that inhibit potently that reaction, was also present in CGRP-TRPV1 positive cells (Fig. 3.3) Therefore, TGNs contain the requisite molecular components to investigate CGRP exocytosis evoked by stimulation of TRPV1 channels and inhibiton by /A and /E BoNTs.

3.3.2 CAP evokes dose-dependent increases of $[Ca^{2+}]_i$, but CGRP exocytosis displays a more complex relationship to [CAP]

Activation by CAP causes the opening of an ion pore in TRPV1 that allows Ca^{2+} to flood inwards due to its much higher concentration outside the cell. This leads to a rapid increase in its intracellular concentration, which is sensed by synaptotagmin on CGRP-containing LDCVs within the vicinity. Binding of Ca^{2+} to synaptotagmin initiates a sequence of molecular reactions that culminate in the promotion of complex formation by unstructured (at least partially) SNAREs, SNAP-25, syntaxin-1, and VAMP/synaptobrevin (Martens and McMahon, 2008), (Sudhof, 2014). The formation of SNARE complexes at the interface between LDCVs and the plasmalemma provides the energy that drives the fusion of their membranes, resulting in the release of CGRP from the neurons (Martens and McMahon, 2008). This process is discussed in more detail below. In the current study, it was demonstrated that the average increase of $[Ca^{2+}]_i$ (as reflected by mean changes in fluorescence intensity) within individual cells, and the number of cells with a detectable increase in $[Ca^{2+}]_i$, depend on the CAP concentration applied (Fig. 3.5 A). This accords with the concentration-dependent elevation by CAP of $[Ca^{2+}]_i$ observed in cultured DRG neurons (Cholewinski et al., 1993) and DRG explants of *pirt*-GCaMP3 mice (Lawrence et al., 2021b). By contrast, the CAP dose-response dependency for CGRP release revealed a more complex relationship. Stimulation of TGNs with 0.01-0.1 μM CAP gave the expected dose-dependent increases in Ca^{2+}-dependent exocytosis of the pain-mediating peptide, with a maximum of 37% of the cell total being released from cells by 0.1 μM CAP. Notably, such CGRP levels equate to the amounts evoked by depolarisation, indicating that 0.1 μM CAP stimulated the release of available CGRP. However, at higher concentrations, 0.25-10 μM CAP, the fraction of CGRP exocytosed decreased (despite the continued dose-dependent increases in $[Ca^{2+}]_i$ up to 1 μM CAP noted above). A similar bell-shaped CAP dose-response relationship,

with maximum release of CGRP at 0.1 μM CAP, was observed in cultures of TGNs from adult rats (Price et al., 2005). The decline in CGRP secretion at high concentrations of CAP seems to be suggestive of the exocytotic process being refractory to high $[Ca^{2+}]_i$. Indeed, an equivalent effect is apparent in adrenal chromaffin cells permeabilised by electrical discharges; lower amounts of catecholamines were released from those permeabilised in the presence of 1 mM Ca^{2+} compared to lesser concentrations (Baker and Knight, 1978). Furthermore, the latter study indicates that it is the intracellular machinery for Ca^{2+}-dependent fusion of vesicles loaded with chemical transmitters that is refractory to high $[Ca^{2+}]$.

3.3.3 BoNT/A inhibits CGRP exocytosis evoked by low, but not high, [CAP]; /E-cleaving chimeras retain their effectiveness against increasing concentration of the vanilloid

In this study, it is shown that the ability of BoNT/A to inhibit CAP-evoked CGRP exocytosis also depend on the concentration of the TRPV1 agonist used. At relatively low [CAP] (0.02 μM), prior incubation of the TGNs with 100 nM BoNT/A reduced the evoked release of neuropeptide, broadly in line with the extent to which its protease had truncated SNAP-25 to a shortened product, $SNAP\text{-}25_A$ (Fig. 3.13). However, BoNT/A pre-treatment proved less effective in reducing the larger amount of CGRP release elicited by the maximally effective concentration of 0.1 μM. Furthermore, further rises in [CAP] continued to evoke more the neuropeptide secretion from BoNT/A-treated cells (Fig. 3.13 B), despite the previously noted decline in neuropeptide release from non-intoxicated cells at the same [CAP] (Fig. 3.9 A). The ineffectiveness of BoNT/A in blocking the release triggered by the higher concentrations of stimulant might be related to the known ability of 1 μM CAP to cause a rapid, prolonged, and large elevation of $[Ca^{2+}]_i$ in TGNs [(Meng et al., 2009) and Fig. 3.5 B, C]; this seems to allow exocytosis under such exceptional circumstances to be mediated by $SNAP\text{-}25_A$. In this regard, it is highly pertinent that $SNAP\text{-}25_A$ remains capable of forming stable complexes (albeit less so than those formed with intact SNAP-25) with the other SNARE partners required for exocytosis (Meng et al., 2009), (Meng et al., 2014), (Hayashi et al., 1994) that can be disassembled by NFS (Otto et al., 1995). Furthermore, the C-terminus of SNAP-25 interacts directly with cytoplasmic domains of the Ca^{2+}-binding, vesicular membrane protein synaptotagmin 1. This association is $[Ca^{2+}]_i$-dependent and the removal of 9 C-terminal residues from SNAP-25 by BoNT/A does not prevent such binding but shifts

the $[Ca^{2+}]_i$-dependency of the interaction rightwards to higher concentrations of the cation. This accords with reports using permeabilised neuroendocrine cells, a format that enables delivery of tightly controlled buffered concentrations of Ca^{2+} directly to the cytoplasm, that BoNT/A decreased the sensitivity to Ca^{2+} of the apparatus for neurotransmitter exocytosis. Consequentially, the neurotoxin inhibited transmitter exocytosis evoked by relatively low (sub-micromolar) Ca^{2+} but was less effective as the cation concentration was increased through the micromolar range (Zhang et al., 2002), (Gerona et al., 2000). Notably, this proposal also explains why raising $[Ca^{2+}]_i$ with an ionophore reverses the inhibition by BoNT/A of transmitter release from both TGNs and motor nerves (Meng et al., 2009), (Meng et al., 2014), (Molgo and Thesleff, 1984).

BoNT/E, like BoNT/A, cleaves a peptide bond at the C-terminus of SNAP-25 but removes a larger 26 residue fragment. The latter encompasses approximately half the residues of a so-called 'SNARE' domain. This is a characteristic coiled-coil forming region. SNAP-25 contains two SNARE domains, one at its N-terminus in addition to the C-terminal region already mentioned. These bind together with two other SNARE domains, one from syntaxin-1 and the other from VAMP, to form a bundle of four helices wound around each other in a super-helix; this is the classic four-helix bundle of the ternary SNARE complex typically illustrated in textbooks. The formation of the ternary SNARE complex releases a large amount of energy (harnessed to catalyse membrane fusion) as many hydrogen bonds are formed within individual helices and hydrophobic interactions are established between helices at their interacting faces. Consequently, the ternary SNARE complex is a low energy, very stable structure. In fact, it is highly resistant to denaturation even in the presence of the ionic detergent sodium dodecyl sulphate (SDS) and, indeed, the SNAREs can only be separated by heating (to >65 °C) in the presence of SDS. The removal of 9 C-terminal residues from SNAP-25 by BoNT/A does not prevent the formation of the SDS-resistant ternary SNARE complex and has only a minor effect on its stability. By contrast, the SNAP-25 product of proteolysis by BoNT/E lacking 26 C-terminal residues is unable to form a SDS-resistant complex, though it can still bind to its cognate SNARE partners via its N-terminal SNARE domain and the remnant portion of its C-terminal domain. Moreover, the 17 extra residues removed by BoNT/E (in addition to the 9 taken off by BoNT/A) contains more of the amino acids essential for the Ca^{2+}-dependent interaction of SNAP-25 with synaptotagmin. The outcome is that BoNT/E abolishes Ca^{2+}-dependent interactions

between synaptotagmin and SNAP-25 (Gerona et al., 2000) and, even though some Ca^{2+}-independent associations remain, it is not possible to overcome the inhibition exerted by BoNT/E by simply raising the [Ca^{2+}] concentration applied to permeabilised neuroendocrine cells or by using ionophores to increase $[Ca^{2+}]_i$ in TGNs. Remarkably, it has been shown using permeabilised neuroendocrine cells that Ca^{2+}-dependent transmitter exocytosis can be restored after its abolition with BoNT/E by the application *in trans* of a polypeptide corresponding to the full length of the C-terminal SNARE domain, elegantly demonstrating the link between the formation of the (SDS-resistant) ternary SNARE complex and catalysis of membrane fusion (Chen et al., 1999). Later studies showed that BoNT/A slows vesicle fusion, even at high $[Ca^{2+}]_i$, whereas, BoNT/E acts at an earlier stage to prevent the complex formation and transmitter release (Khounlo et al., 2017), (Sakaba et al., 2005). Accordingly, herein it is demonstrated that deleting 26 residues from SNAP-25 with LC/E-BoNT/A or BoNT/EA diminished the CGRP release elicited by all the CAP concentrations (Fig. 3.13 B). Likewise, /EA prevents vesicle exocytosis induced by 1 μM of the stimulus, as hinted previously by labelling live TGNs with a tagged marker of exo-/endo-cytosis, antibodies directed against a luminal domain of synaptotagmin I (Syt-Ecto) (Meng et al., 2009). Moreover, electrophysiological recordings in brain stem slices containing sensory neurons proved compatible with the proposal that BoNT/EA, unlike /A, eliminates the excitatory effects of CGRP that result from CAP activating TRPV1 (Meng et al., 2009). Finally, the release of CGRP evoked from TGNs with 1 μM CAP is known to be inhibited by a chimera composed of LC/E attached to a protease-inactive mutant of BoNT/A, termed LC/E-BoTIM/A (Wang et al., 2011). In short, CGRP exocytosis elicited by high concentrations of the TRPV1 activator CAP clearly cannot be mediated by $SNAP\text{-}25_E$.

4 NGF enhances CGRP release evoked by CAP in cultured TGNs which is differently inhibited by SNAP-25 cleaving BoNTs

4.1 Overview

4.1.1 Attenuation of NGF-TrkA signalling is an attractive option for pain management

NGF is a neurotrophin, a protein implicated in the development and differentiation of sensory and sympathetic neurons as well as some neuron types in the CNS. During the early stages of development, it regulates the survival, growth, and density of sensory neuron fibres in peripheral tissues. In humans, congenital loss or impairment of NGF signalling results in a failure to develop peripheral sensory and autonomic neurons, and NGF-dependent central neurons, a condition termed hereditary sensory and autonomic neuropathy (HSAN). Dysfunctional NGF signalling causes HSAN types 4 and 5 characterised by a chronic inability to sense pain (congenital insensitivity to pain, or CIP), often accompanied by complete or partial anhidrosis (CIP with anhidrosis, CIPA) and intellectual deficits (McKelvey et al., 2013). In rodents, it was shown that the dependence on NGF for the survival of sensory neurons is lost after one to two postnatal weeks and in adults its role switches from neuron survival to modulation of sensation (Denk et al., 2017).

NGF has two receptors: the higher affinity tropomyosin receptor kinase A (TrkA) and lower affinity p75 neurotrophin receptor (p75NR) (Denk et al., 2017), (Barker et al., 2020). TrkA is a member of Trk family, which also includes TrkB and TrkC. These are all receptors for members of the neurotrophin family: brain-derived neurotrophic factor (BDNF) and neurotrophin 3 which activate TrkB and TrkC, respectively (Huang and Reichardt, 2003). TrkA is expressed predominantly in nociceptors: it has been detected in cutaneous, muscle, and visceral fibres of the sensory neurons (McMahon et al., 1994). Transgenic mice with KO of genes encoding either NGF or TrkA display a loss compared to wild-type of over 70% of the small-diameter neurons of the TG and DRG, which are considered to be nociceptors. These KO animals also had a reduced sensitivity to noxious heat and mechanical insults (Crowley et al., 1994), (Smeyne et al., 1994), providing solid evidence of a critical role for NGF in pain perception. Unlike in TrkA-KO mice, p75NR-KO mice still develop acute mechanical and heat hyperalgesia after subcutaneous administration of NGF (Bergmann et al., 1998), indicating that TrkA-mediated signalling is more important in nociceptor sensitisation.

4.1.2 NGF is a critical component in acute and chronic pain

Experiments *in vitro* showed that NGF rapidly (in 2-10 minutes) sensitises sensory neurons and enhances currents and Ca^{2+} influx evoked by noxious heat (Galoyan et al., 2003), CAP (Shu and Mendell, 1999), (Bonnington and McNaughton, 2003), (Zhu and Oxford, 2007), and mechanical stimuli (Di Castro et al., 2006). This observation was supported with *in vivo* studies, where a single subcutaneous administration of NGF resulted in persistent local hyperalgesia and/or allodynia in rodents and humans (Barker et al., 2020).

Elevated NGF levels were also observed in injury and inflammatory pain models in rodents (Woolf, 1996) and chronic pain conditions such as osteoarthritis, low back pain, interstitial cystitis, rheumatoid arthritis, and spondyloarthritis in humans (Denk et al., 2017), (Barker et al., 2020). In a complete Freund's adjuvant (CFA) induced model of inflammatory pain, cutaneous injection of anti-NGF antibodies 1 h before and 24 h after CFA administration reduced model-associated mechanical and thermal hypersensitivity in rats (Woolf et al., 1994).

Based on these findings, modulation of NGF/TrkA signalling pathways became an attractive target for chronic pain management. NGF neutralising antibodies were suggested as analgesic treatments for osteoarthritis (Tanezumab, Fulranumab) and lower back chronic pain (Fasinumab). Although anti-NGF treatment showed pain reduction in patients with osteoarthritis in clinical trials phase II and III, a small number of participants that also received non-steroidal anti-inflammatory drugs (NSAIDs) alongside anti-NGF therapy developed progressive osteoarthritis as a side effect (Schnitzer and Marks, 2015), (Denk et al., 2017). Trials were halted and only after careful consideration they have been started again with inclusion of radiographic screening and avoidance of concomitant use of anti-NGF therapy and NSAIDs. Another approach to modulate the NGF signalling pathway is based on inhibition of TrkA with small-molecule antagonists. One of such compounds ONO-4474, a non-selective antagonist of TrkA, TrkB and TrkC, showed an analgesic effect in clinical trials in patients with osteoarthritis (Ishiguro et al., 2020). However, participants received the drug orally and it has not been tested yet if prolonged inhibition of TrkB and TrkC, which promote neuronal survival in CNS, might cause side effects.

Overall, modulation of NGF/TrkA signalling pathways is an attractive goal for pain management. However, to avoid the side effects described above, other components of the NGF-induced sensitisation cascade could be considered as targets for anti-nociceptive management.

4.1.3 NGF rapidly sensitises TRPV1 through TrkA-mediated pathways

Rapid NGF-induced increases in signalling induced by noxious heat and CAP indicated the involvement of TRPV1 channels in nociceptor sensitisation (Shu and Mendell, 1999), (Zhang et al., 2005), (Stein et al., 2006), (Bonnington and McNaughton, 2003). Using pharmacological modulation of NGF/TrkA pathways in heterologous systems and cultured DRG neurons, three mechanisms of TRPV1 potentiation were established. These are (1) modulation of TRPV1 channel-opening probability (Chuang et al., 2001); (2) prevention of agonist-induced desensitisation (Huang et al., 2006b); (3) fast mobilisation of additional channels from intracellular stores to the neuronal membrane (Zhang et al., 2005), (Camprubi-Robles et al., 2009).

All three mechanisms involve phosphorylation of TRPV1, but at different sites. Phosphorylation at Y200 increases trafficking of TRPV1 to the cell membrane, whereas phosphate addition to serines S502 and S801 alters channel opening probability (Fig. 4.1).

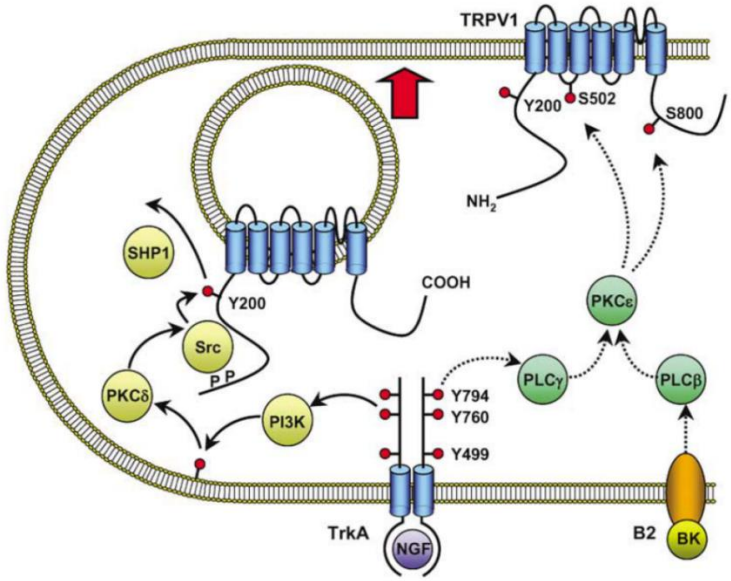

Figure 4.1 NGF acutely sensitises TRPV1 channels
NGF binds to TrkA and activates the PI3K signalling pathway, which leads to phosphorylation of TRPV1 Y200 and trafficking of new channels to the cell surface. NGF-TrkA also activates PLCγ, which via PLCε initiates phosphorylation of S502 and S801 of cell surface TRPV1. This alters channel opening probability

and additionally sustains TRPV1 activity by suppressing its desensitisation. Another pro-inflammatory agent bradykinin (BK) also sensitises surface TRPV1 by phosphorylation of S502 and S801 via PLCβ and PLCε (pathway shown at the lower right of the illustration [adopted from (Zhang et al., 2005)]. Note that numbers beside TrkA indicate residues phosphorylated in the rat isoform, which differ from the positions of the respective phosphorylation sites of human TrkA.

In cultured DRGNs a small peptide (DD04107), which was patterned after the N-terminal domain of SNAP-25 and interferes with the formation of SNARE complexes, reduced surface expression of TRPV1 after acute treatment with the neurotrophin (Camprubi-Robles et al., 2009). Therefore, it seems that attenuation of peripheral sensitisation evoked by NGF could be achieved by disruption of the TRPV1 delivery to the cell surface by regulated exocytosis.

4.2 Results

4.2.1 NGF receptor TrkA, CGRP, and TRV1 are co-expressed by TGNs in vitro

Double co-staining with immunoglobulins against NF-200 and TrkA revealed that the latter was present on all cells which had a positive signal for the neuronal marker (Fig. 4.2 A, B). Such abundant expression of NGF receptor in established cultures agrees with its role as a survival factor for sensory neurons during early development (Barker et al., 2020).

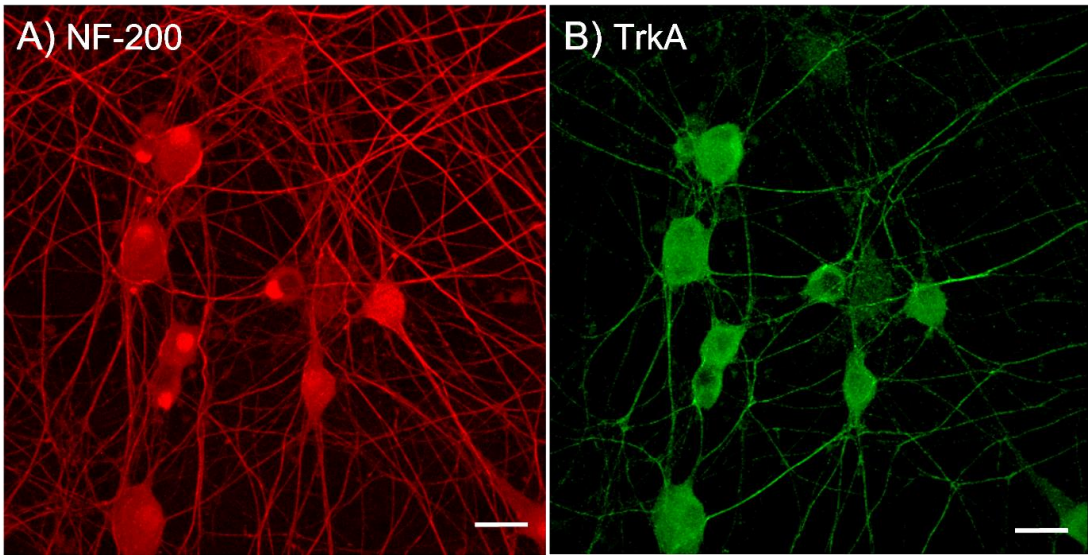

Figure 4.2 The NGF receptor TrkA is found on all NF200-expressing neonatal TGNs *in vitro*
Fixed TGNs were counter-stained with (A) anti-NF-200 and (B) anti-TrkA primary antibodies (2.1.3). After overnight incubation, primary antibodies were removed and TGNs were exposed to the secondary antibodies Alexa-Fluor® 633 (red) and Alexa-Fluor® 488 (green) (anti-mouse and -rabbit, respectively; 1:1000). Scale bar 20 µm. Labeling and confocal imaging was performed by Dr Tomas Zurawski

Considering ubiquitous distribution of TrkA in cultured TGNs, all TRPV1 and CGRP immune-positive cells also expressed NGF receptor (Fig. 4.3 A-D).

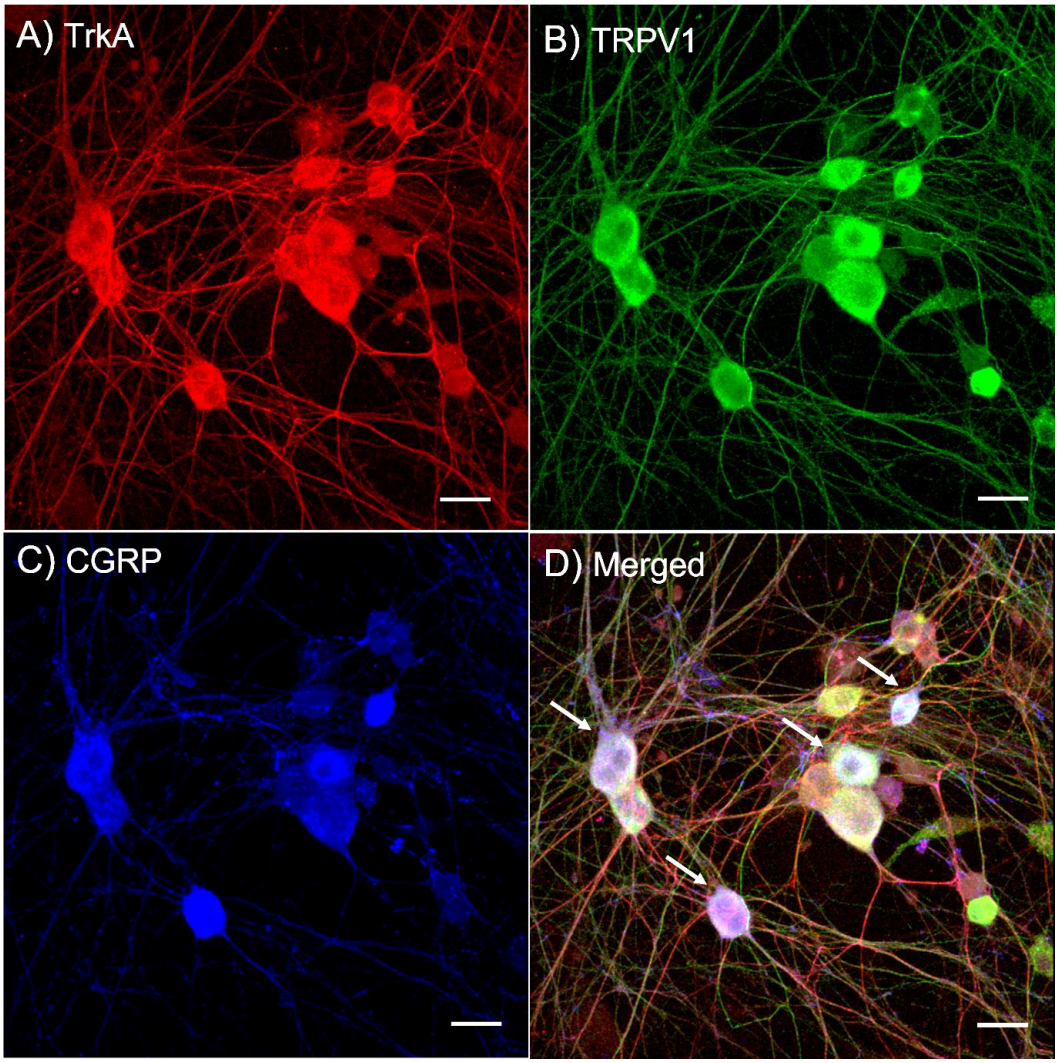

Figure 4.3 CGRP immuno-positive TGNs also contain TRPV1 and the TrkA NGF receptor
Cultured TGNs after 9 DIV were subjected to triple immuno-fluorescence staining with to the following antibodies: (A) TrkA, (B) TRPV1, and (C) CGRP (see 2.1.3). Cells were washed and exposed to secondary antibodies: Alexa-Fluor® 488, Alexa-Fluor® 555, and Alexa-Fluor® 633. (D) Merged image revealing co-expression of CGRP, TRPV1, and TrkA in the same cells (some examples are indicated by white arrows). Scale bar 20 µm. Labeling and confocal imaging was performed by Dr Tomas Zurawski.

4.2.2 NGF deprivation from neonatal TGNs in cultures reduces CAP-evoked CGRP release

As stated in Section 4.1, sensory neurons from neonatal rodents require NGF for growth and survival. However, continuous exposure of the cells to NGF could mask its acute effect on TRPV1 potentiation. Hence, it was essential to establish conditions under which sensory neurons could be grown without compromising cell survival whilst any effects of acute exposure to the neurotrophin would be highlighted.

To achieve this goal, in a pilot experiment, TGNs were cultured with NGF for two days enabling them to grow neurites and establish a neuropil before transfer into "starvation" cell medium (Table 2.2) lacking NGF but containing neutralising anti-NGF antibodies to remove any traces of functional growth factor (Bonnington and McNaughton, 2003). Cells were maintained without the neurotrophin (further referred to as 'starved') for between one to four days before determining total protein, total CGRP, and 0.02 µM CAP-evoked CGRP release (the EC_{50} for CGRP release determined previously, Fig. 3.9). The values obtained for each parameter were compared with the corresponding amounts in cells continuously exposed to NGF for equivalent periods (referred to as 'fed'), which served as controls. Starvation without NGF did not dramatically alter the total protein in cultures, suggesting a lack of cell death, at least up to day 4 when protein levels were lower than in control cells (Fig. 4.4 A). Although the levels of the neuropeptide seemed to decline from day 3 in both fed and starved groups (Fig. 4.4 B), there was no dramatic change in total CGRP relative to fed cells after growth factor withdrawal. More remarkably, within one day of NGF deprivation, the amount of CGRP release stimulated by 0.02 µM CAP was significantly ($p=0.001$) suppressed relative to control cells continuously maintained with NGF (Fig. 4.4 C). A maximum reduction (>50% from the CGRP levels in fed TGNs) in stimulated CGRP release was achieved by day 2 and remained the same on days 3 and 4 (Fig. 4.4 C). Therefore, two days without NGF was considered an optimal period for NGF deprivation because this achieves a maximum reduction in sensitivity to CAP without compromising the levels of total protein and CGRP relative to control cells.

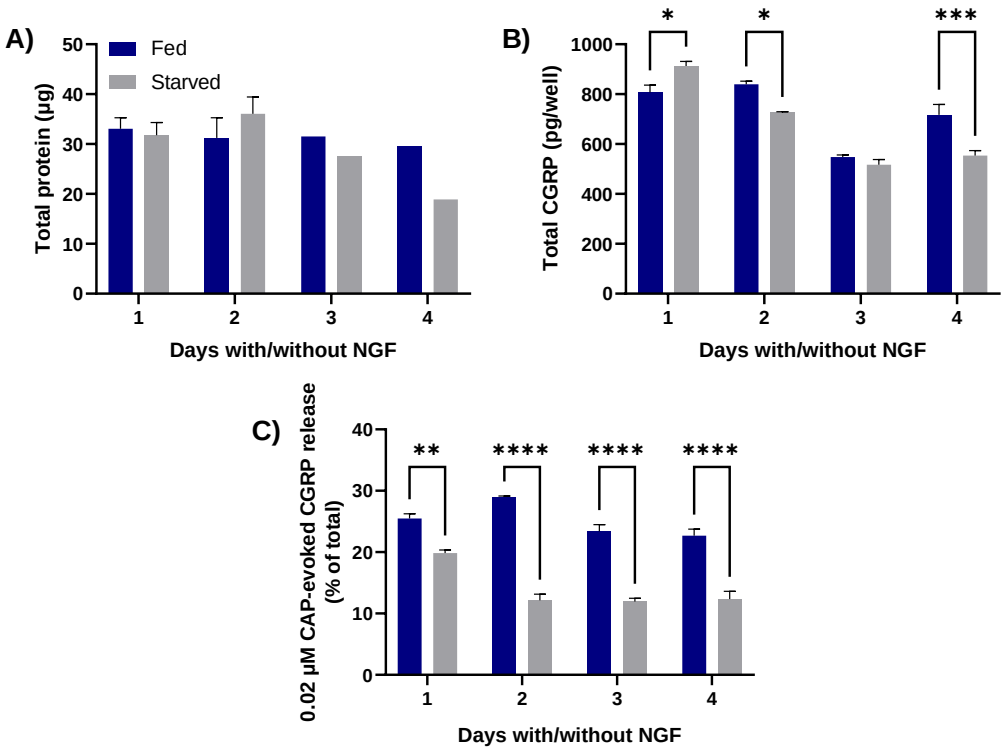

Figure 4.4 NGF withdrawal for 1 to 4 days from cultured TGNs causes reductions of protein content, CGRP and CAP-stimulated CGRP release

TGNs from neonatal rats were cultured in the presence of 50 ng/ml NGF for two days before transferring one cohort to cell medium lacking the neurotrophin and supplemented with 500 ng/ml anti-NGF antibodies (see 2.1.3); another cohort remained in cell medium containing 50 ng/ml NGF. The two cohorts were maintained as described for a further one to four days before stimulation of CGRP release by 0.02 µM CAP. Then cells were lysed in 1% Triton X-100 before quantification of (A) protein by BCA assay, (B) total CGRP and (C) CAP-evoked neuropeptide release by ELISA. Data presented as mean + s.e.m., N=1, n=3, except for day 3 and 4 without NGF in panel (A) where n=1. Two-way ANOVA with Bonferroni multiple comparisons test was applied to panels B and C. ** p<0.01 *** p<0.001, **** p<0.0001.

Another independent set of experiments confirmed that 2 days of NGF starvation had no significant effect on total protein in fed and starved cells (27.3±2.7 vs 24.0±2.4 µg/well, respectively, [mean±s.e.m.]; p=0.38) or total CGRP (1293±125 [fed] vs 1339±127 [starved] pg/well; p=0.8) (Fig. 4.5 B, C). By contrast, NGF deprivation reduced spontaneous CGRP release compared to the levels obtained in fed cultures (0.88±0.06% of total CGRP vs 1.19±0.09%, p=0.009 in starved and fed cells respectively) (Fig. 4.5 D). Likewise, CAP-evoked CGRP release was also ~2-fold reduced in starved cultures (from 16.8±2.7 to 7.7±1.2% of total CGRP; p=0.007) (Fig. 4.5 E). Therefore, the established protocol of 2 days NGF starvation proved to be reproducible.

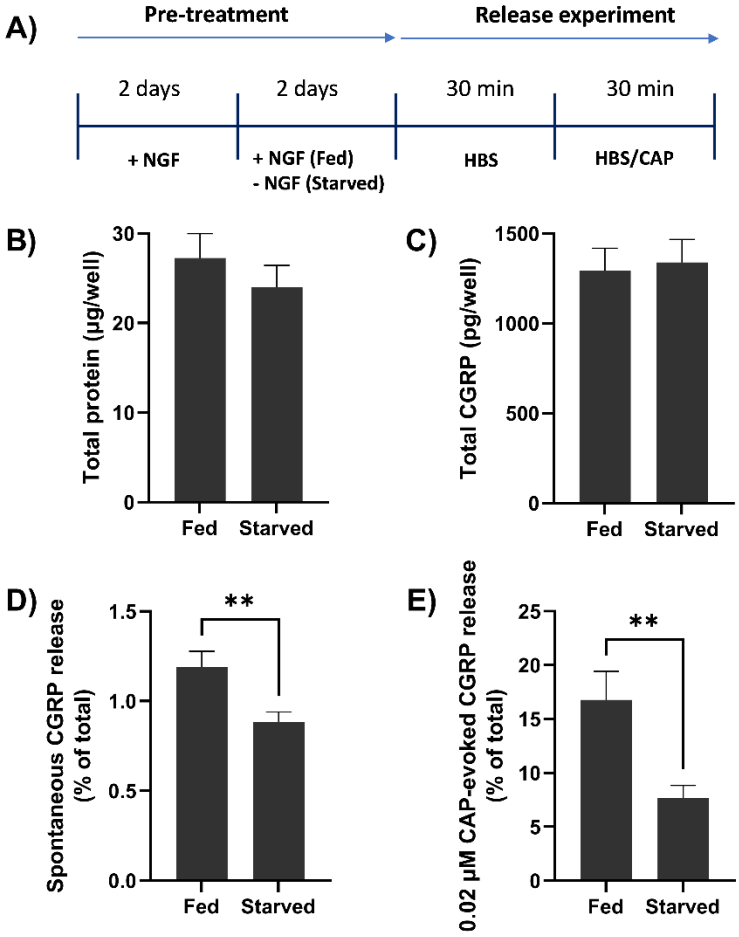

Figure 4.5 Deprival of NGF for 2 days does not significantly alter total protein or CGRP levels in rat cultured TGNs, but reduces both spontaneous and CAP-evoked exocytosis of the neuropeptide
(A) Schematic illustrating the experimental protocol. Rat TGNs were cultivated initially in the presence of 50 ng/ml NGF for 2 days before its withdrawal from half of the wells (starved) or retention for the other cohort over the 4 days (fed). The amounts of CGRP released were quantified during sequential 30 min. exposures, firstly to (D) HBS only (spontaneous release), and then to (E) 0.02 µM CAP in HBS. At the end of experiments, cells were solubilised with 1% (v/v) Triton X-100 in HBS, then total protein (B) and CGRP contents (C) were determined, as detailed in Materials and Methods. Data are presented as mean + s.e.m., N=3, n≥12. Asterisks summarise the results of unpaired t-tests with Welch's correction, ** $p<0.01$ (Belinskaia et al., 2022).

4.2.3 NGF withdrawal from cultured TGNs lowers the amounts of CGRP release evoked by various CAP concentrations

Next, starved and fed cells were exposed to a range of increasing [CAP]: 0.01, 0.025, 0.035, 0.05, 0.1, 0.3, 1 µM, using a slightly modified protocol involving an additional 30 min. incubation with HBS to facilitate acute exposure to NGF (described below) before CAP stimulation (Fig. 4.6 A). As described previously for cells continuously fed with NGF (Fig. 3.9), the dose-response relationship for stimulation of CGRP exocytosis by CAP displayed a bell-shaped pattern in starved and fed cells (Fig.

4.6 B). The inclining phase of each dose-response curve was fit with four-parameter function in the range from 0.01 to 0.1 µM. Importantly, in the starved cells the amounts of CGRP released at each [CAP] were lower than in fed cells exposed to the same concentrations. Moreover, the maximum response at 0.1 µM CAP in the former was 1.5-times lower in starved cells compared to fed (25.2±2.1 vs 37.3±7.1% of the total in starved and fed, respectively). NGF starvation induced a small but just significant increase in EC_{50} values (40.9±1.8 vs 32.6±1.7 in fed cells, p=0.045). The results demonstrate that NGF deprivation from neonatal cultures for 48 h reduces their apparent sensitivity to CAP and the fraction of total CGRP released (Belinskaia et al., 2022).

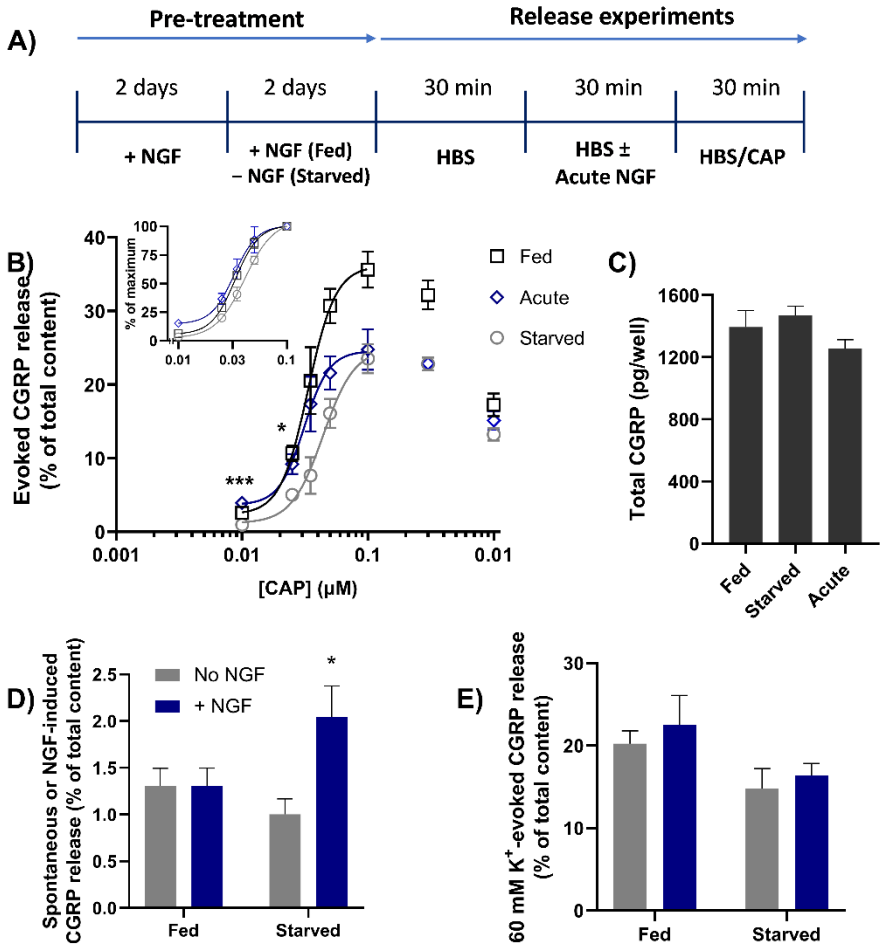

Figure 4.6 NGF withdrawal for 2 days from cultured TGNs decreases CGRP release stimulated by CAP; acute NGF induces exocytosis and enhances that stimulated with low [CAP]

(A) Timeline for pre-treatment and experimental manipulations of TGNs to determine the effect of NGF starvation and its brief re-introduction (100 ng/ml) on CGRP release under requisite conditions. (B) Dose-response relationship between [CAP] and CGRP release expressed as a % of total. Asterisks show significant differences between starved and NGF acutely treated cells (*p<0.05, ***p<0.001, n=8, N≥3, one-way ANOVA followed by Bonferroni's *post hoc* test). Insert: The data obtained with 0.01-0.1 µM CAP replotted as a % of the requisite maximum release evoked by 0.1 µM CAP. (C) Total CGRP contents.

(D) Spontaneous or NGF-induced CGRP released from fed and starved cells (as indicated on abscissa) during the second of three 30 min. periods during which they were exposed to HBS only (grey bars) or HBS containing 100 ng/ml NGF (blue bars). Exposure of starved (but not fed) cells to NGF induced a significant increase in CGRP release (*p<0.05, n=9, N=3, unpaired two-tailed Welch test). (E) In separate experiments, TGNs were incubated for 30 min. with/without NGF and then stimulated with HBS-HK. Data is presented as mean+s.e.m. (Belinskaia et al., 2022)

4.2.4 In starved neonatal TGNs, brief exposure to NGF raises CGRP release and augments the amount exocytosed in response to subsequent stimulation with CAP

It has been established that brief exposure of 2 days-starved DRGNs from neonatal rodents enhances CAP-evoked currents and increases $[Ca^{2+}]_i$ by potentiation of TRPV1 activity (Bonnington and McNaughton, 2003), (Zhu and Oxford, 2007). To determine the outcome of acutely exposing starved cells to NGF for CAP-evoked CGRP release, the experimental protocol was extended to include another 30 min. period of incubation with 100 ng/ml NGF before exposure to CAP. In the control group, cells were incubated with a mixture of 0.1% DMEM in HBS, which served as a vehicle for NGF. In starved TGNs, 30 min. with 100 ng/ml NGF did not alter the total CGRP (Fig. 4.6 C, 'Acute') but induced a 2-fold increase in CGRP release relative to the amount secreted spontaneously (from 1% to 2% of total CGRP. Note, the spontaneous release was not subtracted from these values; Fig. 4.6 D). By contrast, the absence or presence of NGF during the release experiment had no impact on the levels of spontaneous CGRP release from fed cells (1.3% vs. 1.3% of total CGRP). Next, the effect of acute exposure to NGF on CAP-evoked neuropeptide secretion was probed. Immediately after the short application of NGF to the previously starved cells, they were exposed to a range of [CAP] from 0.01 to 0.1 µM. Notably, the brief re-exposure to NGF significantly reversed the starvation-associated reduction of CGRP release evoked only by low 0.01 and 0.025 µM [CAP] (p=0.001 and p=0.036 respectively, Fig. 4.6 B). For intermediate [CAP] of 0.035-0.05 µM, NGF had a partial effect, and at higher 0.1-1 µM CAP, the amounts of released CGRP were similar in NGF-treated and control cells. Fitting the inclining phase with a logistic function, as described before, confirmed that acute exposure of starved TGNs to NGF did not increase the maximum fraction of total CGRP that could be released upon stimulation with CAP (~25%) (Fig. 4.6 B). In contrast, in acutely-treated cells the EC_{50} for [CAP] was lowered from 0.041±0.002 µM (starved cells without acute NGF) to 0.032±0.004 µM (starved cells after acute exposure to NGF), marking a restoration to the sensitivity displayed by TGNs fed continuously with NGF (EC_{50}=0.033±0.002 µM) (Belinskaia et al., 2022). Hence, when CAP-evoked CGRP release was normalised to %

of maximum response (obtained at 0.1 µM), the dose-response functions were similar (Fig. 4.6 B insert; discussed in 4.3.2). The NGF-induced enhancement of CGRP release was selective for CAP-evoked signalling, because CGRP release evoked by depolarisation with HBS-HK was not significantly different from fed and starved cells (Fig. 4.6 E).

4.2.5 NGF requires extracellular Ca^{2+} for direct induction of CGRP release, but not its enhancement of CAP-evoked CGRP exocytosis

Having established that CAP-evoked CGRP release is dependent on extracellular Ca^{2+} (Fig. 3.9), but also being aware that the enhancement of TRPV1 activity following acute exposure to NGF is not (Zhu and Oxford, 2007), (Shu and Mendell, 2001), it was pertinent to investigate whether the direct induction of CGRP release by NGF (Fig. 4.6 D) requires extracellular Ca^{2+}. To answer this question, the experimental protocol was devised as illustrated (Fig. 4.7 A). After an initial period to measure the spontaneous release, starved TGNs were split into two cohorts. The first was exposed to NGF in the presence of extracellular Ca^{2+} whilst the second was incubated with the neurotrophin without added Ca^{2+} but with 2 mM EGTA to chelate any traces of this ion. After 30 min. with NGF, supernatants were removed for CGRP quantification and both neuron cohorts were transferred into bathing solution containing Ca^{2+}. Cells were then stimulated with 0.02 µM CAP for the following 30 min. in the continued presence of Ca^{2+} (Fig. 4.7 A). To confirm that NGF activates the TrkA signalling pathway in the absence of Ca^{2+}, in a separate set of experiments the ratio of total ERK1/2 to p-ERK1/2 was estimated because binding of the growth factor to TrkA triggers phosphorylation of ERK1/2 (p-ERK1/2) (see 4.1.2). For this, TGNs were pre-treated with NGF or vehicle in normal or Ca^{2+}-free HBS and immediately solubilised in 1x LDS as described in 2.2.4. The absence of Ca^{2+} during acute exposure to NGF did not prevent its induction of ERK1/2 phosphorylation (Fig. 4.7 B). In fact, acute exposure of starved cells in the absence of extracellular Ca^{2+} induced a ~4-fold increase of p-ERK1/2 ($p=0.02$), which was indistinguishable from the corresponding increase induced by NGF in the presence of Ca^{2+} (Fig. 4.7 B, C). By contrast, the absence of extracellular Ca^{2+} abolished NGF -induced CGRP release (Fig. 4.7 D). Nevertheless, an ~2.5-fold enhancement by NGF of 0.02 µM CAP-evoked CGRP release was unaffected by the presence or absence of Ca^{2+} during the 30 min. period that the cells were exposed to the neurotrophin (Fig. 4.7 E). These intriguing results (1) indicate that NGF directly stimulates the Ca^{2+}-regulated exocytosis of CGRP and, by

deduction, promotes delivery to the plasma membrane of LDCVs-associated TRPV1, (2) reveal that the latter process does not contribute to the enhancement by NGF of CAP-evoked CGRP release because this occurs by a Ca^{2+}-independent mechanism and is not perturbed to any discernible extent by a lack of NGF-induced CGRP release, (3) concur with previous reports concluding that acute exposure to NGF activates TrkA-mediated intracellular signalling via a Ca^{2+}-independent process that culminates in the sensitisation of the CAP receptor TRPV1. Further detailed interpretation of these results is provided in the Discussion section.

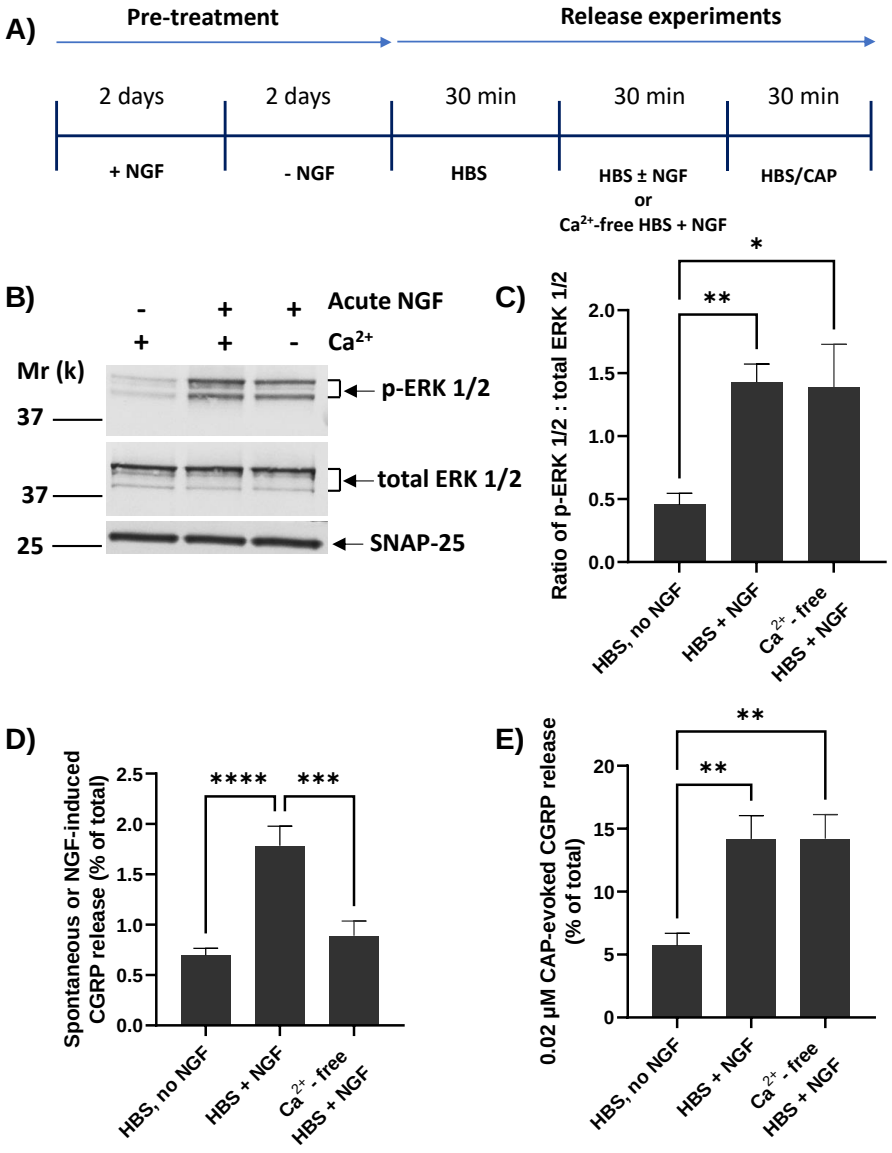

Figure 4.7 Extracellular Ca^{2+} is required for NGF to raise CGRP release but not for its enhancement of CAP-evoked Ca^{2+}-dependent exocytosis

(A) NGF-starved TGNs were exposed in sequence for three 30 min. periods as follows. In the first period, all cells were exposed to HBS only. For period 2, the cells were split into three cohorts and incubated with

Ca^{2+}/HBS modified as follows: Cohort 1, HBS only; Cohort 2, Ca^{2+}/HBS containing 100 ng/ml NGF; Cohort 3, HBS containing 100 ng/ml NGF but with Ca^{2+} replaced by 2 mM EGTA. In period 3, all cells were incubated with Ca^{2+}/HBS containing 0.02 µM CAP. (B) In a separate set of experiments, TGNs were processed as far as period 2 before being lysed in 1x LDS buffer, and the ERK phosphorylation was determined by Western blotting as detailed in the 2.2.4. (C) Histogram showing the ratio of signal intensity for p-ERK1/2 to total ERK1/2 (mean + s.e.m., n≥3, N=2), determined from the requisite immuno-reactive bands detailed in panel B. (D) Spontaneous or NGF-induced CGRP release during incubation period 2 and (E) 0.02 µM CAP-evoked CGRP release in period 3 calculated by subtracting the amount released during incubation 1, both expressed as a % of total CGRP content; n=9, N=3. For all histograms, one-way ANOVA was used followed by Bonferroni's *post hoc* test, and significance indicated with asterisks; * $p<0.05$, ** $p<0.01$, *** $p<0.001$, **** $p<0.0001$. Each column and associated error bar represent mean + s.e.m., respectively.

4.2.6 BoNT/A blocks NGF-induced and NGF-enhanced CAP-stimulated CGRP release

The demonstration that NGF-induced CGRP release is Ca^{2+}-dependent (Fig. 4.7 D) suggests that the neurotrophin might promote fusion between neuropeptide-loaded LDCVs and the plasma membrane. LDCV exocytosis is catalysed by SNARE proteins (see 1.1.3) and is highly susceptible to inhibition by a set of BoNTs. It has been shown in the current study (Fig. 3.10) and by previous members of the research group that BoNT/A effectively enters cultured TGNs, efficiently cleaves SNAP-25 and, consequently, inhibits CGRP release induced by K^+ depolarisation and low [CAP] (Fig. 3.13), (Meng et al., 2007), (Antoniazzi et al., 2022). Thus, to determine whether NGF-induced CGRP release is SNAP-25 mediated, TGNs were exposed to 100 nM of BoNT/A during the 2-day NGF starvation period (Fig. 4.8 A). Control cells were starved without neurotoxin, as normal. Consistent with previously obtained results (Fig. 3.10 A, B), exposure to the toxin led to cleavage of ~75% of the SNAP-25 present in the cells, as revealed by a reduction in the amount intact substrate, and the appearance of a faster migrating immuno-reactive band that was not observed in toxin-free control cells (Fig. 4.8 B). The total CGRP in toxin-treated TGNs displayed a small, but not significant ($p=0.22$), increment compared to control cells (Fig. 4.8 D). Spontaneous CGRP release was nearly two-fold lower in BoNT/A-treated TGNs than in toxin-free cultures (0.40±0.03 vs 0.77±0.11% of total CGRP; mean±s.e.m.; $p=0.005$), suggesting that at least some of this arises from a low level of spontaneous membrane fusion rather than non-exocytotic release (Fig. 4.8 E, grey bars). Likewise, acute NGF-induced release of CGRP was significantly ($p=0.0003$) lower in BoNT/A-intoxicated neurons relative to toxin-free controls, confirming that this also entails SNARE-dependent exocytosis (Fig. 4.8 E, blue bars). Consistent with the experiments reported above (Fig. 4.6 B), acute treatment of starved TGNs with NGF induced a significant ($p=0.006$) increment in subsequent 0.02

µM CAP-evoked release (Fig. 4.8 F). BoNT/A reduced the neurosecretion induced by TRPV1 agonist from starved cells (grey bars, p=0.001) and its enhancement by acute treatment with NGF (blue bars, p=0.005). By contrast, the neurotoxin did not abolish 1 µM CAP-stimulated CGRP release (Fig. 4.8 G, grey bars). Although the enhanced level induced after pre-treatment with NGF was not lowered significantly relative to control cells (Fig. 4.8 G, blue bars), BoNT/A did seem to lower the enhancement of 1 µM CAP-evoked CGRP release induced by NGF as the small but significant increment observed in control cells was absent.

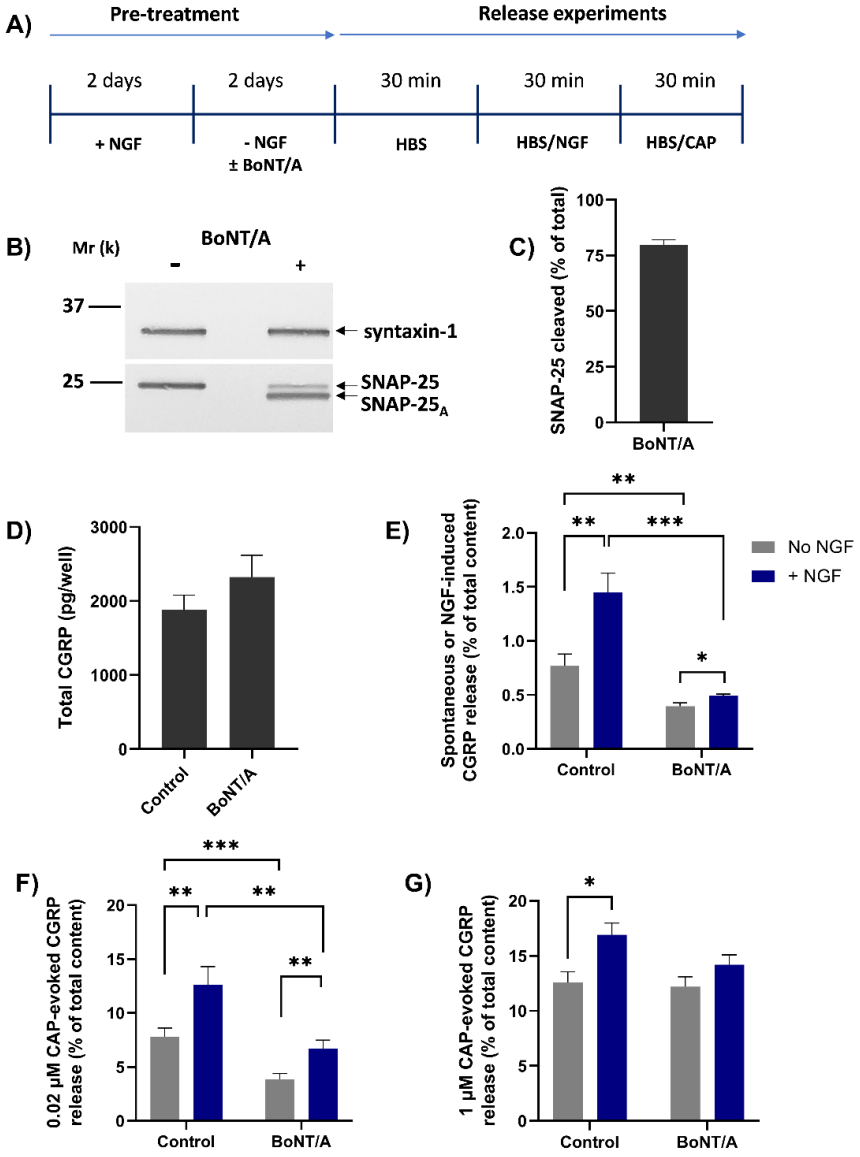

Figure 4.8 BoNT/A blocks NGF-induced CGRP-release and -enhancement of 0.02 µM but not of 1 µM CAP-evoked CGRP release

(A) After 2 days in the presence of 50 ng/ml NGF, TGNs were starved of the neurotrophin as detailed before, without or with the inclusion of 100 nM BoNT/A during this latter step. The release experiment

was performed as described in Fig. 4.6 A. (B) Representative Western Blot showing that BoNT/A cleaves SNAP-25. The bars demonstrate (C) The amount of cleaved SNAP-25 and (D) Total CGRP (pg/well). (E–G) Histograms showing for control or BoNT/A pre-treated cells: (E) spontaneous CGRP release during the second 30 min. incubation into HBS without (grey bars) or induced by 100 ng/ml NGF (blue bars), (F) during the third period evoked by 0.02 µM CAP, and (G) during the third incubation with 1 µM CAP. The data demonstrate mean + s.e.m., N=3, n=9. Asterisks summarise the results of unpaired one-tailed Welch tests applied to the data plotted in panels E, F, and G, * $p<0.05$, ** $p<0.01$, *** $p<0.001$.

4.2.7 Chimera BoNT/EA inhibits CGRP release elicited by high [CAP]

The BoNT/EA chimera was tested to ascertain whether it could cause a greater blockade than BoNT/A of CGRP release evoked by 1 µM CAP and its enhancement by acute NGF, using a protocol identical to the one described above for BoNT/A (Fig. 4.8 A). TGNs were starved of NGF and simultaneously incubated with 100 nM BoNT/EA before being briefly exposed to NGF (or control HBS) followed by stimulation with 1 µM CAP. Exposure to BoNT/EA resulted in the cleavage of more than 85% of the SNAP-25 present (Fig. 4.9 A, B). As found for BoNT/A, total CGRP content was slightly, but not significantly, increased in /EA-treated TGNs (Fig. 4.9 C) but both spontaneous CGRP exocytosis (Fig. 4.9 D, grey bars) and its elevation by NGF (Fig. 4.9 D, blue bars) were markedly reduced. Notably, pre-treatment with /EA reduced the 1 µM CAP-evoked CGRP release from NGF starved cells (Fig. 4.9 E, grey bars), unlike BoNT/A. Moreover, the enhancement of 1 µM CAP-evoked CGRP release observed in control cells after acute exposure to NGF (Fig. 4.9 E, control grey bar vs. control blue bar, $p=0.006$) was absent in TGNs pre-treated with BoNT/EA. Consequently, this chimera clearly blocked responses to 1 µM CAP and its enhancement by NGF to a much greater extent than for BoNT/A (Fig. 4.9 E, c.f. Fig. 4.8 G). These results confirm the involvement of SNARE-dependent membrane trafficking in nociceptor sensitisation by NGF, a key mediator of inflammatory pain (Belinskaia et al., 2022).

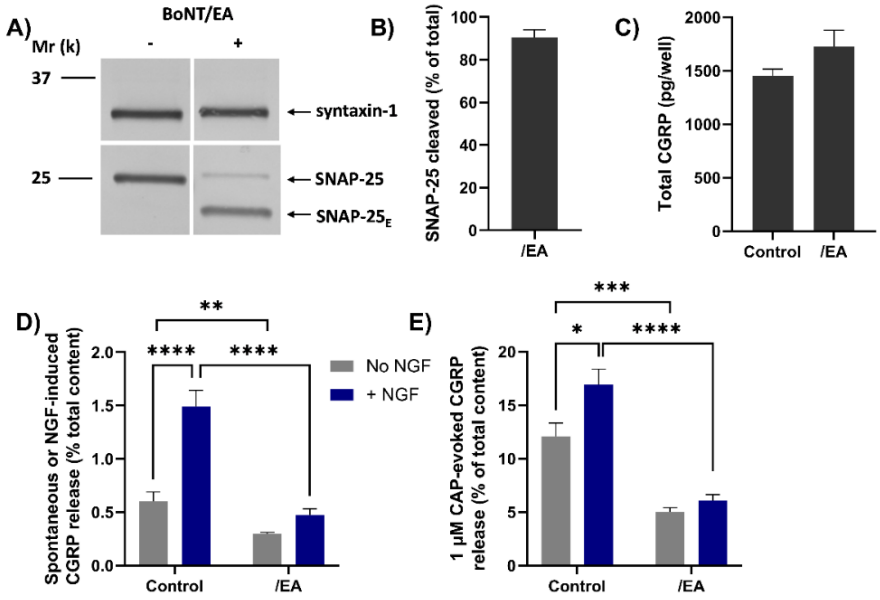

Figure 4.9 Chimera BoNT/EA effectively inhibits 1 µM CAP-evoked CGRP release from starved TGNs, and its enhancement by NGF

TGNs were starved and incubated with 100 nM BoNT/EA using a protocol identical to that described previously for BoNT/A (Fig. 4.8 A). (A) Western blotting with anti-SNAP-25 antibodies confirms the disappearance of intact SNAP-25 and the appearance of a much faster-migrating product in cells exposed to BoNT/EA (+) but not control (-). (B) Histogram displaying the % of SNAP-25 cleaved. (C) Total amounts (pg/well) of CGRP, determined as before, in control and BoNT/EA-treated cells. (D) Amounts of spontaneous CGRP release into HBS only, (grey bars), and that during incubation with 100 ng/ml NGF (blue bars), and (E) upon stimulation with 1 µM CAP (mean + s.e.m. N=3, n=9). Unpaired one-tailed Welch test was applied to the data plotted in panels C–E), * $p<0.05$, ** $p<0.01$, *** $p<0.001$, **** $p<0.0001$ (Belinskaia et al., 2022).

4.3 Discussion

4.3.1 NGF withdrawal from cultured TGNs reduces their sensitivity to CAP

A major goal of the research undertaken in this Chapter was to confirm the involvement of membrane trafficking in nociceptor sensitisation and demonstrate its suitability as a target for therapeutic interventions aimed to ameliorate the heightened pain signalling that ensues from such processes. For this purpose, a "starvation" protocol was established whereby NGF, which is essential for neonatal neurons survival (see 4.1.1) during the first 2 days *in vitro*, was removed from the cell medium for 2 days. This allowed monitoring of the acute effect on CGRP release of re-exposing neurons to the neurotrophin for a brief period at some later time; this protocol overcame masking of the acute effects of NGF by the continuous presence of this growth factor in standard culture procedures (Fig. 4.6 D). Note, that for these experiments the culture period was shortened from 7 DIV to 4, because pilot studies revealed that the younger neuron cultures

responded more robustly to acute application of NGF. Similar to the results described for TGNs fed continuously with NGF for 7 DIV (Fig. 3.9 A), TGNs fed for 4 DIV showed a bell-shaped dose-response to CAP with a maximum of ~37% of the total CGRP being released at 0.1 µM CAP. In starved cells after 48 h of NGF deprivation the amount of CGRP release evoked was depressed at all [CAP] relative to the corresponding levels from fed cells. Notably, the extent of reduction was greatest for 0.1 µM, which (like in fed cultures) also gave the peak amount of CGRP release in the starved TGNs. Importantly, starvation did not impair the expression of CGRP (i.e., total CGRP), so the latter must reflect a depressed ability of CAP to stimulate neuropeptide exocytosis from the cells deprived of NGF.

4.3.2 Brief exposure to NGF enhances CAP-evoked CGRP release from starved TGNs

Consistent with reports that brief exposure of starved DRGNs to NGF just before experimental recordings enhances CAP-induced currents and augments increases in $[Ca^{2+}]_i$ (Bonnington and McNaughton, 2003), it is shown here that acute re-introduction of NGF enhances CAP-evoked CGRP release from starved TGNs, but principally for [CAP] below 0.1 µM. As NGF is known to enhance currents elicited in cultured DRG neurons by 0.03-0.3 µM CAP and escalate the increases in $[Ca^{2+}]_i$ induced by 0.1 or 0.5 µM CAP (Bonnington and McNaughton, 2003), (Zhang et al., 2005), (Camprubi-Robles et al., 2009), it is apparent that 0.1 µM CAP induces adequate $[Ca^{2+}]_i$ for the optimum triggering of CGRP release from TGNs *in vitro*, and that this relationship is unaltered by NGF-starvation. Further increases in $[Ca^{2+}]_i$, which can be achieved using higher [CAP] ((Cholewinski et al., 1993), Fig. 3.5) or acute exposure to NGF of starved neurons (Bonnington and McNaughton, 2003), (Zhang et al., 2005), (Camprubi-Robles et al., 2009), are unable to increase CGRP release above the level evoked by 0.1 µM CAP because the latter already reached the optimum level of $[Ca^{2+}]_i$ for exocytosis. On the other hand, at [CAP] less than 0.1 µM the lower amounts of Ca^{2+} entry triggered by the vanilloid are sub-optimal for stimulating CGRP release (Fig. 4.6 B), so NGF-induced increases in CAP-evoked currents (Zhu and Oxford, 2007) and, consequently, $[Ca^{2+}]_i$ do boost CGRP release [Fig. 4.6 B; (Park et al., 2010)]. The outcome of NGF re-introduction to starved cells, therefore, is an apparent elevation in sensitivity to CAP (Fig. 4.6 B) because the boost to CGRP release, the consequence of augmented Ca^{2+} entry, is analogous to the growth in exocytosis of the neuropeptide observed when [CAP] was increased. Thus, the apparent change of sensitivity to CAP can be explained without there

being an actual alteration in affinity of the vanilloid for its receptor, TRPV1; hence, plotting normalised CGRP release (as a % of the maximum level elicited by 0.1 µM) indicated that there are minimal differences in actual CAP sensitivity between NGF-fed, -starved and -starved then acutely fed TGNs (Fig. 4.6 B insert).

That re-introduction of NGF did not reverse the suppression by starvation of maximum attainable CGRP release (i.e., elicited by 0.1 µM CAP) despite no reduction in CGRP expression is suggestive that the continuous presence of NGF in fed cells must increase the fraction of total CGRP pool available for exocytosis. As the starvation protocol also reduced the amount of CGRP released in response to depolarisation with 60 mM K^+, albeit not significantly (Fig. 4.6 E), targets of NGF signalling other than TRPV1, such as voltage-gated channels or mediators of neuropeptide exocytosis (reviewed by (Barker et al., 2020), (Denk et al., 2017)), likely contribute to maintenance of high levels of CGRP release upon long-term (i.e., 2 days) exposure to NGF. Brief re-introduction of NGF seems to enhance recruitment by lower [CAP] (<0.1 µM) of the smaller fraction of CGRP that remains available after starvation, but cannot recover the increment that appears to be lost during starvation. By contrast, acute (30 min.) exposure to NGF had no effect on 60 mM K^{+-}-depolarisation evoked CGRP release in either fed or starved cells (Fig. 4.6 E). Together, these results highlight a specific fast stimulatory action of NGF on CAP-evoked CGRP release, thereby, implicating TRPV1 as a rapidly modified target of NGF signalling in accordance with current thought (Barker et al., 2020), (Denk et al., 2017). There are various ways by which NGF can modulate TRPV1 activity to boost CAP-stimulated Ca^{2+} entry (Fig. 4.10 A), including altering channel gating and reducing desensitisation (Huang et al., 2006b). However, the main contribution seems to be trafficking of TRPV1 from intracellular organelles to increase their density on the cell surface (Fig. 4.10) (Zhang et al., 2005) and/or replace desensitised forms (Tian et al., 2019).

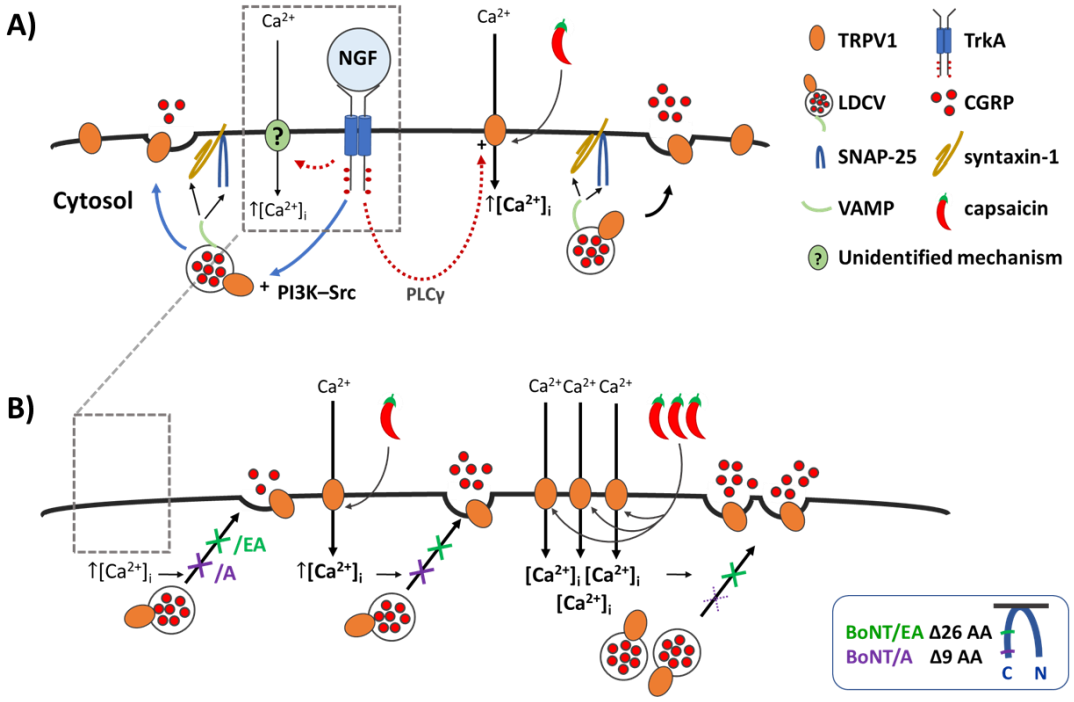

Figure 4.10 NGF induces a minor increase in Ca^{2+}- and SNARE-dependent CGRP release, whereas it greatly enhances the CAP-evoked exocytosis which is blocked by BoNT/A or /EA at low [CAP] but at higher [CAP] is only abolished by BoNT/EA

(A) Illustrates the effect of acute NGF on CGRP exocytosis from control neonatal rat TGNs starved of the neurotrophin for 2 days, and (B) in TGNs pre-treated with BoNT/A or /EA. (A) NGF binds to its receptor TrkA, activates the signalling cascades shown (Zhang et al., 2005), and induces Ca^{2+} influx by an unidentified mechanism (?). Elevated intracellular Ca^{2+} ($[Ca^{2+}]_i$) triggers the fusion of LDCVs via SNARE complexes (VAMP, syntaxin-1 and SNAP-25), thereby, causing exocytotic release of CGRP and surface delivery of vesicle constituents. This acute potentiation by NGF can involve the PI3K-Src pathway, which promotes trafficking of LDCVs, and insertion of their TRPV1 channels into the plasmalemma by Ca^{2+}-regulated exocytosis (blue arrows) c.f. (Zhang et al., 2005), (Camprubi-Robles et al., 2009). Additionally, the PLCγ cascade leads to sensitisation of TRPV1 already on the plasmalemma (red dashed arrows) (Zhang et al., 2005). The outcome of these composite influences of NGF on TRPV1 is that when the channel is activated by CAP $[Ca^{2+}]_i$ is raised even more than normally (Bonnington and McNaughton, 2003), (Zhang et al., 2005), (Camprubi-Robles et al., 2009) and this further enhances CGRP release (Fig. 4.6 B). (B) The proteases of BoNT/A and /EA delete 9 (purple line) and 26 (green line) residues from SNAP-25 (Insert), respectively, preventing the fusion of LDCVs; this blocks the minimal CGRP exocytosis elicited by NGF (arrow with crosses, left) and its enhancement of the release evoked by 0.02 µM CAP (🌶) (arrow with crosses, centre). Stronger stimulation of TRPV1 with 1 µM CAP (🌶🌶🌶) induces a lot more Ca^{2+} influx ($[Ca^{2+}]_i$, $[Ca^{2+}]_i$, $[Ca^{2+}]_i$; Fig. 3.5) which causes a moderate increase in CGRP release but overcomes the inhibition by BoNT/A (purple cross with broken lines, right) while /EA (green cross, right) remains effective in diminishing CGRP release. Acute sensitisation by NGF of TRPV1 selectively enhances neuropeptide exocytosis stimulated by low [CAP] (<0.1 µM) and only moderately affects responses to ≥0.1 µM CAP (Fig. 4.6 B). Despite being impotent against 1 µM CAP-evoked CGRP release in starved cells ((B), 🌶🌶🌶, and Fig. 4.8 G), BoNT/A partially inhibits the moderate NGF-enhancement of 1 µM CAP-evoked CGRP release (Fig. 4.8 G), implicating membrane trafficking in the sensitisation process (B, PI3K-Src stimulated pathway) in accordance with its inhibition of NGF-induced, Ca^{2+}-dependent CGRP exocytosis (Fig. 4.8 E).

4.3.3 Extracellular Ca^{2+} is not required for NGF-provoked sensitisation of TGNs to CAP but essential for CGRP release stimulated by the growth factor

NGF-induced trafficking of TRPV1 via SNARE-mediated membrane fusion in DRGNs has been evidenced using a peptide inhibitor patterned after SNAP-25 (Camprubi-Robles et al., 2009), whilst immuno-cytochemistry revealed TRPV1 (and TRPA1) co-expression on LDCVs, that store CGRP (Meng et al., 2016) (Devesa et al., 2014) and also contain VAMP1 as well as synaptotagmin 1 (Meng et al., 2016). Moreover, exposure of TGNs for 24 h to TNFα induced co-traffic of TRPV1 and TRPA1 to their plasma membrane, and this process was blocked by BoNT/A (Meng et al., 2016). Also, the demonstrated requirement herein for the presence of extracellular Ca^{2+} for acute exposure to NGF to stimulate CGRP release from starved TGNs (Fig. 4.7 D), and its blockade by BoNT/A (Fig. 4.8 E) or /EA (Fig. 4.9 D), supports an involvement of Ca^{2+}- and SNAP-25-dependent LDCVs exocytosis (Fig. 4.10 B). This accords with reports that acute exposure to NGF induces $[Ca^{2+}]_i$ signals in adult mouse DRGNs (Lawrence et al., 2021a), and that in PC12 cells this neurotrophin elicits a small $[Ca^{2+}]_i$ rise (Egea et al., 2000), (Pandiella-Alonso et al., 1986) and evokes catecholamine release that is dependent on extracellular Ca^{2+} [reviewed by (Jiang and Guroff, 1997)]. Thus, in principle, the sensitisation of sensory neurons to CAP caused by NGF may involve the transfer of TRPV1 on LDCVs to the plasmalemma. However, it must also be considered that even in the absence of extracellular Ca^{2+} acute exposure of TGNs to NGF activates TrkA signalling (exemplified here by increased ERK1/2 phosphorylation; Fig. 4.7 B, C) and increases CAP-evoked Na^+ currents indicative of enhanced TRPV1 activity (Zhu and Oxford, 2007). Herein, this was corroborated by the finding that re-introduction to starved cells of NGF in the absence of Ca^{2+} still enhanced subsequent CGRP release triggered by 0.02 μM CAP. It was necessary to include extracellular Ca^{2+} alongside CAP to enable the stimulation of CGRP release but, nevertheless, these novel results clarify that even in the absence of CGRP exocytosis, starved TGNs are sensitised by NGF and subsequent responses to CAP are exaggerated. Such sensitisation might involve phosphorylation of TRPV1 or association of the channel with one or more other signalling molecules (Denk et al., 2017), (Zhang et al., 2005), (Huang et al., 2006a). However, even a low [CAP] such as 0.02 μM evokes far more CGRP release than acute NGF (Fig. 4.6 B c.f. D), so it must cause much more transfer of TRPV1 on LDCVs to the plasma membrane ((Devesa et al., 2014); Fig. 4.10 B). Perhaps in the absence of extracellular Ca^{2+}, NGF modifies

TRPV1 to improve retention of the channel at the cell surface, rather than directly stimulating its transfer, or promotes docking of LDCVs containing TRPV1 in advance of Ca^{2+}-triggered fusion. The results presented here do not exclude that a component of NGF sensitisation to CAP occurs without trafficking of supplementary TRPV1 to the plasma membrane. In collaboration with Dr Seshu Kumar Kaza attempts were made to demonstrate directly the trafficking of additional TRPV1 channels to the cell surface by biotinylation of surface proteins, enrichment with streptavidin beads and Western blotting with several commercially available TRPV1 antibodies. The detection of surface channels and its quantification with or without 30 min. incubation with NGF appeared to be challenging and results were inconclusive. It may be that short incubation with the neurotrophin does not elicit a large enough increment in the amount of TRPV1 on the neuron surface for reliable detection of the change. In this regard, it has been reported that a 24 h exposure of TGNs to TNFα produced a >12-fold larger increase in surface TRPV1 compared to 30 min only (Meng et al., 2016). The incubation period with NGF in this study was kept deliberately short to ensure that only rapid signalling events were being assessed without influence of changes in gene expression. Therefore, quantitative assay of CAP-induced CGRP release is used as an indirect approach to evaluate the delivery of TRPV1 to the plasmalemma. The extensive inhibition of NGF-induced sensitisation by SNAP-25-cleaving BoNTs, particularly by /EA, accords with evidence that delivery of TRPV1 to the cell surface is the major factor (Zhang et al., 2005).

4.3.4 BoNT/EA abolishes NGF-enhanced CGRP release evoked by high [CAP]

The findings reported here clarify a possible basis for the prevention of nociceptor sensitisation by BoNT/A that may be relevant to its limited analgesic action in migraineurs with elevated CGRP (see 1.3.2); this notion arises because of its blockade of CAP-evoked CGRP release and of the enhancement by NGF, but only under conditions of relatively mild nociceptor activation (Fig. 4.9 B). The declining ability of BoNT/A to reduce neuropeptide exocytosis elicited by high [CAP] despite extensive proteolysis of SNAP-25 (75% of the cells' complement) is likely related to the larger increase in $[Ca^{2+}]_i$ induced, relative to the respective signal brought about by 0.02 μM CAP [Fig. 3.5 A, B and (Cholewinski et al., 1993)], and the prolonged persistence of raised $[Ca^{2+}]_i$ during 30 min. exposure to high concentrations of the vanilloid (Fig. 3.5 A and (Meng et al., 2009)). Similarly, extensive proteolysis of SNAP-25 was observed for BoNT/EA but with production of the shorter, more functionally disabled, product typical for /E ($SNAP\text{-}25_E$),

(Fig. 4.9 A, B). Strikingly, the latter was accompanied by large reductions in CGRP release evoked by either high [CAP] (Fig. 4.9 E) and the augmentation by NGF of exocytosis was prevented (Fig. 4.9 E), highlighting the superiority of BoNT/EA relative to /A for attenuation of CGRP release under strong stimulation conditions represented by 1 μM CAP (Fig. 4.8 E). As other nocisensive channels are implicated in migraine, TRPA1 (Benemei and Dussor, 2019) and P_2X_3 (Fabbretti et al., 2006), and also reportedly transfer to the surface of sensitised nociceptors, BoNTs could potentially provide more broadly effective analgesia than selective antagonism of any single channel. It is also suggested that modified BoNTs with /E protease activity might be a more effective option for suffers exhibiting exceptionally excessive neuropeptide secretion, particularly if caused by over-excitable sensory neurons with high $[Ca^{2+}]_i$ loads (Meng et al., 2009). Moreover, the recombinant engineering utilised here facilitates further potentially beneficial improvements such as to prolong the /E protease lifetime (Wang et al., 2017) and enhance selectivity for sensory relative to other peripheral neurons (Foster and Chaddock, 2010).

4.3.5 Chimera LC/E-BoNT/A shows a long-lasting analgesic effect in a model of CAP-induced acute nociception in rats

Much pain research is being focused on migraine and trigeminal neuralgia, because of the prevalence of these debilitating conditions that involve the trigeminal sensory system. Current migraine pathophysiology theories propose that the first trigger of the attack comes from the hypothalamus followed by activation of the TNC. This leads to activation of the TG neurons and the release of CGRP, resulting in vasodilatation and promoting neurogenic inflammation. In addition, CGRP sensitises nearby Aδ-fibres by activating its receptor (a complex of the calcitonin receptor-like receptor, receptor activity-modifying protein 1, and two cytoplasmic receptor coupling proteins). In these conditions, innoxious stimuli are sensed as painful [reviewed in (Haanes and Edvinsson, 2019)]. Because BoNT/EA and LC/E-BoNT/A are shown to be more effective in the blocking of CGRP release evoked by high [CAP] *in vitro* (Fig. 3.13), it was essential to evaluate the anti-nociceptive versatility of LC/E-BoNT/A in a model of acute pain induced by CAP in rats, and this was performed by a colleague in the host laboratory (Antoniazzi et al., 2022). As one of the three TG branches innervate a rat whisker pad, this region was used for subcutaneous injection of the TRPV1 agonist. Administration of CAP sensitises peripheral and central nociceptive circuits causing pain-related behaviour such as grooming and freezing. LC/E-BoNT/A significantly reduced nocifensive

behaviour compared to the control group, and the effect of a single injection lasted up to 15 days. The toxin treatment had no impact on the rats' weight gain or normal grooming behaviour over the period studied, indicating an absence of adverse effects. Importantly, pain attenuation after LC/E-BoNT/A pre-treatment was observed in both males and females (Antoniazzi et al., 2022). This is noteworthy as females are more sensitive to pain and less responsive to analgesics. As TNC contributes to the transmission of craniofacial pain, acute noxious stimulation of the trigeminal innervation induces the expression of c-Fos in the nuclei of neuronal cell bodies within this region; thus, it serves as a marker of neuronal activation. Evidence that LC/E-BoNT/A acted at peripheral terminals to supress the activity of the primary nociceptors was found by immuno-histochemical staining for c-Fos in the brainstem from rats pre-treated with the toxin and controls. In rats not treated with LC/E-BoNT/A, the vanilloid injection induced a significant increase in c-Fos expression, while in the toxin-treated animals, the number of activated cells did not change. This indicates that pre-injection of LC/E-BoNT/A into the peripheral sensory field inhibited the generation of pain signals in primary sensory neurons and/or their passage to second-order sensory neurons in the CNS (Antoniazzi et al., 2022).

Overall, the data reported here demonstrated that /E cleaving chimeras BoNT/EA and LC/E-BoNT/A are valid potential candidates for the treatment of pain conditions, which involve the trigeminal sensory system. Their profound inhibition of CGRP release from cultures of TGNs *in vitro*, even when intensely stimulated with CAP and sensitised by a pro-inflammatory compound (NGF), raises the possibility of these chimeras providing more effective relief from painful conditions that respond poorly to BoNT/A.

5 Bipartite activation of TGNs by TRPA1 agonist AITC is reflected by complex Ca^{2+} influx and CGRP release patterns: enhancement by NGF and inhibition with VAMP and SNAP-25 cleaving BoNTs

5.1 Overview

Transient receptor potential subfamily A member 1 (TRPA1) is a pain-related cation channel from the TRP family that has been implicated in the pathophysiology of pain and migraine. It is predominantly expressed in sensory neurons of TGs and DRGs, although it is also present on some types of non-neuronal cells. In the sensory fibres that innervate meninges, the channels are highly co-localised with TRPV1 and CGRP [reviewed in (Dux et al., 2020)]. TRPA1 is activated by numerous endogenous and exogenous compounds. They include nitrogen and oxygen species, formaldehyde, acrolein (a compound found in cigarette smoke and automobile exhaust), and headache-inducing plant extracts such as mustard oil or umbellulone. TRPA1 agonists can be divided into two groups. The first composes reactive electrophiles (allyl isothiocyanate (AITC) from mustard oil, formalin, acrolein) that covalently modify the channel by interaction with intracellular cysteine and lysine residues (Detailed in 5.3). The second group includes non-electrophilic compounds (menthol, carvacrol, thymol) that activate the channel non-covalently. It is not known how non-covalent agonists interact with TRPA1 and whether they induce physiological responses similar to those produced by covalent bond forming agonists [reviewed in (Meents et al., 2019)]. When TRPA1 is activated, an integral channel is opened that permits Ca^{2+} flux into the neuronal cytosol. The resulting increase in cytosolic [Ca^{2+}] induces the release of neurotransmitters and neuropeptides.

Experiments *in vivo* have demonstrated the role of TRPA1 in pain signalling; its activators induce pain behaviour in rodents, while knockout of the TRPA1 gene or treatment with its antagonists reduced the pain sensitivity (Kwan et al., 2006), (McNamara et al., 2007), (Eid et al., 2008). As TRPA1 is activated by number of environmental irritants, a lot of attention has been given to its role in migraine and other types of headaches. It was demonstrated in rodents that intranasal administration or topical application to the dura (one of the three membranes comprising meninges) of mustard oil or acrolein induces CGRP release and meningeal vasodilatation which can be blocked by a TRPA1 antagonist HC-030031 (Kunkler et al., 2011), (Denner et al., 2017). Experiments in humans suffering from migraine demonstrated that administration of NO donors induces symptoms typical of a migraine attack, which was associated with increased levels of CGRP in blood samples obtained from the jugular vein [reviewed in

(Iyengar et al., 2017)]. This supports the important role of TRPA1 in pathophysiology of this debilitating disease.

Immuno-histochemical studies indicate that TRPA1 and TRPV1 are co-localised in sensory fibres innervating meninges. Moreover, in TGN cultures it was demonstrated that TRPA1 co-locates with TRPV1 on CGRP-containing intracellular vesicles inside sensory neurons (Meng et al., 2016), (Devesa et al., 2014). When these cultures were exposed to a pro-inflammatory cytokine TNFα the neurons became sensitised to CAP such that evoked currents and intracellular Ca^{2+} signals were amplified. Evidence that this involved the transfer of TRPA1 to the cell surface has been accrued by the inhibition of neuron sensitisation to CAP using SNAP-25 inactivating BoNT/A (Meng et al., 2016) or LC/E-BoNT/A (Nugent et al., 2018), as well as knock-down of another SNARE VAMP1. However, the relationships between activation of TRPA1 with different [AITC] and CGRP release, its enhancement by NGF and susceptibility to BoNTs are poorly defined.

5.2 Results

5.2.1 AITC dose-dependently stimulates Ca^{2+}-regulated CGRP release from cultured TGNs, which is extensively inhibited by the TRPA1 antagonists HC-030031 and A967079

To document a functional link between activation of TRPA1 and CGRP release from TGNs, primary cultures isolated from rat neonates were exposed to various concentrations of the TRPA1 agonist AITC as described in section 2.2.2.3 and Fig. 5.1. Interestingly, a detectable increase in CGRP exocytosis (relative to the level observed in the absence of any stimulus) was elicited by as little as 0.001 mM AITC, but the amount of secreted neuropeptide plateaued between 0.01-0.05 mM, at a level of ~7% of the total content expressed in the neurons (Fig. 5.1 A). However, raising [AITC] further provoked more neuropeptide secretion, reaching a maximum of ~24% of the total at 0.35 mM AITC and then declining for >0.5 mM. The data was best fit by a two-site model with separate curve-fitting performed on two overlapping [AITC] sub-ranges 0.0001-0.05 mM and 0.01 to 0.5 mM (Fig. 5.1 A, green line, R^2=0.75; black line, R^2=0.86, respectively). This yielded an EC_{50}=0.006 mM for an apparent higher affinity site for AITC that can elicit release of a small fraction of CGRP (~7% of the total) and a lower affinity site EC_{50}=0.093 mM responsible for an additional ~17%. Omission of extracellular Ca^{2+}

prevented the CGRP release evoked by 0.01-1 mM [AITC] (Fig. 5.1 A, squares), confirming it involves Ca^{2+}-regulated exocytosis. In pilot experiments, TGNs were exposed to 0.05, 0.1, 0.5, and 1 mM AITC in presence of 10 µM HC-030031 a TRPA1 antagonist. This resulted in 58, 68, 43, and 43% reductions of AITC-evoked CGRP release (data not shown). A higher concentration of the antagonist, 100 µM, inhibited the response to 0.01 mM AITC by ~90% but was less effective against higher [AITC] (Fig. 5.1 B). An alternative TRPA1 antagonist, A967079, blocked CGRP release elicited by 0.05 and 1 mM AITC by 94 and 88%, respectively (Fig. 5.1 B). Thus, TRPA1 is implicated in Ca^{2+}-dependent CGRP release that appears to involve high- and low-affinity mechanisms for its activation by AITC.

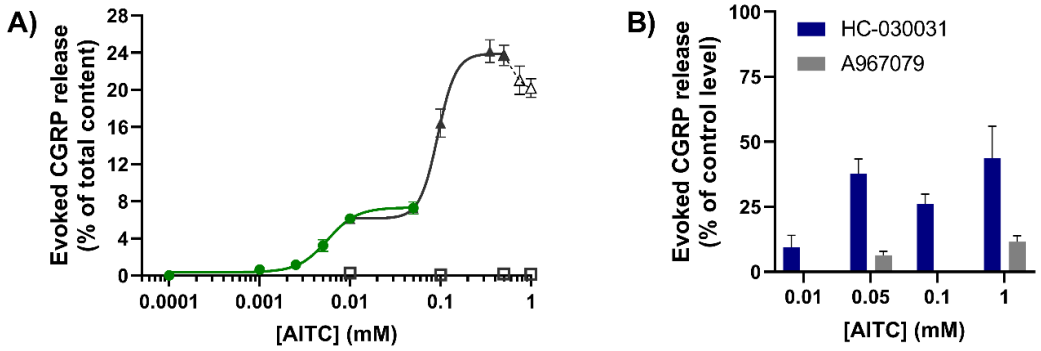

Figure 5.1 AITC induces Ca^{2+}-regulated CGRP release from TGNs via apparently high- and low-affinity mechanisms, which are attenuated by TRPA1 antagonists, HC-030031 and A967079
Cultured TGNs were sequentially exposed for 30 min. to vehicle (0.1% DMSO) followed by [AITC] and the cell bathing solutions removed after each period for respective measurements of spontaneous and AITC-evoked CGRP release. (A) The dose-response relationship between [AITC] and CGRP release suggests two mechanisms for the agonist evoking the response, apparently involving distinct affinities for TRPA1. The seemingly higher- (green: 0.0001-0.05 mM AITC) and lower-affinity (black: 0.01-0.5 mM AITC) mechanisms were separately fit with four-parameter logistic functions (see section 2.2.9). The response peaked at 0.35 mM AITC and declined for higher concentrations; data points between 0.5 and 1 mM AITC, connected with a broken line, were not included in the fitting. Note that some error bars are obscured by symbols. The amounts of CGRP released into Ca^{2+}-free HBS containing 2 mM EGTA in the presence of 0.01, 0.1, 0.5 or 1 mM AITC are plotted with black squares; N≥3, n≥6. (B) TGNs were exposed to 100 µM HC-030031, 100 µM A967079 or vehicle only for 30 min. before determining spontaneous release and that for stimulation with various [AITC]. After subtraction of the spontaneous efflux, the amounts of CGRP released in the presence of antagonist were calculated, as detailed in the Materials and Methods, and plotted (blue bars, HC-030031; grey bars, A967079) as a % of the requisite control level elicited by each [AITC]; N=2, n≥6. Data are presented as mean±s.e.m.

5.2.2 AITC provokes bi-phasic Ca^{2+} signals in cultured TGNs with differential stimulation of the distinct phases being dependent on the concentration applied

The neurons were loaded with Fluo-4 AM (detailed in 2.2.7) prior to monitoring responses by fluorescence microscopy before and during their exposure to AITC for 30 min. (the period used previously to assess CGRP release). Separate experiments were performed for each [AITC]. Responding cells were determined as detailed in 2.2.7 and used to calculate the mean increases in signal intensity ($F\text{-}F_0/F_0$). The resultant data are plotted against time (Fig. 5.2 A, B). Whilst fluorescence remained stable at a low level prior to the addition of AITC (Fig. 5.2 A, B white background), 0.01 mM of this TRPA1 agonist induced an increase in the mean intensity that rose steadily over the first 10 min. (Fig. 5.2 A, yellow line, pink background) and plateaued over the following 10-15 min. (Fig. 5.2 A, yellow line, light blue background). In neurons exposed to 0.05 mM AITC (Fig. 5.2 A, blue line), the mean signal rose more rapidly and reached a higher maximum within 5 min., but then declined over the next 25 min. despite the continuous presence of the agonist throughout this period. An even faster onset of the response occurred in cells exposed to 0.1 mM AITC (Fig. 5.2 A, red line), reaching a maximum value within 2 min., but this was notably lower than that observed in cells exposed to 0.05 mM AITC. This trend of faster onset (at least up to 0.35 mM) but lower maximum continued upon raising [AITC] to 0.35 and 0.5 mM (Fig. 5.2 B grey and green line, respectively). These recordings suggest that the AITC receptor in TGNs undergoes an [agonist]-dependent desensitisation, as has been reported by others (Wang et al., 2008b), (Ibarra and Blair, 2013), (Zhao et al., 2020). An interesting feature in neurons exposed to 0.1 or 0.35 mM AITC is a delayed slow secondary phase of fluorescence accumulation observed after near-complete desensitisation (Fig. 5.2 A red and 5.2 B grey). At 0.5 mM AITC, the secondary phase started before desensitisation of the first response had finished (Fig. 5.2 B, green line). With 1 mM AITC, the secondary signal rose so rapidly it almost completely obscured the primary signal (Fig. 5.2 B, pink line). Collectively, these measurements indicate that AITC elevates $[Ca^{2+}]_i$ in TGNs in two phases with different concentration dependencies. A notable consequence of AITC causing activation and subsequent desensitisation is that the AUC of fluorescence changes proved similar in cells exposed to 0.01 or 0.05 mM AITC (despite their radically different profiles) and is reduced in TGNs exposed to 0.1 mM (Fig. 5.2 C). Only in cells treated with 0.5 and 1 mM AITC did large concentration-dependent increases in AUC become apparent.

Consistent with its extensive inhibition of AITC-induced CGRP release, the TRPA1 antagonist A967079 almost completely abolished the large primary phase increase in $[Ca^{2+}]_i$ induced by 0.05 mM AITC and dramatically reduced signals elicited by 1 mM AITC (Fig. 5.2 C).

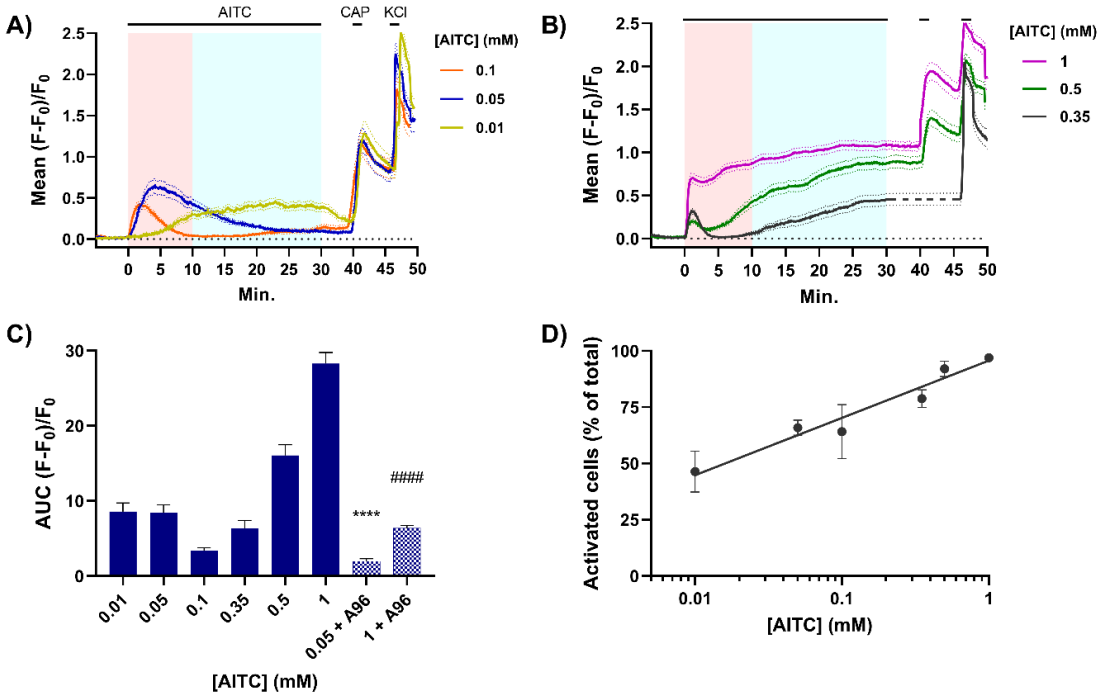

Figure 5.2 AITC elicits bi-phasic increases in $[Ca^{2+}]_i$ with a complex relationship to agonist concentration

Cultured TGNs were loaded with Fluo-4 AM and fluorescence intensity was recorded by time-lapse confocal microscopy. (A, B) Solid lines indicate the mean increases of fluorescence intensity ($F-F_0$) evoked by various [AITC] relative to initial fluorescence (F_0), plotted against time. Dotted lines above and below the solid traces indicate ± s.e.m. The black lines above the traces indicate the period AITC, CAP, and 100 mM KCl were present. Note, in experiments with 0.35 mM AITC, the trace between 30-45 min. (dashed line) is artificially created in GraphPad as cells were exposed only to AITC followed by KCl. (C) AUC of mean fluorescence change recorded over 30 min. for each [AITC] in the absence (N=3, n≥100) or presence of 100 µM A967079 [(A96), N=2, n≥30]; data were analysed using unpaired t-test with Welch's correction; **** p≤0.0001, 0.05 mM AITC vs 0.05 mM AITC+A967079; #### p≤0.0001 1 mM AITC vs 1 mM AITC+A967079. (D) The % of excitable cells; that responded to different concentrations of AITC; N=3, n ≥80. In (C, D) data are present as mean±s.e.m.

5.2.3 Raising [AITC] increases the fraction of TGNs that exhibit an increase in $[Ca^{2+}]_i$

Another factor pertinent to the amount of CGRP release elicited is the number of cells activated by each [AITC]. To evaluate this, after exposure to AITC as detailed in Fig. 5.2, TGNs were subsequently treated for 1 min. with 1 µM CAP and then 100 mM KCl at the end of each experiment. Cells were identified as AITC responders if AITC

caused their fluorescence intensity to increase by more than 10 x s.d. of the baseline signal whereas total responders incorporated cells that responded to any of the stimuli (detailed in 2.2.7). As observed before for raising [CAP] (Fig. 3.5 A), the % of excitable cells that were stimulated by AITC, increased linearly in a dose-dependent manner from 46% for 0.01 mM to 97% at 1 mM (Fig. 5.2 D).

5.2.4 CAP provokes larger increases of $[Ca^{2+}]_i$ in TGNs than AITC

To compare Ca^{2+}-signalling induced by 30 min. stimulations with 1 mM AITC or 1 μM CAP in the same cell population, TGNs were loaded with Fluo-4 AM before sequential exposures, (as described in Section 5.2.2), to AITC followed by CAP. In addition, after exposure to CAP, the cultures were washed for 30 min. then stimulated with 100 mM KCl to identify viable excitable cells. 1 mM AITC induced a rapid initial elevation in mean fluorescence followed by a slower phase of increase in signal intensity (Fig. 5.3 A; 5-35 min.). Notably, replacing AITC with 1 μM CAP immediately led to a sharp larger increment in fluorescence that was sustained throughout the period that the CAP remained present (Fig. 5.3 A; 35-65 min.). This plateau decreased only slightly during the subsequent 30 min. washout before brief application of 100 mM KCl induced a third sharp rise in the mean signal. On repeating the recordings (Fig. 5.3 B) but with a reversal of the application sequence of AITC and CAP, the latter caused a sharper initial rise in fluorescence (Fig. 5.3 B) that was larger than was the corresponding initial response to 1 mM AITC (Fig. 5.3 A). In the continued presence of CAP, after falling back slightly from the initial peak, fluorescence was sustained at a high level until this agonist was replaced with 1 mM AITC at which point the intensity declined slowly over the next 30 min. in the presence of AITC. During the subsequent washout of AITC the signal continued to decline slowly before brief exposure to 100 mM KCl induced a short sharp increase. In summary, the response provoked by 1 μM CAP was larger than that resulting from 1 mM AITC in TGNs exposed sequentially to each noxious substance one after the other, irrespective of the order of their application.

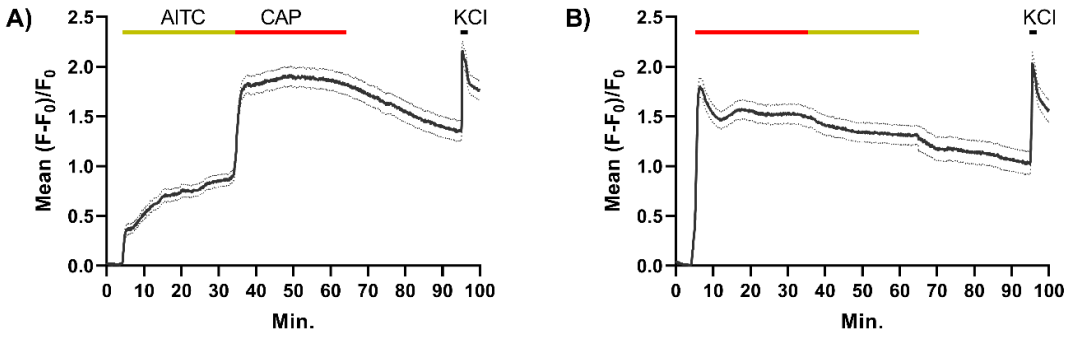

Figure 5.3 1 mM AITC induces less intense Ca^{2+} signals than 1 µM CAP in TGNs
After 5 min. of baseline recordings, the cells were exposed in sequence for 30 min. each to: (A) 1 mM AITC followed by 1 µM CAP or (B) 1 µM CAP before 1 mM AITC. In both experiments after 30 min. washout, 100 mM KCl was also applied for 1 min. Bars above the traces indicate the periods when the neurons were exposed to AITC (yellow), CAP (red bar) and KCl (black). N=3, n≥100. Solid and dotted black lines indicate the mean increase in fluorescence as a fraction of initial signal intensity ± s.e.m.

5.2.5 Dose dependencies for the cleavage in TGNs of requisite SNARE substrates by BoNT/A, LC/E-BoNT/A or BoNT/DA and the inhibition of AITC-evoked CGRP release reveals a marked hysteresis

To compare the potencies of the toxins in cleaving their substrates and inhibiting CGRP release evoked by 1 mM AITC, TGNs were exposed for 48 h to an exponential series of BoNT/A, LC/E-BoNT/A or /DA concentrations. The neurotoxins induced dose-dependent truncation of SNAP-25 (BoNT/A or LC/E-BoNT/A; Fig. 5.4 A, B, C, D) or VAMP1/2 (/DA; Fig. 5.4 E, F). Interestingly, at 0.01-10 nM of each BoNT the inhibition of AITC evoked CGRP exocytosis was relatively small compared to the extent of SNAP-25 or VAMP1/2 proteolysis; however, at the highest tested concentration of 100 nM, /DA extensively reduced CGRP exocytosis and VAMP1/2 by similar extents. These results highlight a hysteresis between the degradation of SNAREs and the consequent perturbation of membrane fusion. This phenomenon suggests a redundancy in the level of SNAREs expressed such that small reductions have minimal effect on exocytosis because the cells express much more than they actually require. Therefore, in most experiments 100 nM toxin was used to extensively reduce the contents of SNAREs and to maximise the inhibition of exocytosis without excessive depletion of the resource available.

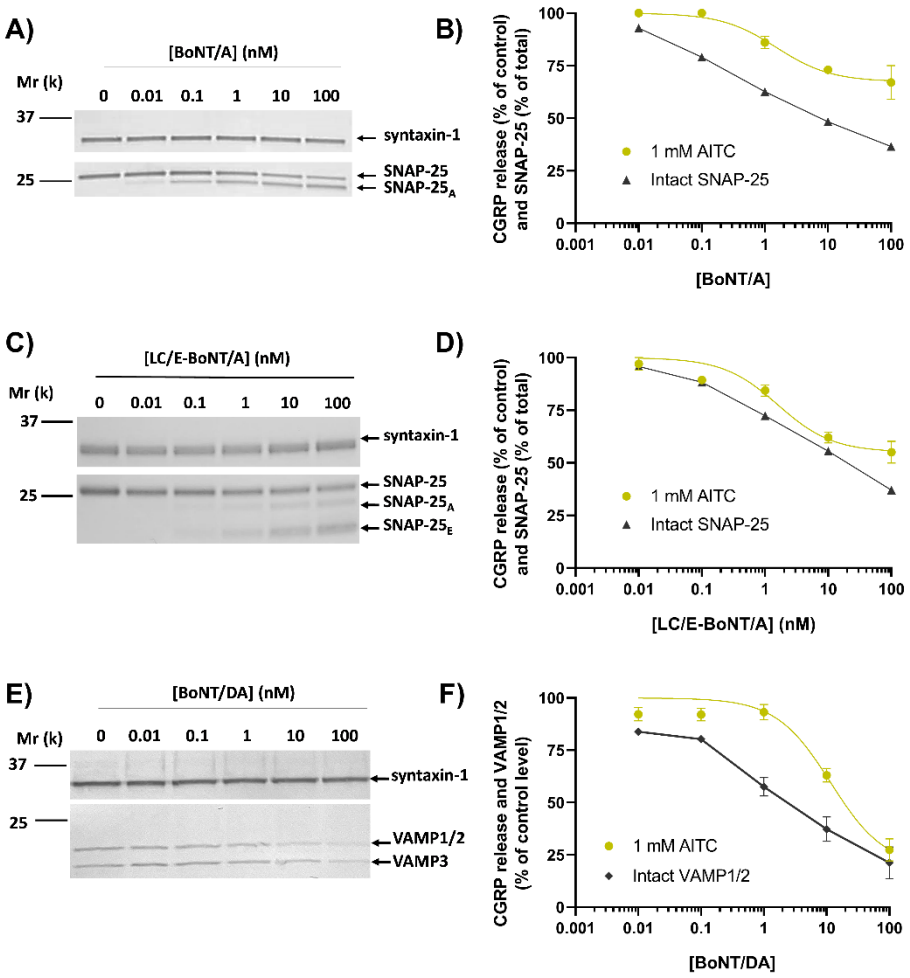

Figure 5.4 BoNT/A, LC/E-BoNT/A, and BoNT/DA dose-dependently cleave SNAP-25 or VAMP1/2 and inhibit AITC-evoked CGRP release

TGNs after 4 DIV were intoxicated for 48 h with 0.01, 0.1, 1, 10, and 100 nM BoNT/A, LC/E-BoNT/A, or BoNT/DA in growth medium before stimulation of CGRP release for 30 min. with 1 mM AITC as described in 2.2.3; control cells were exposed to growth medium only. Then, after removal of the cell bathing fluid for CGRP assay, the TGNs were solubilised for Western blotting with (A, C) anti-SNAP-25 and (E) anti-VAMP1/2/3 antibodies. Reactivity to immunoglobulins for syntaxin-1 served as a loading control in all cases. Numbers above lanes indicate the concentration of each toxin applied, with 0 indicating toxin-free control cells. (B, D, F) The amounts of released CGRP and (F) intact VAMP1/2 normalised to control levels. In (B, D) intact SNAP-25 is expressed as a % of total. Dose-dependent relationships are shown fit with three-parameter logistic functions with maximum values constrained to 100. Data are presented as mean±s.e.m., N=1, n≥2 (for CGRP assay) and n=1 for quantification of fraction of SNAP-25 remaining intact in cells exposed to BoNT/A and LC/E-BoNT/A; N=2, n=5 (CGRP assay) and n=2 (quantification of VAMP1/2). The experiment to determine the dose-dependent effect of LC/E-BoNT/A on CGRP exocytosis and proteolysis of SNAP-25 was performed in collaboration with Dr. Seshu Kumar Kaza, DCU.

5.2.6 AITC-induced CGRP release is inhibited by BoNTs: a VAMP-cleaving recombinant chimera proved more efficacious than variants that proteolyse SNAP-25

Next, to investigate blocking effect of BoNT/A, LC/E-BoNT/A, and BoNT/DA on CGRP release evoked by different stimulation conditions, pre-treated for 48 h with 100 nM BoNTs or control TGNs were exposed to a range of [AITC]. Two days incubation with toxins resulted in an extensive cleavage of their substrates (Fig. 5.5 A, B). Although no changes occurred in the total CGRP content (Fig. 5.5 C), spontaneous exocytosis of this peptide was reduced by all BoNT variants (Fig. 5.5 D). Surprisingly, BoNT/A blocked only ~40% of the CGRP release evoked by a broad range of agonist concentrations (Fig. 5.5 E). Despite truncating a larger fragment from SNAP-25 (resulting in a smaller product; Fig. 5.5 A), LC/E-BoNT/A was no more effective than BoNT/A at reducing CGRP-exocytosis even though the fractional blockade by the /E-cleaving chimera rose slightly as the [AITC] was increased (Fig. 5.5 E). The pre-treatment of TGNs with BoNT/DA, caused the largest inhibition of AITC-evoked CGRP release, ~75% across the whole range of agonist concentrations tested (Fig. 5.5 E). Also, it gave an ~80% inhibition of 0.1 μM CAP-evoked CGRP release and, like LC/E-BoNT/A (Fig. 3.13 B), remained effective against 1 μM CAP (Fig. 5.5 F) that promotes much larger increases in $[Ca^{2+}]_i$ (Fig. 3.5 B, C).

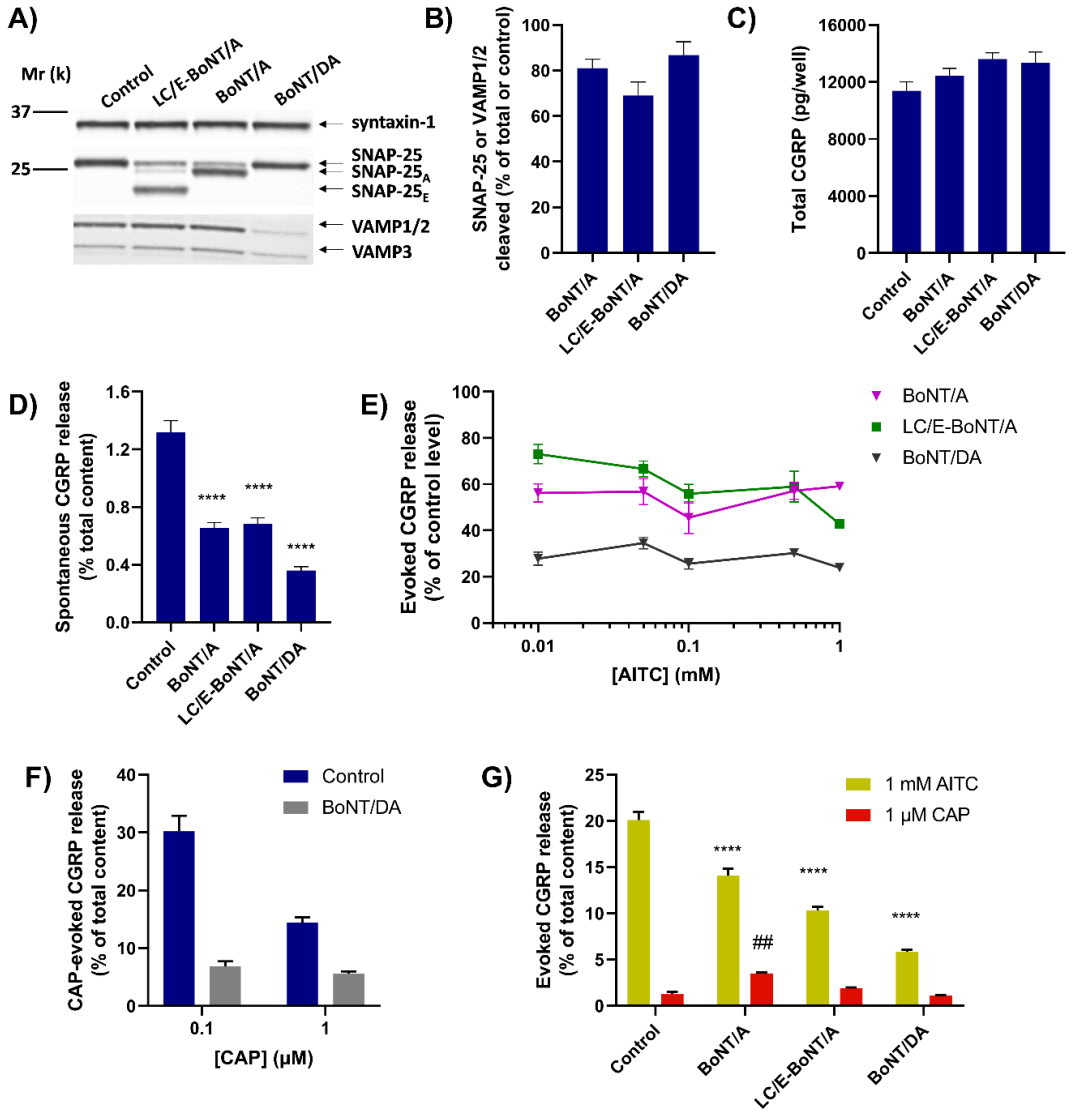

Figure 5.5 VAMP-cleaving BoNT/DA inhibits AITC-evoked CGRP release from TGNs more extensively than BoNT/A or LC/E-BoNT/A, which proteolyse SNAP-25 at different bonds

Cultured TGNs were pre-treated with 100 nM BoNT/A, LC/E-BoNT/A, BoNT/DA or control medium for 48 h, before determining spontaneous and evoked CGRP release over 30 min. (A) Representative Western blot showing that LC/E-BoNT/A and BoNT/A both cleaved SNAP-25 at distinct sites, yielding products of dissimilar sizes, whereas BoNT/DA proteolysed and, thereby, diminished detectable VAMPs 1/2, and 3 (note that VAMPs 1 and 2 co-migrate). Syntaxin-1 is not affected by any of the toxins, so was used as a loading control. (B) The amounts of cleaved and intact SNAP-25, as well as intact VAMP1/2, were quantified by densitometric analysis (described in Materials and Methods). SNAP-25 proteolysis is presented as a % of total SNAP-25 content (sum of intact and cleaved), whilst VAMP1/2 cleavage was determined from the % reduction in signal intensity relative to the level in untreated control cells; N=5, n=5. Note that VAMP3 was not included in densitometric analysis. (C) Total content of CGRP (pg/well). (D) Histogram displaying spontaneous CGRP release, in control cells and those treated with the various BoNT variants, calculated as % of the total CGRP content; N≥3, n=16. (E) TGNs were pre-treated with BoNTs, as described above, before exposing the cells to various [AITC] for 30 min. The amounts of CGRP released were quantified and expressed as % of requisite control values (i.e., the amounts elicited from non-intoxicated control cells); N≥2, n≥5. (F) Amounts of CGRP release upon stimulation with indicated [CAP] in cells pre-treated with 100 nM BoNT/DA and in control cells. (G) TGNs were sequentially stimulated

with 1 mM AITC (yellow) and then with 1 µM CAP (red) for 30 min each; evoked CGRP release is expressed as a % of control level. Data are presented as mean±s.e.m. One- or two-way ANOVA was used in D and G followed by Bonferroni's post hoc test; ## $p<0.01$ for CAP-evoked in control vs BoNTs; **** $p<0.0001$ for AITC-evoked in control vs BoNTs.

5.2.7 CAP fails to evoke CGRP release from TGNs previously depleted by AITC stimulation

To ascertain whether or not AITC and CAP stimulate CGRP release from the same TGNs, sequential exposure to AITC was followed by CAP, and the amounts of CGRP released during stimulation with each of the TRP channel agonists were quantified. During 30 min. incubation with 1 mM AITC, 20% of the total neuropeptide present was exocytosed (Fig. 5.5 G, control), leaving 80% retained inside the cells. Nevertheless, subsequent stimulation with 1 µM CAP proved unable to evoke more than a minimal amount of additional CGRP release, meaning either that prior exposure to 1 mM AITC depleted virtually all the CGRP that can be mobilised by 1 µM CAP or prior exposure of CAP-excitable TGNs to 1 mM AITC causes extensive desensitisation of TRPV1 (a less likely scenario, see 5.3). Either way, it could be deduced that the vast majority of TGNs co-expressing CGRP and TRPV1 very likely express TRPA1 too.

5.2.8 In BoNT/A pre-treated neurons CAP elicits a fraction of CGRP exocytosis when applied after AITC

CGRP release upon sequential stimulation by AITC and then CAP was next investigated in TGNs incubated for 48 h with BoNT/A. As noted in Section 5.2.6, such pre-treatment effected a partial reduction only in the amount of CGRP released during 30 min. exposure to AITC; BoNT/A-treated cells released 14% of their CGRP, a reduction of 6% compared to non-treated control cells (Fig. 5.5 G). Upon subsequent stimulation with 1 µM CAP some additional CGRP was released though this only represented 3.5% of the total content; it seems that CAP could mobilise the small fraction of releasable neuropeptide that was unresponsive to AITC after BoNT/A intoxication. This accords with the ability of 1 µM CAP to rescue CGRP release from BoNT/A-intoxicated TGNs (see Fig. 3.13) more effectively than 1 mM AITC (Fig. 5.5 E). Moreover, as AITC and CAP stimulate the same population of cells (see Sections 5.2.3 & 5.2.7), this cannot be due to the recruitment by CAP of cells that are unresponsive to AITC. By contrast, LC/E-BoNT/A and BoNT/DA inhibited responses to 1 mM AITC more extensively, with CAP being unable to elicit any more CGRP release from TGNs treated with either of these variants (Fig. 5.5 G).

5.2.9 NGF enhances the release of CGRP evoked by low [AITC]

Ca^{2+} imaging experiments and electrophysiology have shown that NGF potentiates the activity of TRPV1 channels (detailed in 4.1.4). In Chapter 4 it was demonstrated that NGF potentiation resulted in enhanced CAP-evoked CGRP release (Fig. 4.6). In view of TRPV1 and A1 channels being co-expressed in TGNs, the effect of NGF on TRPA1 activity was investigated using the experimental protocol similar to that described in Fig. 4.6 A except that instead of using CAP cells were stimulated by various [AITC]. As shown previously (Fig. 4.6 D), exposure to NGF for 30 min. induced a small but significant ($p<0.0001$) increase in CGRP secretion compared to the amount recorded in the absence of NGF (Fig. 5.6 A). Incubation of TGNs with the neurotrophin for 30 min. prior to stimulation with AITC significantly ($p=0.03$) enhanced the amount of CGRP secreted during exposure to the TRPA1 agonist but only at the lowest concentration, 0.01 mM (Fig. 5.6 B); the amounts of CGRP release evoked by 0.05 or 0.1 mM AITC were also augmented slightly but these changes were not significant. Also, NGF showed no effect on the amount of CGRP exocytosis stimulated by 0.5 mM AITC (Fig. 5.6 B).

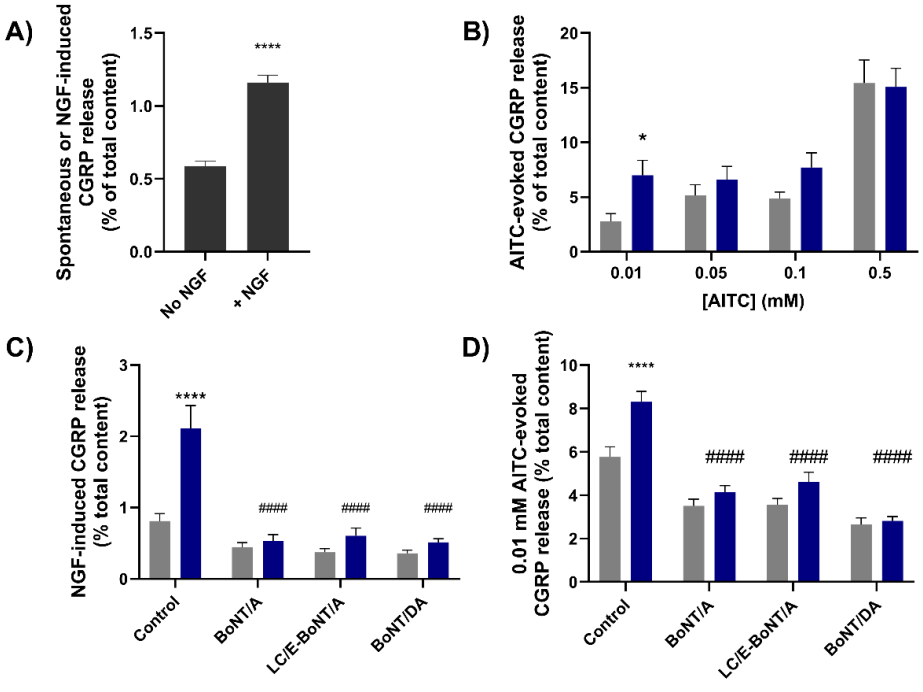

Figure 5.6 BoNT/A, LC/E-BoNT/A, and BoNT/DA inhibit both the induction by NGF of CGRP exocytosis and its enhancement of AITC-evoked neuropeptide secretion

(A-D) Histograms showing: (A) the levels of CGRP secreted from 2-day NGF-starved TGNs during a subsequent 30 min. exposure to HBS in the absence (No NGF) or presence of 100 ng/ml NGF (+NGF); (B) amounts of CGRP released during 30 min. exposure to various [AITC] from TGNs that had previously been starved of NGF for 2 days, then exposed to HBS without (grey bars) or including 100 ng/ml NGF

(blue bars) just prior to stimulation with the noxious substance. Two-tailed Welch tests were applied to compare responses between NGF-free and -30 min. treated groups at each AITC concentration, * $p<0.05$; (C) levels of CGRP released during 30 min. incubation with HBS only (grey bars) or HBS+100 ng/ml NGF (blue bars) from TGNs that had been deprived of NGF for 48 h in the absence (Control) or presence of 100 nM of the indicated toxins; (D) amounts of CGRP release evoked by 0.01 mM AITC from control or BoNT-pre-treated, 2-day NGF-starved TGNs that had just been exposed for 30 min. to 100 ng/ml NGF (blue bars) or HBS only (grey bars). (C, D) Two-way ANOVA followed by Bonferroni's post hoc test was used; (C) **** $p<0.0001$ for pre-treatment with NGF vs no NGF; #### $p<0.0001$ for NGF-induced in control vs pre-treated with indicated BoNTs cells; (D) **** $p<0.0001$ for AITC evoked CGRP release in pre-treatment with NGF vs no NGF TGNs; #### $p<0.0001$ for NGF-enhanced AITC-stimulated release in control vs pre-treated with indicated BoNTs cells; $N\geq2$, n=6 for /A and LC/E-BoNT/A, n=10 for /DA.

5.2.10 CGRP release induced by NGF and its enhancement of secretion evoked by low [AITC] are both blocked by BoNTs that cleave SNAP-25 or VAMP1/2/3

To evaluate if SNAP-25 and VAMP1/2/3 are involved in the NGF-induced enhancement of CGRP release evoked by 0.01 mM AITC, cultured TGNs were pre-treated with 100 nM of BoNT/A, LC/E-BoNT/A, or BoNT/DA during the 2-day NGF withdrawal period. The release assay was then performed, as described above in 5.2.9. BoNT/DA prevented the induction by NGF of CGRP exocytosis (Fig. 5.6 C), confirming that VAMP1/2 and/or 3 is involved in this process; furthermore, the inhibition observed with the other two variants is in accordance with Fig. 4.8 E and Fig. 4.9 D also reaffirming the requirement for SNAP-25. Notably, BoNT/DA as well as LC/E-BoNT/A, and BoNT/A, all reduced CGRP release evoked by 0.01 mM AITC from NGF-starved cells that were not acutely exposed to the growth factor (Fig. 5.6 D, grey bars). More strikingly, each toxin also prevented augmentation of 0.01 mM AITC-evoked CGRP release by the brief re-introduction of NGF relative to that observed in control cells. Thus, VAMP1/2/3 and SNAP-25 are essential mediators of TGN sensitisation by NGF to AITC, implicating SNARE-mediated membrane fusion in the process.

5.3 Discussion

Regarding molecular mechanisms that contribute to pathological pain, there has been great interest in the roles of TRP channels that excite nociceptors and neuropeptides such as CGRP which are released consequently (Julius, 2013), (Benemei and Dussor, 2019), (Iannone et al., 2022), (Edvinsson et al., 2018). Nevertheless, the details of how these processes are linked to each other and to pain signalling are still not clear. Here, AITC was used to activate TRPA1 in cultures of rat TGNs and the resultant increases in $[Ca^{2+}]_i$ were correlated for the first time with the extents of CGRP release. Notably, this revealed that there are two mechanisms for AITC to evoke CGRP exocytosis, apparently,

implicating distinct affinities of this electrophilic agonist for the TRPA1 channel (Fig. 5.1 A). Furthermore, the effect of NGF, a neurotrophin implicated in inflammation, on AITC-induced CGRP release was found to enhance significantly only CGRP release elicited by a low [AITC], 0.01 mM, indicating a selective action via the more AITC-sensitive mechanism. Finally, with a view to expected therapeutic benefits of lowering CGRP release and its enhancement by NGF (Edvinsson, 2022), (Sarchielli and Gallai, 2004), (Barker et al., 2020), inhibition of both processes by BoNT/A was examined, as well as by recombinant variants that retain the neurotropism of BoNT/A but either cleave a larger fragment off SNAP-25 (LC/E-BoNT/A) or target the latter's cognate SNARE complex partners VAMP1/2 and 3 (BoNT/DA). Notably, this unveiled that whilst all three BoNTs attenuated sensitisation of TGNs by NGF, the VAMP-cleaving /DA was more efficacious in reducing AITC-evoked CGRP release than either of the two SNAP-25-targetting variants.

The complex AITC-dependency of CGRP release observed herein accords with the intricacy of TRPA1 activation by electrophiles. The initial activation at low concentrations of AITC that elicits release of ~7% of the total CGRP content (Fig. 5.1 A) is compatible with the AITC sensitivity of cysteines (C621, C641 and C655) that occupy a pocket in the so-called 'coupling domain' on the cytoplasmic side of TRPA1 (Bahia et al., 2016), (Hinman et al., 2006), (Macpherson et al., 2007). A triple mutant [TRPA1-3C (Hinman et al., 2006) C621S, C641S, C655S] exhibited a greatly reduced sensitivity to AITC <100 μM. Covalent modification by small electrophiles such as AITC of C621 and C655 stabilises an open pocket conformation that, in turn, facilitates opening of the TRPA1 channel pore. The second and larger increment of CGRP release would seem to imply activation of TRPA1 at another site. In this regard, TRPA1-3C was shown to be activated upon prolonged exposure to high [AITC] (>100 μM), and only rendered insensitive to the electrophile by an additional mutation in TRPA1-3C of K708R. Although exposure to such high AITC concentrations for a prolonged time (30 min.) will modify other cell proteins (Macpherson et al., 2007) including other TRP channels that may consequently be activated (Everaerts et al., 2011), even the CGRP release induced by 1 mM AITC was inhibited by either of two selective TRPA1 antagonists, HC-030031 or A967079 (Fig. 5.1 B). Thus, the big increment in CGRP exocytosis evoked by the higher [AITC] may be attributable to such further activation of TRPA1, but a small contribution from other channels cannot be excluded. Confirmation of this model will

require analysis of CGRP release from sensory neurons in which the wild-type TRPA1 has been substituted for the TRPA1-3C or TRPA1-3C-K708R mutants, a challenging endeavour outside the scope of this study.

Notably, TRPA1-3C activated by high [AITC] displays the same unitary conductance as the wild-type channel at low [AITC] (Hinman et al., 2006). If heterologous expression of TRPA1 in HEK cells faithfully reflects the activity of this channel in neurons, it seems unlikely alteration of Ca^{2+} conductance could underlie the large increase in CGRP release at high [AITC]. So, the relationship between [AITC] and $[Ca^{2+}]_i$ during prolonged exposure to the agonist was investigated in TGNs loaded with Fluo-4 AM. When exposed to the lowest [AITC], 0.01 mM, there was a slow progressive rise in fluorescence (Fig. 5.2 A). As this is reminiscent of TRPA1 activation by low concentrations of an electrophile, it appears attributable to involvement of a chemical reaction that would slowly yield modified cysteines and, thereby, open channels (Hinman et al., 2006). Collision theory predicts that increasing the concentration of one of the reactants (AITC) accelerates the chemical reaction and, thereby, the build-up of product (TRPA1 with modified cysteines and an open channel). Accordingly, exposing dye-loaded TGNs to 0.05 mM AITC induced a much faster increase in fluorescence than observed with 0.01 mM (Fig. 5.2 A). However, after a few minutes exposure to 0.05 mM AITC the intensity of fluorescence started to decline despite the continued presence of the agonist; this invokes another well-established characteristic of TRPA1, Ca^{2+}-dependent desensitisation (Akopian et al., 2007), (Wang et al., 2008b), (Zhao et al., 2020). As Ca^{2+} permeates through the channel, it is captured by a cytoplasmic Ca^{2+}-binding site proximal to the pore (Zhao et al., 2020), (Wang et al., 2008b); this initially potentiates TRPA1 channel conductance but is followed by a delayed reduction in conductivity termed desensitisation (Wang et al., 2008b). Interestingly, a single mutation E788S in the Ca^{2+}-binding site is sufficient to prevent Ca^{2+}-mediated potentiation of TRPA1 activity, whilst two additional mutations Q791S and N805S are required to prevent Ca^{2+}-mediated desensitisation (Zhao et al., 2020). This delayed TRPA1 desensitisation could explain the contrary effects of increasing [AITC] on fluorescence intensity (Fig. 5.2 A); an initial rise in fluorescence is accelerated with rising [AITC], but signals crest and then decline sooner as desensitisation ensues. A consequence of such desensitisation is that the integrated Ca^{2+}-signal (AUC of time course) does not increase upon raising [AITC] from 0.01 to 0.05 mM (Fig. 5.2 C); hence, similar amounts of CGRP

exocytosis were evoked (Fig. 5.1 A). When AITC was increased to ≥0.1 mM, secondary delayed elevations of fluorescence appeared (Fig. 5.2 B, C). These might correspond to slower TRPA1 activation by AITC reacting with the weaker amine nucleophile, K708 (Zhao et al., 2020), so it is tempting to speculate that the secondary response signal is minimal at low [AITC], delayed at intermediate [AITC], and accelerated by high [AITC], the pattern observed experimentally. Notably, channels activated by K708 modification are resistant to Ca^{2+}-dependent desensitisation (Zhao et al., 2020). Hence, large and sustained increases in the time integrated Ca^{2+}-signals were observed for TGNs exposed to 0.35, 0.5 and 1 mM AITC (Fig. 5.2 B, C), and a larger fraction of the cells responded (Fig. 5.2 D). This accounts for the large increases in the amounts of CGRP exocytosis evoked by 0.35 and 0.5 mM AITC, though the extent of exocytosis in response to 1 mM AITC was somewhat lower. A similar outcome has been observed for CGRP release elicited from TGNs by high [CAP] (Belinskaia et al., 2022).

In summary, complex patterns of increases in $[Ca^{2+}]_i$ were observed in TGNs exposed to different [AITC], but these can be nominally reconciled with current knowledge of the multi-site chemical activation and desensitisation of TRPA1. Consequently, Ca^{2+} influx is limited in amount and duration at low [AITC], despite initial activation of the signal, due to desensitisation restricting the stimulation of CGRP release to a relatively low level (~7%). By contrast, relatively high [AITC] [known to additionally activate TRPA1 by a secondary mechanism resistant to desensitisation (Hinman et al., 2006)] elicit large and persistent increases in $[Ca^{2+}]_i$ that evoke a large extra increment in CGRP exocytosis.

The large and sustained increase in $[Ca^{2+}]_i$ induced by CAP after AITC pre-treatment (Fig. 5.3 A) is not compatible with the proposal that cross-desensitisation of TRPV1 by AITC impairs CAP evoked CGRP release (Ruparel et al., 2008). An alternative possible explanation is that pre-exposure to 1 mM AITC extensively depletes the cells of readily releasable CGRP (Fig. 5.1 A). To investigate this notion advantage was taken of the poor inhibition by BoNT/A of CGRP release evoked by 1 μM CAP (Meng et al., 2007), (Belinskaia et al., 2022). Pre-exposure to BoNT/A reduced the amount of CGRP released in response to 1 mM AITC, relative to untreated control cells (Fig. 5.5 G), so the releasable reserve was depleted but only partly. Subsequent stimulation of the BoNT/A-treated TGNs with 1 μM CAP was able to stimulate the exocytosis of a residual portion of releasable CGRP (Fig. 5.5 G). This ability of CAP to

release the residual CGRP corroborates the Ca^{2+} imaging data to confirm that pre-exposure to AITC does not cause extensive cross-desensitisation of TRPV1 in TGNs but, rather, depletes the neurons of releasable CGRP.

Neurotrophins such as NGF might modulate TRPA1 activity by the activation of phospholipase C and degradation of phosphatidyl inositol polyphosphates (PIPs) that directly bind to TRPA1 channels and suppress their activity (Macpherson et al., 2007), (Zhao et al., 2020). Alternatively, NGF might mobilise to the cell surface intracellular reserves of TRPA1 residing on CGRP-containing secretory granules (Morenilla-Palao et al., 2004), like observed for TNFα (Meng et al., 2016). Here, using a protocol that reliably reports an enhancement of TRPV1 activity by NGF (Belinskaia et al., 2022), it was found that NGF pre-treatment furnishes a modest enhancement of AITC-evoked CGRP release but only for low [AITC] (Fig. 5.6 B). The lack of enhancement of CGRP release evoked by 0.5 mM AITC is probably due to the maximum stimulation of CGRP release having been reached even in the absence of NGF; a similar outcome was observed previously for the enhancement by NGF of CGRP release evoked by low but not high [CAP] [(Fig. 4.6 B, (Belinskaia et al., 2022)]. TRPA1 trafficking also underlies AITC enhancement of cell excitability to AITC and this has been attenuated by tetanus toxin (Schmidt et al., 2009), which cleaves VAMP1/2/3. The likely involvement of the channels' delivery to the cell surface from intracellular reserves was highlighted by pre-treatment of the TGNs with BoNT/A, LC/E-BoNT/A or BoNT/DA, as all three inhibitors of SNARE-mediated membrane fusion prevented the NGF- enhancement of 0.01 mM AITC-evoked CGRP release (Fig. 5.6 D) as well as its induction of exocytosis (Fig. 5.6 C).

BoNTs potentially offer a prospect of analgesia through specific inhibition of membrane fusion, encompassing TRP channel trafficking and CGRP release. BoNT/A has been approved and is used clinically with some success for intransigent chronic migraine and off-label for other severe headaches (Becker, 2020). However, it was found here that BoNT/A caused only a partial inhibition of AITC-evoked CGRP release (Fig. 5.5 E) and only at high toxin concentrations (Fig. 5.4 B) despite extensive proteolysis of SNAP-25 (Fig. 5.4 A, B and Fig. 5.5 A, B) to an extent previously found to result in lowering CGRP release evoked by K^+ depolarisation, bradykinin or low [CAP] (Meng et al., 2007), (Belinskaia et al., 2022). Inhibition of CAP-evoked CGRP release by BoNT/A is overcome by raising [CAP], which has been attributed to this causing larger and more persistent increases in $[Ca^{2+}]_i$ (Meng et al., 2009), (Belinskaia et al., 2022). However,

persistent high [Ca^{2+}] is unable to account for the partial inhibition of AITC-evoked CGRP release by BoNT/A, as a similar incomplete blockade was observed over a broad range of [AITC] (Fig. 5.5 E) that elicited a diverse range of $[Ca^{2+}]_i$ signals (Fig. 5.2 A, B). Moreover, LC/E-BoNT/A could only partly reduce AITC-evoked CGRP release, matching the level of inhibition by BoNT/A, despite its extensive inhibition of CAP-evoked CGRP release even at high [CAP] (Antoniazzi et al., 2022), (Wang et al., 2017). Thirdly, even 1 mM AITC proved incapable of raising $[Ca^{2+}]_i$ to anywhere near the level induced by 1 µM CAP (Fig. 5.3 A, B). By contrast, in TGNs pre-treated with BoNT/DA, evoked CGRP release was consistently inhibited by ~70% at all [AITC] tested (Fig. 5.5 E), in closer alignment with the observed 85% reduction of intact VAMP1/2 (Fig. 5.5 A, B). This confirms that AITC-evoked CGRP exocytosis is SNARE-mediated, so the reasons for relatively weak inhibition by BoNT/A and LC/E-BoNT/A remain unknown. It might be that the residual intact SNAP-25 (~20% of the total content) is disproportionately capable of mediating AITC-evoked CGRP release.

6 General discussion and recommendations for future work

6.1 BoNT/A is a condition-dependent inhibitor of CGRP release when it is evoked by activation of TRP channels

Exocytotic processes in sensory neurons contribute to chronic migraine, other types of headaches, and to chronic pain in other areas of the body. Elevated levels have been reported of a secreted neuropeptide, CGRP, during and between migraine attacks and therapeutic strategies aimed at neutralising CGRP with antibodies or CGRP receptor antagonists have proven beneficial for many patients (Edvinsson, 2022). However, for others the side effects of directly targeting CGRP signalling have been intolerable (Gonzalez-Hernandez et al., 2018). An alternative strategy has been to block the release of the neuropeptide with an inhibitor of exocytosis, BoNT/A, a major advantage being precise delivery by injection of the drug (e.g., in BOTOX®) to localised peripheral sensory fields; thereby, adverse reactions are minimised and systemic effects avoided. Based on a large-scale clinical trial demonstrating that BOTOX® injections were safe and reduced the frequency and severity of headaches in a significant proportion of chronic migraineurs refractory to other drugs, it has been licensed since 2010 as a third order treatment (Finnerup et al., 2015) for this very common and highly disabling disorder. Furthermore, clinical studies have found that 70% of the patients selected for BOTOX® responded well and that this was a cohort that specifically exhibited higher than average serum levels of CGRP (Cernuda-Morollón et al., 2015), which become normalised after the treatment. Nevertheless, a large proportion of patients receiving BOTOX® reported no improvement in their symptoms and even in responders the frequency and severity of attacks were only partially reduced (Dodick et al., 2010); the reasons for such incomplete relief of symptoms are obscure.

An understanding of molecular mechanisms behind migraine pain will define BoNT/A's site of action and the basis of its therapeutic effect, which will provide an opportunity for further improvements. According to current research, stimulation of TRPV1 and A1 channels on nociceptors that innervate the meninges is involved in the development of headaches (Meents et al., 2010), (Iyengar et al., 2017). Such channel activation causes the entry of Ca^{2+} through the opened pore, leading to build-up of this cation inside the sensory afferent fibres that provokes their secretion of CGRP. Additionally, *in vitro* experiments revealed, that the type of stimulation and its intensity (agonist concentration) influence the levels of $[Ca^{2+}]_i$ achieved and, consequently, the amounts of neuropeptide released. For instance, depolarisation of the TGNs cultures

evokes more CGRP release than high [CAP] (Chapter 3), but the latter induces more extensive and sustained levels $[Ca^{2+}]_i$ (Meng et al., 2009), which effects exocytotic machinery and the inhibitory effect of BoNTs (see below). By contrast to TRPV1, TRPA1 stimulated by AITC undergoes a bi-phasic activation which both limits the amount of $[Ca^{2+}]_i$ attained and alters its kinetic profile. This impacts the amounts of neuropeptide that is released. Moreover, even with intense stimulation of A1, the levels of $[Ca^{2+}]_i$ and CGRP release is lower than at activation of TRPV1 by high [CAP] (Fig. 6.1 A centre and left).

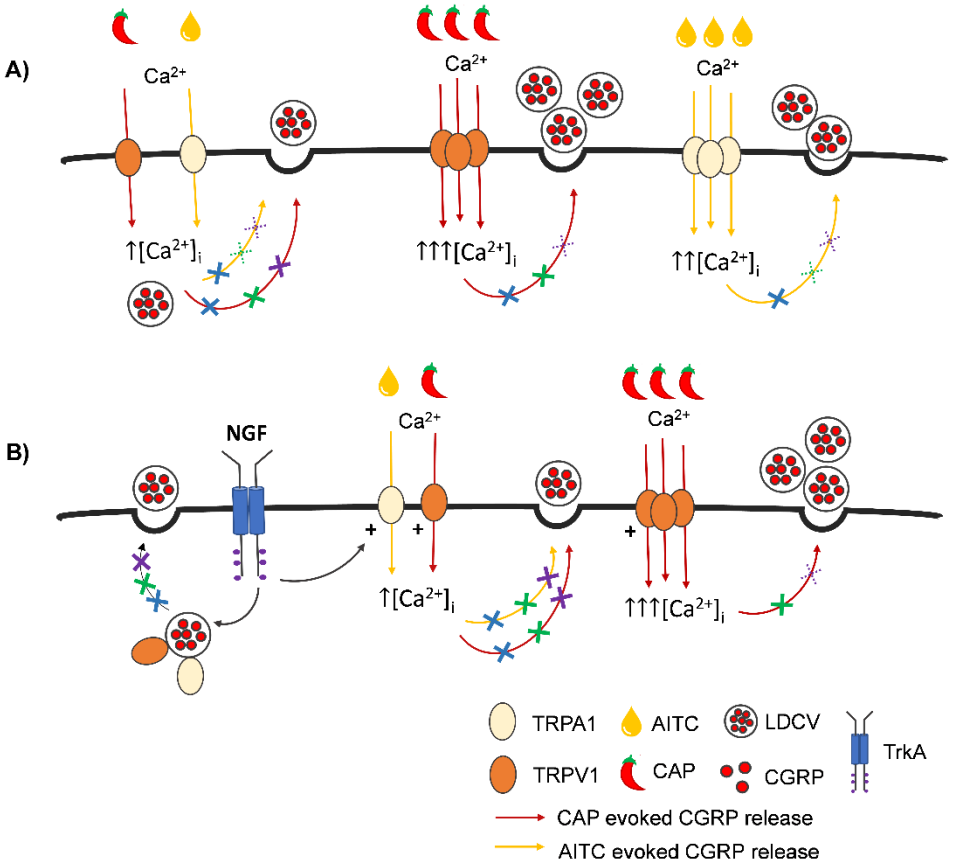

Figure 6.1 Recombinant BoNTs with /E and /D proteases abolish CGRP release under a wider range of conditions than BoNT/A

(A) Left: mild stimulation of cultured TGNs with low [CAP] or [AITC] (0.02 and 10 µM, respectively) induce small elevation of $[Ca^{2+}]_i$. BoNT/A, /E and /D cleaving chimeras diminish CAP-elicited CGRP release (purple, green, and blue crosses, respectively). Only /D-cleaving BoNT retained full blocking efficacy when the neuropeptide exocytosis was evoked by low AITC, as /A and /E caused only partial inhibition. Middle: intensive stimulation with high [CAP] provokes extensive elevation of $[Ca^{2+}]_i$ and only /E and /D containing BoNTs reduce evoked CGRP release. Right: at high [AITC] the levels of $[Ca^{2+}]_i$ are smaller than at high [CAP], but only BoNT/DA extensively reduced stimulated CGRP exocytosis. (B) Left: NGF binds to its receptor TrkA and induces CGRP release which is blocked by /A, /E, and /D-cleaving

BoNTs. Middle: NGF sensitises TRPV1 and TRPA1 and enhances CGRP release, evoked by low [CAP] or [AITC], which is abolished by A, /E, and /D-cleaving BoNTs. Right: NGF enhances CGRP release evoked by high [CAP] (but not by high [AITC]), which can be blocked by /E protease, while /A is ineffective. Note, BoNT/DA was not tested on NGF-enhanced CGRP release, evoked by high [CAP].

Released CGRP contributes to a process termed neurogenic inflammation by eliciting vasodilatation, the recruitment of immune cells, and release of inflammatory mediators including (but not limited to) NGF and TNFα (Ji et al., 2014). The latter exacerbate pain sensation by binding to their respective receptors and activating intracellular signalling cascades that, amongst other things, promote the trafficking of additional TRP channels to the cell surface (Khan et al., 2008), (Meng et al., 2016). Additionally, NGF by itself induces Ca^{2+} dependent CGRP exocytosis, which can also contribute to the development of sensitisation and neurogenic inflammation (Chapter 4, 5; Figure 6.1 B left). Increased levels of surface TRPs leads to enhanced Ca^{2+} influx (Bonnington and McNaughton, 2003), (Camprubi-Robles et al., 2009), (Zhang et al., 2005). Consequently, release of vasodilating CGRP (Chapters 4 and 5) and other neurotransmitters [reviewed in (Julius, 2013)] is increased. These in turn promote neurogenic inflammation and the release of yet more factors that enhance TRP channel activity, and so on, in a positively reinforcing loop. Moreover, prolonged exposure of the sensory fibres to NGF promotes the upregulation of TRP and CGRP genes expression [reviewed in (Barker et al., 2020)]. Altogether, this results in increased sensitivity of nociceptors to the noxious stimuli and amplification of pain signalling. The involvement of regulated exocytosis in both CGRP release from nociceptors and the delivery of extra TRP channels to the cell surface suggests that both process might be susceptible to inhibition by BoNT/A with a desirable anti-nociceptive outcome (Ferrandiz-Huertas et al., 2014).

Pre-treatment with BoNT/A of rodent peptidergic sensory neurons inhibits their release of neuropeptides (e.g. CGRP, Substance P) evoked by depolarisation (Purkiss et al., 2000), (Welch et al., 2000), (Meng et al., 2007) or bradykinin (Meng et al., 2007). However, the same pre-treatment resulted in a feeble reduction in the amount of CGRP secretion evoked by the activation of TRPV1 with CAP [Chapter 3, (Meng et al., 2007)] (Fig. 6.1 A, purple). Fluorescence imaging revealed that high concentrations (1 μM) of CAP induced much larger increases in the $[Ca^{2+}]_i$ compared to those evoked by K^+ depolarisation [Chapter 3, (Cholewinski et al., 1993), (Meng et al., 2009)], whilst binding

experiments *in vitro* showed that SNAP-25$_A$ lacking only nine amino acids from its C-terminus retained the ability to form complexes with cognate partner SNAREs, syntaxin-1 and VAMP1 that were stable, being resistant to denaturation with the ionic detergent SDS (Hayashi et al., 1994). Hence, it was deduced that under conditions of extensive and sustained levels of $[Ca^{2+}]_i$ induced by 1 μM CAP SNAP-25$_A$ remains capable of supporting exocytosis. As detailed in Chapter 3, the C-terminus of SNAP-25 is required for Ca^{2+}-dependent interaction of the protein with a Ca^{2+}-sensor, synaptotagmin I, located on synaptic vesicles. Studies in permeabilised neuroendocrine cells demonstrated that at low $[Ca^{2+}]_i$ BoNT/A inhibited neurosecretion, but this effect was abolished upon increasing cytosolic Ca^{2+} levels up to millimolar concentrations (Gerona et al., 2000). In this regard, it is notable that the ability of 4-aminopyridine or CAP (Lundh et al., 1977), (Thyagarajan et al., 2009) to restore neurotransmission to rodent neuromuscular junctions that had been paralysed with BoNT/A is thought to involve the induction of abnormally high $[Ca^{2+}]_i$ due to the blockade of hyperpolarising K^+ channels or activation of TRPV1, respectively. It has been deduced that BoNT/A only reduces the sensitivity of regulated exocytosis to Ca^{2+}; hence, its therapeutic efficacy can be limited by the intensity of nociceptor stimulation.

BoNT/A proved herein to be a partial inhibitor of the AITC-stimulated CGRP release too, despite such stimulation inducing much less Ca^{2+} flux (and, consequently, CGRP release) into the cells compared to CAP (Chapter 5 and Fig. 6.1 A). The lower $[Ca^{2+}]_i$ (relative to CAP-induced signals) may underlie the ability of AITC to partially overcome the inhibition by BoNT/A but less extensively than CAP (Chapter 5). The complex relationship between $[Ca^{2+}]_i$ and CGRP release precludes a full understanding of the reasons why BoNT/A is only partly effective. Altogether, these findings highlight that BoNT/A is a conditional inhibitor of CGRP exocytosis that is more effective against CGRP exocytosis when it is elicited by K^+-depolarisation or bradykinin, rather than AITC and (especially) high concentrations of CAP, apparently due to larger and more prolonged increases in $[Ca^{2+}]_i$ by the agonists of TRPA1 and, most extensively, TRPV1.

6.2 Recombinant chimeras LC/E-BoNT/A, BoNT/EA, and BoNT/DA blocked CGRP exocytosis under conditions that proved insensitive to /A

Targeting other SNAREs (syntaxin-1, VAMP) or removal of a larger portion of SNAP-25 are alternative strategies for reducing neuropeptide exocytosis that could be more effective. BoNTs that block CGRP exocytosis, even when induced by relatively

high $[Ca^{2+}]_i$ persisting for prolonged durations, could be useful for the treatment of pain conditions insensitive to BoNT/A. The benefit in /E-cleaving BoNTs is in the faster than /A proteolytic activity in neuronal cultures (Keller et al., 2004), (Wang et al., 2008a) and removal of a larger fragment from the C-terminus of SNAP-25, which contains amino acids essential for interaction with synaptotagmin I (Gerona et al., 2000). Recombinant BoNT/EA inhibited CGRP exocytosis stimulated by 1 μM CAP and evoked release which was enhanced by NGF (Chapter 4, Fig. 6.1 B green). However, there is also the disadvantage that this protease is short lived within cells (Wang et al., 2008a). Combination of the powerful LC/E by its fusion to a full molecule of BoNT/A stabilised the /E protease activity and extended its persistence up to 15 days (Wang et al., 2017). Thus, LC/E-BoNT/A has the advantage of longevity over BoNT/EA as a potential therapeutic molecule. It demonstrated a major inhibitory effect on CGRP exocytosis stimulated by CAP [Chapter 3, (Wang et al., 2017)] but, surprisingly, was no more effective in diminishing AITC-evoked exocytosis than BoNT/A (Chapter 5, Fig. 6.1 B green). Nevertheless, in animal models of CAP- or AITC-induced pain after injection of agonist into rat whisker pad, the chimera showed a long-lasting (15 days) pain-relief effect for both agonists without altering spontaneous behaviour or locomotor performance [(Antoniazzi et al., 2022); unpublished data]. Moreover, LC/E-BoNT/A displayed better anti-nociceptive effect (up to 20 days) than BoNT/A on mechanical and cold hypersensitivity in a model of neuropathic pain in rats, which represents a more severe impairment of the sensory system (Wang et al., 2017). BoNT/A showed analgesic effects in animal models of CAP and AITC-induced pain as well (Luvisetto et al., 2015), (Matak et al., 2014); however, contradictory results occurred when the toxin was tested in humans. Several studies (Gazerani et al., 2006), (Gazerani et al., 2009), (Tugnoli et al., 2007) reported a reduction of CAP-induced nociception in humans after BoNT/A pre-treatment, while in (Schulte-Mattler et al., 2007) a higher [CAP] was used and BoNT/A had no effect on CAP-evoked nociception. Such discrepancies might arise from different types of CAP application on the skin (subcutaneous injection vs topical application) and the concentration of the TRPV1 agonist used. Considering that LC/E-BoNT/A is a better inhibitor than BoNT/A of CGRP release *in vitro* evoked by any [CAP], the molecule should be tested in pre-clinical studies of CAP-induced pain in humans.

Another BoNT serotype, /D, cleaves VAMP1/2/3 and in cultured TGNs inhibits CGRP release evoked by depolarisation, CAP, and bradykinin (Meng et al., 2007), (Meng

et al., 2014). Although an acceptor protein, SV2A/B/C, and gangliosides that are essential for BoNT/D binding to neurons are both present in rodents and humans, it was found that this neurotoxin has no paralytic effect in human muscles (Coffield et al., 1997), (Eleopra et al., 2013); the reason for such a lack of susceptibility to /D in humans remains unknown. Nevertheless, a study in human stem cell derived neurons (Pellett et al., 2015) has reported that after a brief (10 min) treatment the BoNT/D protease activity can be detected inside the cells for up to 14 days (which is similar to LC/E-BoNT/A). The replacement of the binding domain of /D with the corresponding region from /A (creating chimera BoNT/DA) enabled the delivery LC/D into rat TGNs *in vitro*. Herein it was demonstrated, that the chimera inhibited both CAP and AITC-evoked (Chapter 5, Fig. 6.1 B blue) CGRP exocytosis, so targeting VAMP1/2/3 could also form a feasible basis for an alternative analgesic in patients resistant to BoNT/A. In fact, VAMP-cleaving BoNT serotype B (trade names rimabotulinumtoxin B, NeuroBloc, Myobloc) is already in use for treatments of dystonia, a movement disorder which induces pain associated with muscle constrictions [reviewed in (Marques et al., 2016)]. BoNT/B has proven to be safe, well tolerated and effective in /A-resistant patients. Its antinociceptive effect has also been demonstrated in rodent inflammatory pain models (Luvisetto et al., 2006), (Sikandar et al., 2016). Thus, further investigation of VAMP-cleaving BoNTs is warranted to provide insights into their effectiveness as anti-pain treatment.

6.3 Factors that might influence the sensitivity of sensory neurons to BoNTs: a comparison with previous studies

With regard to the BoNT concentrations required in this study to inhibit CAP- or AITC-evoked CGRP exocytosis from TGNs (see 5.2.5), it is intriguing that another research group has reported significant inhibition of 2 µM CAP-evoked CGRP exocytosis in cultured TGNs pre-treated with much lower doses of BoNT/A akin to those used therapeutically [1.6 or 3.1 Units, which is equivalent to a few picograms of the neurotoxin (Durham et al., 2004)]. These researchers exposed cells to /A after only 1 DIV in presence of a low concentration of NGF (10 ng/ml). Under such conditions these immature cultures will not have established a neuropil (Fig. 3.1 A). Moreover, NGF upregulates the expression of CGRP and TRPV1 and enhances cell sensitivity to CAP (Price et al., 2005), characteristics that increase over days to weeks especially in the presence of the NGF concentrations used herein. These factors were not investigated by Durham and co-workers, but the work of others (Price et al., 2005) indicate that immature 1 DIV neurons

grown with low [NGF] express relatively low amounts of TRPV1 and CGRP. Indeed, the CAP-induced increment of CGRP was much lower (only 5-fold over the baseline) in (Durham et al., 2004), compared to the present study (~15-fold increase). It is possible that the immature cultures used in (Durham et al., 2004) were more sensitive to BoNT/A, but this cannot be verified because the only metric used was inhibition of CGRP release; they did not measure SNAP-25 cleavage. By contrast, Western blotting was performed routinely in this study to verify that the blockade of the neuropeptide secretion was reconcilable with SNARE proteolysis by each of the toxins investigated. In this regard, the potency of BoNT/A reported herein is consistent with previous results from the host laboratory (Meng et al., 2007), (Meng et al., 2014) and from other groups (Welch et al., 2000), (Purkiss et al., 2000). These latter studies detected only a minor proportion of SNAP-25 being cleaved at sub-nanomolar [BoNT/A] and a similarly small reduction in CGRP exocytosis; these reports contradict the extensive inhibition claimed in (Durham et al., 2004) but do indicate that a limited inhibition of CGRP release by therapeutically-relevant concentrations of BoNT/A is detectable in cultured sensory neurons. However, whilst inhibition by BoNT/A or LC/E-BoNT/A of KCl-evoked CGRP or Substance P release was observed at 1-50 pM of each toxin (Meng et al., 2007), (Wang et al., 2017), (Welch et al., 2000), a higher concentration (10 nM) of either chimera LC/E-BoNT/A or BoNT/DA inhibited only ~15-20% of the neuropeptide release evoked upon TRP channels activation (Chapter 5). However, CGRP is known to be a very potent vasodilator (Brain et al., 1986), and it is possible that even a small reduction in its release could reduce the promotion of neurogenic inflammation, nociceptors sensitisation, and pain development.

6.4 Selective delivery of BoNT LC into sensory neurons is a strategy for improved pain therapy

The doses of BoNT used therapeutically must be restricted in amount and delivery sites (for example, BOTOX® is used in femtomole concentrations) because BoNTs are potent inhibitors of neurotransmission at neuromuscular junctions, at ganglionic synapses of the autonomic nervous system and at parasympathetic neuroeffector junctions (Rossetto et al., 2014). Such restrictions are necessary to minimise or avoid side-effects ranging in scope from discomfort (e.g., dry mouth, one of the most common adverse reactions) to severely disabling neuromuscular paralysis or potentially even lethality. Moreover, the need for nanomolar BoNT concentrations and prolonged cell treatments

in vitro (see 5.2.5) indicate that sensory neurons (in culture) are less sensitive to the toxins than motor neurons in living animals. However, as immunotherapy targeting CGRP or its receptor has highlighted the likely benefits of suppressing nociceptor CGRP signalling (Edvinsson et al., 2018), and it seems feasible that clinical BoNT/A injections do reduce such signalling to some extent, it is possible that a more extensive blockade of CGRP exocytosis from nociceptors would provide even more effective pain management. Employment of gene engineering to retarget recombinant BoNTs specifically to sensory neurons could provide safer therapeutics by reducing the concentrations of BoNTs required to target sensory nerves. Alternatively, the apparent preference of natural BoNTs for motor nerves could be selectively ablated so that higher doses can be tolerated by the organism and in this way more of the therapeutic might be able to enter sensory neurons. The latter appears to have been an unforeseen but beneficial outcome of a recombinant BoNT created by expressing individual domains separately but with fused affinity tags that enable them to bind each other *in vitro* (Ferrari et al., 2011). Cleverly, this technology called "protein-stapling" used so called SNARE domains from VAMP, SNAP-25 and syntaxin-1 to mediate the specific high-affinity binding interaction to create a molecule called BiTox (Ferrari et al., 2011). Further improvements could be performed with this technique by replacing the /A proteolytic chain with the /E or /D enzyme, which are similar (/E) or better (/D) inhibitors of AITC evoked CGRP exocytosis and more effective in the inhibition of neurosecretion induced by CAP. Another strategy involves the modification of one or more of each of the three basic domains of BoNTs (binding, translocation, and proteolytic LC) to tailor the therapeutic effect for certain pathological conditions. To this purpose, a number of different methodologies are being developed. They include the delivery of neurotoxin proteases into neurons by herpes simplex virus type 1 vectors that express transgenic BoNT LC (Joussain et al., 2019). Moreover, for a more precise targeting these vectors can also contain a specific promotor for a certain type of cells, like *Pirt* (phosphoinositide interacting regulator of TRP) which expresses exclusively in peripheral sensory neurons (Wang et al., 2021). In cultured DRGNs or TGNs such lentiviruses demonstrated inhibition of CGRP release (Joussain et al., 2019), (Wang et al., 2021). Other studies have focused on modification or replacement of the receptor-binding domain of BoNT/A. For example, (Nugent et al., 2017) used a coupling strategy where the LC and translocation domain of /A was conjugated to anti-TrkA IgG (immunoglobulin G). The advantage of such an approach is that in adult rodents and humans, this NGF receptor is expressed on nociceptors but not motor nerve endings;

therefore, it provides a means of selectively delivering the BoNT LC into pain-sensing neurons. To summarise, there are several strategies for BoNT LC delivery into the sensory neurons actively being investigated with the aim of improving the safety and efficacy of neurotoxins in pain management. However, the ability for scaled production, storage, and ease of use for clinicians must also be considered during their further development.

References

AKOPIAN, A. N., RUPAREL, N. B., JESKE, N. A. & HARGREAVES, K. M. 2007. Transient receptor potential TRPA1 channel desensitization in sensory neurons is agonist dependent and regulated by TRPV1-directed internalization. *J Physiol,* 583**,** 175-93.

ANTONIAZZI, C., BELINSKAIA, M., ZURAWSKI, T., KAZA, S. K., DOLLY, J. O. & LAWRENCE, G. W. 2022. Botulinum neurotoxin chimeras suppress stimulation by capsaicin of rat trigeminal sensory neurons in vivo and In vitro. *Toxins (Basel),* 14.

ARAUJO, M. C., SOCZEK, S. H. S., PONTES, J. P., MARQUES, L. A. C., SANTOS, G. S., SIMAO, G., BUENO, L. R., MARIA-FERREIRA, D., MUSCARA, M. N. & FERNANDES, E. S. 2022. An Overview of the TRP-Oxidative Stress Axis in Metabolic Syndrome: Insights for Novel Therapeutic Approaches. *Cells,* 11.

AURORA, S. K., DODICK, D. W., TURKEL, C. C., DEGRYSE, R. E., SILBERSTEIN, S. D., LIPTON, R. B., DIENER, H. C., BRIN, M. F. & GROUP, P. C. M. S. 2010. OnabotulinumtoxinA for treatment of chronic migraine: results from the double-blind, randomized, placebo-controlled phase of the PREEMPT 1 trial. *Cephalalgia,* 30**,** 793-803.

BAHIA, P. K., PARKS, T. A., STANFORD, K. R., MITCHELL, D. A., VARMA, S., STEVENS, S. M., JR. & TAYLOR-CLARK, T. E. 2016. The exceptionally high reactivity of Cys 621 is critical for electrophilic activation of the sensory nerve ion channel TRPA1. *J Gen Physiol,* 147**,** 451-65.

BAKER, P. F. & KNIGHT, D. E. 1978. Calcium-dependent exocytosis in bovine adrenal medullary cells with leaky plasma membranes. *Nature,* 276**,** 620-2.

BARKER, P. A., MANTYH, P., ARENDT-NIELSEN, L., VIKTRUP, L. & TIVE, L. 2020. Nerve growth factor signaling and its contribution to pain. *J Pain Res,* 13**,** 1223-1241.

BASBAUM, A. I., BAUTISTA, D. M., SCHERRER, G. & JULIUS, D. 2009. Cellular and molecular mechanisms of pain. *Cell,* 139**,** 267-84.

BECKER, W. J. 2020. Botulinum toxin in the treatment of headache. *Toxins (Basel),* 12.

BELINSKAIA, M., ZURAWSKI, T., KAZA, S. K., ANTONIAZZI, C., DOLLY, J. O. & LAWRENCE, G. W. 2022. NGF enhances CGRP release evoked by capsaicin from rat trigeminal neurons: differential inhibition by SNAP-25-cleaving proteases. *Int J Mol Sci,* 23.

BENEMEI, S. & DUSSOR, G. 2019. TRP channels and migraine: recent developments and new therapeutic opportunities. *Pharmaceuticals (Basel),* 12.

BERGMANN, I., REITER, R., TOYKA, K. V. & KOLTZENBURG, M. 1998. Nerve growth factor evokes hyperalgesia in mice lacking the low-affinity neurotrophin receptor p75. *Neurosci Lett,* 255**,** 87-90.

BONNINGTON, J. K. & MCNAUGHTON, P. A. 2003. Signalling pathways involved in the sensitisation of mouse nociceptive neurones by nerve growth factor. *J Physiol,* 551**,** 433-46.

BOWEN, E. J., SCHMIDT, T. W., FIRM, C. S., RUSSO, A. F. & DURHAM, P. L. 2006. Tumor necrosis factor-alpha stimulation of calcitonin gene-related peptide expression and secretion from rat trigeminal ganglion neurons. *J Neurochem,* 96**,** 65-77.

BRAIN, S. D., TIPPINS, J. R., MORRIS, H. R., MACINTYRE, I. & WILLIAMS, T. J. 1986. Potent vasodilator activity of calcitonin gene-related peptide in human skin. *J Invest Dermatol,* 87**,** 533-6.

BREIDENBACH, M. A. & BRUNGER, A. T. 2005. New insights into clostridial neurotoxin-SNARE interactions. *Trends Mol Med,* 11**,** 377-81.

BURSTEIN, R., BLUMENFELD, A. M., SILBERSTEIN, S. D., MANACK ADAMS, A. & BRIN, M. F. 2020. Mechanism of action of onabotulinumtoxinA in chronic migraine: a narrative review. *Headache,* 60**,** 1259-1272.

CAMPRUBI-ROBLES, M., PLANELLS-CASES, R. & FERRER-MONTIEL, A. 2009. Differential contribution of SNARE-dependent exocytosis to inflammatory potentiation of TRPV1 in nociceptors. *FASEB J,* 23**,** 3722-33.

CARMINE BELIN, A., RAN, C. & EDVINSSON, L. 2020. Calcitonin Gene-Related Peptide (CGRP) and Cluster Headache. *Brain Sci,* 10.

CATERINA, M. J., LEFFLER, A., MALMBERG, A. B., MARTIN, W. J., TRAFTON, J., PETERSEN-ZEITZ, K. R., KOLTZENBURG, M., BASBAUM, A. I. & JULIUS, D. 2000. Impaired nociception and pain sensation in mice lacking the capsaicin receptor. *Science,* 288**,** 306-13.

CERNUDA-MOROLLÓN, E., RAMÓN, C., MARTÍNEZ-CAMBLOR, P., SERRANO-PERTIERRA, E., LARROSA, D. & PASCUAL, J. 2015. OnabotulinumtoxinA decreases interictal CGRP plasma levels in patients with chronic migraine. *Pain,* 156**,** 820-824.

CHAPMAN, E. R. 2002. Synaptotagmin: a Ca^{2+} sensor that triggers exocytosis? *Nat Rev Mol Cell Biol,* 3**,** 498-508.

CHEN, Y. A., SCALES, S. J., PATEL, S. M., DOUNG, Y. C. & SCHELLER, R. H. 1999. SNARE complex formation is triggered by Ca^{2+} and drives membrane fusion. *Cell,* 97**,** 165-74.

CHOLEWINSKI, A., BURGESS, G. M. & BEVAN, S. 1993. The role of calcium in capsaicin-induced desensitization in rat cultured dorsal root ganglion neurons. *Neuroscience,* 55**,** 1015-23.

CHUANG, H. H., PRESCOTT, E. D., KONG, H., SHIELDS, S., JORDT, S. E., BASBAUM, A. I., CHAO, M. V. & JULIUS, D. 2001. Bradykinin and nerve growth factor release the capsaicin receptor from PtdIns(4,5)P2-mediated inhibition. *Nature,* 411**,** 957-62.

COFFIELD, J. A., BAKRY, N., ZHANG, R. D., CARLSON, J., GOMELLA, L. G. & SIMPSON, L. L. 1997. In vitro characterization of botulinum toxin types A, C and D action on human tissues: combined electrophysiologic, pharmacologic and molecular biologic approaches. *J Pharmacol Exp Ther,* 280**,** 1489-98.

CROWLEY, C., SPENCER, S. D., NISHIMURA, M. C., CHEN, K. S., PITTS-MEEK, S., ARMANINI, M. P., LING, L. H., MCMAHON, S. B., SHELTON, D. L., LEVINSON, A. D. & ET AL. 1994. Mice lacking nerve growth factor display perinatal loss of sensory and sympathetic neurons yet develop basal forebrain cholinergic neurons. *Cell,* 76**,** 1001-11.

DENK, F., BENNETT, D. L. & MCMAHON, S. B. 2017. Nerve Growth Factor and Pain Mechanisms. *Annu Rev Neurosci,* 40**,** 307-325.

DENNER, A. C., VOGLER, B., MESSLINGER, K. & DE COL, R. 2017. Role of transient receptor potential ankyrin 1 receptors in rodent models of meningeal nociception - Experiments in vitro. *Eur J Pain,* 21**,** 843-854.

DEVESA, I., FERRANDIZ-HUERTAS, C., MATHIVANAN, S., WOLF, C., LUJAN, R., CHANGEUX, J. P. & FERRER-MONTIEL, A. 2014. alphaCGRP is essential for algesic exocytotic mobilization of TRPV1 channels in peptidergic nociceptors. *Proc Natl Acad Sci U S A,* 111**,** 18345-50.

DI CASTRO, A., DREW, L. J., WOOD, J. N. & CESARE, P. 2006. Modulation of sensory neuron mechanotransduction by PKC- and nerve growth factor-dependent pathways. *Proc Natl Acad Sci U S A,* 103**,** 4699-704.

DIENER, H. C., DODICK, D. W., AURORA, S. K., TURKEL, C. C., DEGRYSE, R. E., LIPTON, R. B., SILBERSTEIN, S. D., BRIN, M. F. & GROUP, P. C. M. S. 2010. OnabotulinumtoxinA for treatment of chronic migraine: results from the double-blind, randomized, placebo-controlled phase of the PREEMPT 2 trial. *Cephalalgia,* 30**,** 804-14.

DODICK, D. W., TURKEL, C. C., DEGRYSE, R. E., AURORA, S. K., SILBERSTEIN, S. D., LIPTON, R. B., DIENER, H. C., BRIN, M. F. & GROUP, P. C. M. S. 2010. OnabotulinumtoxinA for treatment of chronic migraine: pooled results from the double-blind, randomized, placebo-controlled phases of the PREEMPT clinical program. *Headache,* 50**,** 921-36.

DOMINGUEZ, C., POZO-ROSICH, P., TORRES-FERRUS, M., HERNANDEZ-BELTRAN, N., JURADO-COBO, C., GONZALEZ-ORIA, C., SANTOS, S., MONZON, M. J., LATORRE, G., ALVARO, L. C., GAGO, A., GALLEGO, M., MEDRANO, V., HUERTA, M., GARCIA-ALHAMA, J., BELVIS, R.,

LEIRA, Y. & LEIRA, R. 2018. OnabotulinumtoxinA in chronic migraine: predictors of response. A prospective multicentre descriptive study. *Eur J Neurol,* 25**,** 411-416.

DURHAM, P. L., CADY, R. & CADY, R. 2004. Regulation of calcitonin gene-related peptide secretion from trigeminal nerve cells by botulinum toxin type A: implications for migraine therapy. *Headache,* 44**,** 35-42; discussion 42-3.

DURHAM, P. L. & MASTERSON, C. G. 2013. Two mechanisms involved in trigeminal CGRP release: implications for migraine treatment. *Headache,* 53**,** 67-80.

DUSSOR, G., YAN, J., XIE, J. Y., OSSIPOV, M. H., DODICK, D. W. & PORRECA, F. 2014. Targeting TRP channels for novel migraine therapeutics. *ACS Chem Neurosci,* 5**,** 1085-96.

DUX, M., ROSTA, J. & MESSLINGER, K. 2020. TRP Channels in the Focus of Trigeminal Nociceptor Sensitization Contributing to Primary Headaches. *Int J Mol Sci,* 21.

ECKERT, S. P., TADDESE, A. & MCCLESKEY, E. W. 1997. Isolation and culture of rat sensory neurons having distinct sensory modalities. *J Neurosci Methods,* 77**,** 183-90.

EDVINSSON, L. 2022. Calcitonin gene-related peptide (CGRP) is a key molecule released in acute migraine attacks-Successful translation of basic science to clinical practice. *J Intern Med,* 292**,** 575-586.

EDVINSSON, L., HAANES, K. A., WARFVINGE, K. & KRAUSE, D. N. 2018. CGRP as the target of new migraine therapies - successful translation from bench to clinic. *Nat Rev Neurol,* 14**,** 338-350.

EGEA, J., ESPINET, C., SOLER, R. M., PEIRO, S., ROCAMORA, N. & COMELLA, J. X. 2000. Nerve growth factor activation of the extracellular signal-regulated kinase pathway is modulated by $Ca^{(2+)}$ and calmodulin. *Mol Cell Biol,* 20**,** 1931-46.

EID, S. R., CROWN, E. D., MOORE, E. L., LIANG, H. A., CHOONG, K. C., DIMA, S., HENZE, D. A., KANE, S. A. & URBAN, M. O. 2008. HC-030031, a TRPA1 selective antagonist, attenuates inflammatory- and neuropathy-induced mechanical hypersensitivity. *Mol Pain,* 4**,** 48.

ELEOPRA, R., MONTECUCCO, C., DEVIGILI, G., LETTIERI, C., RINALDO, S., VERRIELLO, L., PIRAZZINI, M., CACCIN, P. & ROSSETTO, O. 2013. Botulinum neurotoxin serotype D is poorly effective in humans: an in vivo electrophysiological study. *Clin Neurophysiol,* 124**,** 999-1004.

EVERAERTS, W., GEES, M., ALPIZAR, Y. A., FARRE, R., LETEN, C., APETREI, A., DEWACHTER, I., VAN LEUVEN, F., VENNEKENS, R., DE RIDDER, D., NILIUS, B., VOETS, T. & TALAVERA, K. 2011. The capsaicin receptor TRPV1 is a crucial mediator of the noxious effects of mustard oil. *Curr Biol,* 21**,** 316-21.

FABBRETTI, E., D'ARCO, M., FABBRO, A., SIMONETTI, M., NISTRI, A. & GINIATULLIN, R. 2006. Delayed upregulation of ATP P_2X_3 receptors of trigeminal sensory neurons by calcitonin gene-related peptide. *J Neurosci,* 26**,** 6163-71.

FERRANDIZ-HUERTAS, C., MATHIVANAN, S., WOLF, C. J., DEVESA, I. & FERRER-MONTIEL, A. 2014. Trafficking of thermo TRP channels. *Membranes (Basel),* 4**,** 525-64.

FERRARI, E., MAYWOOD, E. S., RESTANI, L., CALEO, M., PIRAZZINI, M., ROSSETTO, O., HASTINGS, M. H., NIRANJAN, D., SCHIAVO, G. & DAVLETOV, B. 2011. Re-assembled botulinum neurotoxin inhibits CNS functions without systemic toxicity. *Toxins (Basel),* 3**,** 345-55.

FINNERUP, N. B., ATTAL, N., HAROUTOUNIAN, S., MCNICOL, E., BARON, R., DWORKIN, R. H., GILRON, I., HAANPAA, M., HANSSON, P., JENSEN, T. S., KAMERMAN, P. R., LUND, K., MOORE, A., RAJA, S. N., RICE, A. S., ROWBOTHAM, M., SENA, E., SIDDALL, P., SMITH, B. H. & WALLACE, M. 2015. Pharmacotherapy for neuropathic pain in adults: a systematic review and meta-analysis. *Lancet Neurol,* 14**,** 162-73.

FOSTER, K. & CHADDOCK, J. 2010. Targeted secretion inhibitors-innovative protein therapeutics. *Toxins (Basel),* 2**,** 2795-815.

GALOYAN, S. M., PETRUSKA, J. C. & MENDELL, L. M. 2003. Mechanisms of sensitization of the response of single dorsal root ganglion cells from adult rat to noxious heat. *Eur J Neurosci,* 18**,** 535-41.

GARDNER, A. P. & BARBIERI, J. T. 2018. Light chain diversity among the botulinum neurotoxins. *Toxins (Basel),* 10.

GAZERANI, P., PEDERSEN, N. S., STAAHL, C., DREWES, A. M. & ARENDT-NIELSEN, L. 2009. Subcutaneous Botulinum toxin type A reduces capsaicin-induced trigeminal pain and vasomotor reactions in human skin. *Pain,* 141**,** 60-9.

GAZERANI, P., STAAHL, C., DREWES, A. M. & ARENDT-NIELSEN, L. 2006. The effects of Botulinum Toxin type A on capsaicin-evoked pain, flare, and secondary hyperalgesia in an experimental human model of trigeminal sensitization. *Pain,* 122**,** 315-325.

GERONA, R. R., LARSEN, E. C., KOWALCHYK, J. A. & MARTIN, T. F. 2000. The C terminus of SNAP-25 is essential for Ca^{2+}-dependent binding of synaptotagmin to SNARE complexes. *J Biol Chem,* 275**,** 6328-36.

GONZALEZ-HERNANDEZ, A., MARICHAL-CANCINO, B. A., MAASSENVANDENBRINK, A. & VILLALON, C. M. 2018. Side effects associated with current and prospective antimigraine pharmacotherapies. *Expert Opin Drug Metab Toxicol,* 14**,** 25-41.

GUDES, S., BARKAI, O., CASPI, Y., KATZ, B., LEV, S. & BINSHTOK, A. M. 2015. The role of slow and persistent TTX-resistant sodium currents in acute tumor necrosis factor-alpha-mediated increase in nociceptors excitability. *J Neurophysiol,* 113**,** 601-19.

HAANES, K. A. & EDVINSSON, L. 2019. Pathophysiological mechanisms in migraine and the identification of new therapeutic targets. *CNS Drugs,* 33**,** 525-537.

HAYASHI, T., MCMAHON, H., YAMASAKI, S., BINZ, T., HATA, Y., SUDHOF, T. C. & NIEMANN, H. 1994. Synaptic vesicle membrane fusion complex: action of clostridial neurotoxins on assembly. *EMBO J,* 13**,** 5051-61.

HEINRICHER, M. M., TAVARES, I., LEITH, J. L. & LUMB, B. M. 2009. Descending control of nociception: Specificity, recruitment and plasticity. *Brain Res Rev,* 60**,** 214-25.

HENSELLEK, S., BRELL, P., SCHAIBLE, H. G., BRAUER, R. & SEGOND VON BANCHET, G. 2007. The cytokine TNFalpha increases the proportion of DRG neurones expressing the TRPV1 receptor via the TNFR1 receptor and ERK activation. *Mol Cell Neurosci,* 36**,** 381-91.

HINMAN, A., CHUANG, H. H., BAUTISTA, D. M. & JULIUS, D. 2006. TRP channel activation by reversible covalent modification. *Proc Natl Acad Sci U S A,* 103**,** 19564-8.

HUANG, E. J. & REICHARDT, L. F. 2003. Trk receptors: roles in neuronal signal transduction. *Annu Rev Biochem,* 72**,** 609-42.

HUANG, J., ZHANG, X. & MCNAUGHTON, P. A. 2006a. Inflammatory pain: the cellular basis of heat hyperalgesia. *Curr Neuropharmacol,* 4**,** 197-206.

HUANG, J., ZHANG, X. & MCNAUGHTON, P. A. 2006b. Modulation of temperature-sensitive TRP channels. *Semin Cell Dev Biol,* 17**,** 638-45.

IANNONE, L. F., DE LOGU, F., GEPPETTI, P. & DE CESARIS, F. 2022. The role of TRP ion channels in migraine and headache. *Neurosci Lett,* 768**,** 136380.

IBARRA, Y. & BLAIR, N. T. 2013. Benzoquinone reveals a cysteine-dependent desensitization mechanism of TRPA1. *Mol Pharmacol,* 83**,** 1120-32.

ISHIGURO, N., OYAMA, S., HIGASHI, R. & YANAGIDA, K. 2020. Efficacy, safety, and tolerability of ONO-4474, an orally available pan-tropomyosin receptor kinase inhibitor, in japanese patients with moderate to severe osteoarthritis of the knee: a randomized, placebo-controlled, double-blind, parallel-group comparative study. *J Clin Pharmacol,* 60**,** 28-36.

IYENGAR, S., OSSIPOV, M. H. & JOHNSON, K. W. 2017. The role of calcitonin gene-related peptide in peripheral and central pain mechanisms including migraine. *Pain,* 158**,** 543-559.

JI, R. R., SAMAD, T. A., JIN, S. X., SCHMOLL, R. & WOOLF, C. J. 2002. p38 MAPK activation by NGF in primary sensory neurons after inflammation increases TRPV1 levels and maintains heat hyperalgesia. *Neuron,* 36**,** 57-68.

JI, R. R., XU, Z. Z. & GAO, Y. J. 2014. Emerging targets in neuroinflammation-driven chronic pain. *Nat Rev Drug Discov,* 13**,** 533-48.

JIANG, H. & GUROFF, G. 1997. Actions of the neurotrophins on calcium uptake. *J Neurosci Res,* 50**,** 355-60.

JOUSSAIN, C., LE COZ, O., PICHUGIN, A., MARCONI, P., LIM, F., SICURELLA, M., SALONIA, A., MONTORSI, F., WANDOSELL, F., FOSTER, K., GIULIANO, F., EPSTEIN, A. L. & ARANDA MUNOZ, A. 2019. Botulinum Neurotoxin Light Chains Expressed by Defective Herpes Simplex Virus Type-1 Vectors Cleave SNARE Proteins and Inhibit CGRP Release in Rat Sensory Neurons. *Toxins (Basel),* 11.

JULIUS, D. 2013. TRP channels and pain. *Annu Rev Cell Dev Biol,* 29**,** 355-84.

KALLIOLIAS, G. D. & IVASHKIV, L. B. 2016. TNF biology, pathogenic mechanisms and emerging therapeutic strategies. *Nat Rev Rheumatol,* 12**,** 49-62.

KELLER, J. E., CAI, F. & NEALE, E. A. 2004. Uptake of botulinum neurotoxin into cultured neurons. *Biochemistry,* 43**,** 526-32.

KHALIL, M., ZAFAR, H. W., QUARSHIE, V. & AHMED, F. 2014. Prospective analysis of the use of OnabotulinumtoxinA (BOTOX) in the treatment of chronic migraine; real-life data in 254 patients from Hull, U.K. *J Headache Pain,* 15**,** 54.

KHAN, A. A., DIOGENES, A., JESKE, N. A., HENRY, M. A., AKOPIAN, A. & HARGREAVES, K. M. 2008. Tumor necrosis factor alpha enhances the sensitivity of rat trigeminal neurons to capsaicin. *Neuroscience,* 155**,** 503-9.

KHOUNLO, R., KIM, J., YIN, L. & SHIN, Y. K. 2017. Botulinum toxins A and E inflict dynamic destabilization on t-SNARE to impair SNARE assembly and membrane fusion. *Structure,* 25**,** 1679-1686 e5.

KOIVISTO, A. P., BELVISI, M. G., GAUDET, R. & SZALLASI, A. 2022. Advances in TRP channel drug discovery: from target validation to clinical studies. *Nat Rev Drug Discov,* 21**,** 41-59.

KOPLAS, P. A., ROSENBERG, R. L. & OXFORD, G. S. 1997. The role of calcium in the desensitization of capsaicin responses in rat dorsal root ganglion neurons. *J Neurosci,* 17**,** 3525-37.

KRESS, M. & REEH, P. W. 1996. More sensory competence for nociceptive neurons in culture. *Proc Natl Acad Sci U S A,* 93**,** 14995-7.

KUNKLER, P. E., BALLARD, C. J., OXFORD, G. S. & HURLEY, J. H. 2011. TRPA1 receptors mediate environmental irritant-induced meningeal vasodilatation. *Pain,* 152**,** 38-44.

KWAN, K. Y., ALLCHORNE, A. J., VOLLRATH, M. A., CHRISTENSEN, A. P., ZHANG, D. S., WOOLF, C. J. & COREY, D. P. 2006. TRPA1 contributes to cold, mechanical, and chemical nociception but is not essential for hair-cell transduction. *Neuron,* 50**,** 277-89.

LAWRENCE, G. W., ZURAWSKI, T. H. & DOLLY, J. O. 2021a. Ca^{2+} signalling induced by NGF identifies a subset of capsaicin-excitable neurons displaying enhanced chemo-nociception in dorsal root ganglion explants from adult pirt-GCaMP3 mouse. *Int J Mol Sci,* 22.

LAWRENCE, G. W., ZURAWSKI, T. H., DONG, X. & DOLLY, J. O. 2021b. Population coding of capsaicin concentration by sensory neurons revealed using Ca^{2+} imaging of dorsal root ganglia explants from adult pirt-GCaMP3 mouse. *Cell Physiol Biochem,* 55**,** 428-448.

LIAO, M., CAO, E., JULIUS, D. & CHENG, Y. 2013. Structure of the TRPV1 ion channel determined by electron cryo-microscopy. *Nature,* 504**,** 107-12.

LUNDH, H., LEANDER, S. & THESLEFF, S. 1977. Antagonism of the paralysis produced by botulinum toxin in the rat. The effects of tetraethylammonium, guanidine and 4-aminopyridine. *J Neurol Sci,* 32**,** 29-43.

LUVISETTO, S., MARINELLI, S., LUCCHETTI, F., MARCHI, F., COBIANCHI, S., ROSSETTO, O., MONTECUCCO, C. & PAVONE, F. 2006. Botulinum neurotoxins and formalin-induced pain: central vs. peripheral effects in mice. *Brain Res,* 1082**,** 124-31.

LUVISETTO, S., VACCA, V. & CIANCHETTI, C. 2015. Analgesic effects of botulinum neurotoxin type A in a model of allyl isothiocyanate- and capsaicin-induced pain in mice. *Toxicon,* 94**,** 23-8.

MACPHERSON, L. J., DUBIN, A. E., EVANS, M. J., MARR, F., SCHULTZ, P. G., CRAVATT, B. F. & PATAPOUTIAN, A. 2007. Noxious compounds activate TRPA1 ion channels through covalent modification of cysteines. *Nature,* 445**,** 541-5.

MALIN, S. A., DAVIS, B. M. & MOLLIVER, D. C. 2007. Production of dissociated sensory neuron cultures and considerations for their use in studying neuronal function and plasticity. *Nat Protoc,* 2**,** 152-60.

MANTYH, P. W., KOLTZENBURG, M., MENDELL, L. M., TIVE, L. & SHELTON, D. L. 2011. Antagonism of nerve growth factor-TrkA signaling and the relief of pain. *Anesthesiology,* 115**,** 189-204.

MARLIN, M. C. & LI, G. 2015. Biogenesis and function of the NGF/TrkA signaling endosome. *Int Rev Cell Mol Biol,* 314**,** 239-57.

MARQUES, R. E., DUARTE, G. S., RODRIGUES, F. B., CASTELAO, M., FERREIRA, J., SAMPAIO, C., MOORE, A. P. & COSTA, J. 2016. Botulinum toxin type B for cervical dystonia. *Cochrane Database Syst Rev,* 2016**,** CD004315.

MARTENS, S. & MCMAHON, H. T. 2008. Mechanisms of membrane fusion: disparate players and common principles. *Nat Rev Mol Cell Biol,* 9**,** 543-56.

MARTINS, L. B., DUARTE, H., FERREIRA, A. V., ROCHA, N. P., TEIXEIRA, A. L. & DOMINGUES, R. B. 2015. Migraine is associated with altered levels of neurotrophins. *Neurosci Lett,* 587**,** 6-10.

MATAK, I., ROSSETTO, O. & LACKOVIC, Z. 2014. Botulinum toxin type A selectivity for certain types of pain is associated with capsaicin-sensitive neurons. *Pain,* 155**,** 1516-1526.

MCKELVEY, L., SHORTEN, G. D. & O'KEEFFE, G. W. 2013. Nerve growth factor-mediated regulation of pain signalling and proposed new intervention strategies in clinical pain management. *J Neurochem,* 124**,** 276-89.

MCMAHON, S. B., ARMANINI, M. P., LING, L. H. & PHILLIPS, H. S. 1994. Expression and coexpression of Trk receptors in subpopulations of adult primary sensory neurons projecting to identified peripheral targets. *Neuron,* 12**,** 1161-71.

MCNAMARA, C. R., MANDEL-BREHM, J., BAUTISTA, D. M., SIEMENS, J., DERANIAN, K. L., ZHAO, M., HAYWARD, N. J., CHONG, J. A., JULIUS, D., MORAN, M. M. & FANGER, C. M. 2007. TRPA1 mediates formalin-induced pain. *Proc Natl Acad Sci U S A,* 104**,** 13525-30.

MEENTS, J. E., CIOTU, C. I. & FISCHER, M. J. M. 2019. TRPA1: a molecular view. *J Neurophysiol,* 121**,** 427-443.

MEENTS, J. E., NEEB, L. & REUTER, U. 2010. TRPV1 in migraine pathophysiology. *Trends Mol Med,* 16**,** 153-9.

MENG, J., DOLLY, J. O. & WANG, J. 2014. Selective cleavage of SNAREs in sensory neurons unveils protein complexes mediating peptide exocytosis triggered by different stimuli. *Mol Neurobiol,* 50**,** 574-88.

MENG, J., OVSEPIAN, S. V., WANG, J., PICKERING, M., SASSE, A., AOKI, K. R., LAWRENCE, G. W. & DOLLY, J. O. 2009. Activation of TRPV1 mediates calcitonin gene-related peptide release, which excites trigeminal sensory neurons and is attenuated by a retargeted botulinum toxin with anti-nociceptive potential. *J Neurosci,* 29**,** 4981-92.

MENG, J., WANG, J., LAWRENCE, G. & DOLLY, J. O. 2007. Synaptobrevin I mediates exocytosis of CGRP from sensory neurons and inhibition by botulinum toxins reflects their anti-nociceptive potential. *J Cell Sci,* 120**,** 2864-74.

MENG, J., WANG, J., STEINHOFF, M. & DOLLY, J. O. 2016. TNFalpha induces co-trafficking of TRPV1/TRPA1 in VAMP1-containing vesicles to the plasmalemma via Munc18-1/syntaxin1/SNAP-25 mediated fusion. *Sci Rep,* 6**,** 21226.

MOLGO, J. & THESLEFF, S. 1984. Studies on the mode of action of botulinum toxin type A at the frog neuromuscular junction. *Brain Res,* 297**,** 309-16.

MORENILLA-PALAO, C., PLANELLS-CASES, R., GARCIA-SANZ, N. & FERRER-MONTIEL, A. 2004. Regulated exocytosis contributes to protein kinase C potentiation of vanilloid receptor activity. *J Biol Chem,* 279**,** 25665-72.

NICHOLLS, D. G. 1994. Exocytosis of large dense-core vesicles from neurons and secretory cells. *Proteins, Transmitters and Synapses.* Blackwell Scientific Publications.

NUGENT, M., WANG, J., LAWRENCE, G., ZURAWSKI, T., GEOGHEGAN, J. A. & DOLLY, J. O. 2017. Conjugate of an IgG Binding Domain with Botulinum Neurotoxin A Lacking the Acceptor Moiety Targets Its SNARE Protease into TrkA-Expressing Cells When Coupled to Anti-TrkA IgG or Fc-betaNGF. *Bioconjug Chem,* 28**,** 1684-1692.

NUGENT, M., YUSEF, Y. R., MENG, J., WANG, J. & DOLLY, J. O. 2018. A SNAP-25 cleaving chimera of botulinum neurotoxin /A and /E prevents TNFalpha-induced elevation of the activities of native TRP channels on early postnatal rat dorsal root ganglion neurons. *Neuropharmacology,* 138**,** 257-266.

OTTO, H., HANSON, P. I., CHAPMAN, E. R., BLASI, J. & JAHN, R. 1995. Poisoning by botulinum neurotoxin A does not inhibit formation or disassembly of the synaptosomal fusion complex. *Biochem Biophys Res Commun,* 212**,** 945-52.

PANDIELLA-ALONSO, A., MALGAROLI, A., VICENTINI, L. M. & MELDOLESI, J. 1986. Early rise of cytosolic Ca^{2+} induced by NGF in PC12 and chromaffin cells. *FEBS Lett,* 208**,** 48-51.

PARK, K. A., FEHRENBACHER, J. C., THOMPSON, E. L., DUARTE, D. B., HINGTGEN, C. M. & VASKO, M. R. 2010. Signaling pathways that mediate nerve growth factor-induced increase in expression and release of calcitonin gene-related peptide from sensory neurons. *Neuroscience,* 171**,** 910-23.

PAULSEN, C. E., ARMACHE, J. P., GAO, Y., CHENG, Y. & JULIUS, D. 2015. Structure of the TRPA1 ion channel suggests regulatory mechanisms. *Nature,* 520**,** 511-7.

PELLETT, S., TEPP, W. H., SCHERF, J. M., PIER, C. L. & JOHNSON, E. A. 2015. Activity of botulinum neurotoxin type D (strain 1873) in human neurons. *Toxicon,* 101**,** 63-9.

PHILLIPS, E., REEVE, A., BEVAN, S. & MCINTYRE, P. 2004. Identification of species-specific determinants of the action of the antagonist capsazepine and the agonist PPAHV on TRPV1. *J Biol Chem,* 279**,** 17165-72.

PRICE, T. J., LOURIA, M. D., CANDELARIO-SOTO, D., DUSSOR, G. O., JESKE, N. A., PATWARDHAN, A. M., DIOGENES, A., TROTT, A. A., HARGREAVES, K. M. & FLORES, C. M. 2005. Treatment of trigeminal ganglion neurons in vitro with NGF, GDNF or BDNF: effects on neuronal survival, neurochemical properties and TRPV1-mediated neuropeptide secretion. *BMC Neurosci,* 6**,** 4.

PURKISS, J., WELCH, M., DOWARD, S. & FOSTER, K. 2000. Capsaicin-stimulated release of substance P from cultured dorsal root ganglion neurons: involvement of two distinct mechanisms. *Biochem Pharmacol,* 59**,** 1403-6.

RAY, J. C., KAPOOR, M., STARK, R. J., WANG, S. J., BENDTSEN, L., MATHARU, M. & HUTTON, E. J. 2021. Calcitonin gene related peptide in migraine: current therapeutics, future implications and potential off-target effects. *J Neurol Neurosurg Psychiatry,* 92**,** 1325-1334.

RIZO, J. & ROSENMUND, C. 2008. Synaptic vesicle fusion. *Nat Struct Mol Biol,* 15**,** 665-74.

ROSSETTO, O., PIRAZZINI, M. & MONTECUCCO, C. 2014. Botulinum neurotoxins: genetic, structural and mechanistic insights. *Nat Rev Microbiol,* 12**,** 535-49.

ROZEN, T. & SWIDAN, S. Z. 2007. Elevation of CSF tumor necrosis factor alpha levels in new daily persistent headache and treatment refractory chronic migraine. *Headache,* 47**,** 1050-5.

RUPAREL, N. B., PATWARDHAN, A. M., AKOPIAN, A. N. & HARGREAVES, K. M. 2008. Homologous and heterologous desensitization of capsaicin and mustard oil responses utilize different cellular pathways in nociceptors. *Pain,* 135**,** 271-279.

RUSSELL, F. A., KING, R., SMILLIE, S. J., KODJI, X. & BRAIN, S. D. 2014. Calcitonin gene-related peptide: physiology and pathophysiology. *Physiol Rev,* 94**,** 1099-142.

SAKABA, T., STEIN, A., JAHN, R. & NEHER, E. 2005. Distinct kinetic changes in neurotransmitter release after SNARE protein cleavage. *Science,* 309**,** 491-4.

SARCHIELLI, P. & GALLAI, V. 2004. Nerve growth factor and chronic daily headache: a potential implication for therapy. *Expert Rev Neurother,* 4**,** 115-27.

SCHMIDT, M., DUBIN, A. E., PETRUS, M. J., EARLEY, T. J. & PATAPOUTIAN, A. 2009. Nociceptive signals induce trafficking of TRPA1 to the plasma membrane. *Neuron,* 64**,** 498-509.

SCHNITZER, T. J. & MARKS, J. A. 2015. A systematic review of the efficacy and general safety of antibodies to NGF in the treatment of OA of the hip or knee. *Osteoarthritis Cartilage,* 23 Suppl 1**,** S8-17.

SCHULTE-MATTLER, W. J., OPATZ, O., BLERSCH, W., MAY, A., BIGALKE, H. & WOHLFAHRT, K. 2007. Botulinum toxin A does not alter capsaicin-induced pain perception in human skin. *J Neurol Sci,* 260**,** 38-42.

SHU, X. & MENDELL, L. M. 1999. Nerve growth factor acutely sensitizes the response of adult rat sensory neurons to capsaicin. *Neurosci Lett,* 274**,** 159-62.

SHU, X. & MENDELL, L. M. 2001. Acute sensitization by NGF of the response of small-diameter sensory neurons to capsaicin. *J Neurophysiol,* 86**,** 2931-8.

SIKANDAR, S., GUSTAVSSON, Y., MARINO, M. J., DICKENSON, A. H., YAKSH, T. L., SORKIN, L. S. & RAMACHANDRAN, R. 2016. Effects of intraplantar botulinum toxin-B on carrageenan-induced changes in nociception and spinal phosphorylation of GluA1 and Akt. *Eur J Neurosci,* 44**,** 1714-22.

SMEYNE, R. J., KLEIN, R., SCHNAPP, A., LONG, L. K., BRYANT, S., LEWIN, A., LIRA, S. A. & BARBACID, M. 1994. Severe sensory and sympathetic neuropathies in mice carrying a disrupted Trk/NGF receptor gene. *Nature,* 368**,** 246-9.

STEIN, A. T., UFRET-VINCENTY, C. A., HUA, L., SANTANA, L. F. & GORDON, S. E. 2006. Phosphoinositide 3-kinase binds to TRPV1 and mediates NGF-stimulated TRPV1 trafficking to the plasma membrane. *J Gen Physiol,* 128**,** 509-22.

STUDIER, F. W. 2005. Protein production by auto-induction in high density shaking cultures. *Protein Expr Purif,* 41**,** 207-34.

SUDHOF, T. C. 2012. Calcium control of neurotransmitter release. *Cold Spring Harb Perspect Biol,* 4**,** a011353.

SUDHOF, T. C. 2014. The molecular machinery of neurotransmitter release (Nobel lecture). *Angew Chem Int Ed Engl,* 53**,** 12696-717.

THYAGARAJAN, B., KRIVITSKAYA, N., POTIAN, J. G., HOGNASON, K., GARCIA, C. C. & MCARDLE, J. J. 2009. Capsaicin protects mouse neuromuscular junctions from the neuroparalytic effects of botulinum neurotoxin a. *J Pharmacol Exp Ther,* 331**,** 361-71.

TIAN, Q., HU, J., XIE, C., MEI, K., PHAM, C., MO, X., HEPP, R., SOARES, S., NOTHIAS, F., WANG, Y., LIU, Q., CAI, F., ZHONG, B., LI, D. & YAO, J. 2019. Recovery from tachyphylaxis of TRPV1 coincides with recycling to the surface membrane. *Proc Natl Acad Sci U S A,* 116**,** 5170-5175.

TUGNOLI, V., CAPONE, J. G., ELEOPRA, R., QUATRALE, R., SENSI, M., GASTALDO, E., TOLA, M. R. & GEPPETTI, P. 2007. Botulinum toxin type A reduces capsaicin-evoked pain and neurogenic vasodilatation in human skin. *Pain,* 130**,** 76-83.

VAN HECKE, O., TORRANCE, N. & SMITH, B. H. 2013. Chronic pain epidemiology and its clinical relevance. *Br J Anaesth,* 111**,** 13-8.

VOLLER, B., SYCHA, T., GUSTORFF, B., SCHMETTERER, L., LEHR, S., EICHLER, H. G., AUFF, E. & SCHNIDER, P. 2003. A randomized, double-blind, placebo controlled study on analgesic effects of botulinum toxin A. *Neurology,* 61**,** 940-4.

WANG, J., CASALS-DIAZ, L., ZURAWSKI, T., MENG, J., MORIARTY, O., NEALON, J., EDUPUGANTI, O. P. & DOLLY, O. 2017. A novel therapeutic with two SNAP-25 inactivating proteases shows long-lasting anti-hyperalgesic activity in a rat model of neuropathic pain. *Neuropharmacology,* 118**,** 223-232.

WANG, J., MENG, J., LAWRENCE, G. W., ZURAWSKI, T. H., SASSE, A., BODEKER, M. O., GILMORE, M. A., FERNANDEZ-SALAS, E., FRANCIS, J., STEWARD, L. E., AOKI, K. R. & DOLLY, J. O. 2008a. Novel chimeras of botulinum neurotoxins A and E unveil contributions from the binding, translocation, and protease domains to their functional characteristics. *J Biol Chem,* 283**,** 16993-7002.

WANG, J., ZURAWSKI, T. H., MENG, J., LAWRENCE, G., OLANGO, W. M., FINN, D. P., WHEELER, L. & DOLLY, J. O. 2011. A dileucine in the protease of botulinum toxin A underlies its long-lived neuroparalysis: transfer of longevity to a novel potential therapeutic. *J Biol Chem,* 286**,** 6375-85.

WANG, W., KONG, M., DOU, Y., XUE, S., LIU, Y., ZHANG, Y., CHEN, W., LI, Y., DAI, X., MENG, J. & WANG, J. 2021. Selective Expression of a SNARE-Cleaving Protease in Peripheral Sensory Neurons Attenuates Pain-Related Gene Transcription and Neuropeptide Release. *Int J Mol Sci,* 22.

WANG, Y. Y., CHANG, R. B., WATERS, H. N., MCKEMY, D. D. & LIMAN, E. R. 2008b. The nociceptor ion channel TRPA1 is potentiated and inactivated by permeating calcium ions. *J Biol Chem,* 283**,** 32691-703.

WEBSTER, J. D. & VUCIC, D. 2020. The Balance of TNF Mediated Pathways Regulates Inflammatory Cell Death Signaling in Healthy and Diseased Tissues. *Front Cell Dev Biol,* 8**,** 365.

WEI, S., QIU, C. Y., JIN, Y., LIU, T. T. & HU, W. P. 2021. TNF-alpha acutely enhances acid-sensing ion channel currents in rat dorsal root ganglion neurons via a p38 MAPK pathway. *J Neuroinflammation,* 18**,** 92.

WELCH, M. J., PURKISS, J. R. & FOSTER, K. A. 2000. Sensitivity of embryonic rat dorsal root ganglia neurons to Clostridium botulinum neurotoxins. *Toxicon,* 38**,** 245-58.

WOOLF, C. J. 1996. Phenotypic modification of primary sensory neurons: the role of nerve growth factor in the production of persistent pain. *Philos Trans R Soc Lond B Biol Sci,* 351**,** 441-8.

WOOLF, C. J., SAFIEH-GARABEDIAN, B., MA, Q. P., CRILLY, P. & WINTER, J. 1994. Nerve growth factor contributes to the generation of inflammatory sensory hypersensitivity. *Neuroscience,* 62**,** 327-31.

ZHANG, L., HOFF, A. O., WIMALAWANSA, S. J., COTE, G. J., GAGEL, R. F. & WESTLUND, K. N. 2001. Arthritic calcitonin/alpha calcitonin gene-related peptide knockout mice have reduced nociceptive hypersensitivity. *Pain,* 89**,** 265-73.

ZHANG, S., MASUYER, G., ZHANG, J., SHEN, Y., LUNDIN, D., HENRIKSSON, L., MIYASHITA, S. I., MARTINEZ-CARRANZA, M., DONG, M. & STENMARK, P. 2017. Identification and characterization of a novel botulinum neurotoxin. *Nat Commun,* 8**,** 14130.

ZHANG, X., HUANG, J. & MCNAUGHTON, P. A. 2005. NGF rapidly increases membrane expression of TRPV1 heat-gated ion channels. *EMBO J,* 24**,** 4211-23.

ZHANG, X., KIM-MILLER, M. J., FUKUDA, M., KOWALCHYK, J. A. & MARTIN, T. F. 2002. Ca^{2+}-dependent synaptotagmin binding to SNAP-25 is essential for Ca^{2+}-triggered exocytosis. *Neuron,* 34**,** 599-611.

ZHAO, J., LIN KING, J. V., PAULSEN, C. E., CHENG, Y. & JULIUS, D. 2020. Irritant-evoked activation and calcium modulation of the TRPA1 receptor. *Nature,* 585**,** 141-145.

ZHU, W. & OXFORD, G. S. 2007. Phosphoinositide-3-kinase and mitogen activated protein kinase signaling pathways mediate acute NGF sensitization of TRPV1. *Mol Cell Neurosci,* 34**,** 689-700.